Faculty of Science and Engineering

School of Civil and Mechanical Engineering

Development of a Hybrid Conceptual-Statistical Framework to Evaluate Catchment-Scale Water Balance

Hamideh Kazemi Alamouti

This thesis is presented for the degree of

Doctor of Philosophy of Curtin University

February 2021

Abstract

Catchment water balance provides useful information for sustainable water management, catchment development, and policymaking. Streamflow is one of the main components in the catchment water balance; accordingly, streamflow study is critical for better understanding the catchment's water balance. Streamflow studies can be conducted using two approaches (i.e., long-term and short-term studies). This study applied both approaches to investigate streamflow change in several catchments with different physical and hydrological characteristics, around the world (i.e., Harvey Catchment in Western Australia, Beardy and Goulburn Catchments in New South Wales and Karkheh basin in Iran). For the long-term approach, two types of models (i.e., a conceptual model (the Budyko) and hydrological models (HBV and HBV-light)) were used to investigate impacts of climate change and human activities on annual streamflow and the models' performances were compared. To further enhance the results, image processing and remote sensing techniques were employed to quantify the impact of land use change on streamflow variation. It was shown that, in most of the cases, climate change and regional human activities play equally significant roles in streamflow change. It was also confirmed that water storage change is negligible when the study period is sufficiently long. Moreover, the study successfully applied the Budyko model for estimating streamflow under two future climate scenarios and the results were cross validated with HBV model.

For the short-term study, the conceptual models (i.e., Budyko, Budyko-Du, ABCD, ABCD-GE models) were employed to estimate monthly streamflow variation in the case study. The models showed that for inter-annual studies, the water storage change is significant and cannot be ignored. To investigate the importance of groundwater storage variation in streamflow change, groundwater level data was required. However, uniform groundwater data is not accessible in most of the catchments. Therefore spatiotemporal analysis has been conducted to assess the spatially and temporally non-uniform groundwater data. The Regression Kriging code was written in R STUDIO to spatiotemporally estimate the groundwater level in the catchment. The assessed groundwater level information was adapted by the conceptual models (i.e., Budyko-Du and ABCD-GE) and showed a significant improvement, proving the importance of groundwater change in streamflow estimation. To further improve the estimation, a hybrid conceptual statistical model was integrated using the ARIMA model. The result showed notable improvement in the performance of the models, affirming that using only conceptual models may not be able to grasp all the aspects required for accurate streamflow estimation, due to the simplifying assumptions imbedded in conceptual models. The current framework can be adapted to other catchments, particularly, study areas with non-uniform data or where only limited data is available. The research outcome provides useful information for policymaking and sustainable development of catchments while using very limited information, without requiring complicated data or time-consuming simulation.

Declaration

To the best of my knowledge and belief, this thesis contains no material previously published by and other person except where due acknowledgement has been made.

This thesis contains no material which has been accepted for the award of any other degree or diploma in any university.

Signature:

Hamideh Kazemi

Date: February 2021

Acknowledgment

This work would not have been achievable without the support of several people to whom I will always be deeply grateful.

First and foremost I wish to single out my supervisor Dr Ranjan Sarukkalige and express my sincere gratitude for his continuous guidance, support and encouragement throughout this study. He changed my view of dealing with science and supported me all along with great passion and novel ideas. From day one, he encouraged me to think outside the box and supported me to grasp every opportunity to expand my professional network. He kindly and patiently participated in all after-hours meetings with external institutes and helped me find extra financial and technical support to extend the research beyond the initial scopes.

I would like to acknowledge the financial support of the International Postgraduate Research Scholarship from the Curtin University and the top-up scholarship from CSIRO-Data61. Also, I would like to thank Dr Quanxi Shao who provided me with his unsurpassed knowledge and great technical advice.

I take this opportunity to express my deepest appreciation to the love of my life, Amir, for his understanding and unending inspiration. He was always beside me in hard days and assured me with his unfailing kindness and patience. I owe much gratitude to my dearest parents for their permanent encouragement, understanding and unwavering support during my whole life to this day that I am submitting the thesis, and my beautiful siblings (Mohsen, Zeinab and Hamidreza) whose love and support are with me in whatever I pursue. You all made it possible for me to complete this dissertation.

Publications from this thesis

1- Al-Safi, H. I. J., Kazemi, H., & Sarukkalige, P. R. (2020). Comparative study of conceptual versus distributed hydrologic modelling to evaluate the impact of climate change on future runoff in unregulated catchments. *Journal of Water and Climate Change*, 11(2), 341-366.

2- Kazemi, H., Sarukkalige, R., & Badrzadeh, H. (2019). Evaluation of streamflow changes due to climate variation and human activities using the Budyko approach. *Environmental Earth Sciences*, 78(24), 713.

3- Kazemi, H., Hashemi, H., Maghsood, F. F., Hosseini, S. H., Sarukkalige, R., Jamali, S., & Berndtsson, R. (**Under review**) Assessment of streamflow decrease due to climate vs. human influence in a semiarid area. *Journal of hydro-environment research.*

4- Kazemi, H., Sarukkalige, R., Shao, Q. (**Under review**) Evaluation of non-uniform groundwater level data using spatiotemporal modelling. *Journal of Groundwater for Sustainable Development.*

5- Kazemi, H., Sarukkalige, R., Shao, Q. (**Under review**) On the application of hybrid conceptual-statistical models to detect streamflow variation. *Journal of Hydrology.*

Contents

List of Figures

List of Tables

Abbreviations

E0	Potential Evapotranspiration	ε_P	Precipitation elasticity
E	Actual Evapotranspiration	ΔQ_h	Streamflow change due to human activities
FDCs	Flow Duration Curves	ΔQ_c	Streamflow change due to climate change
GA	Genetic Algorithm	ΔG	Groundwater change
GWL	Groundwater level	ΔGWL	Groundwater Level Change
KGE	Kling Gupta Efficiency	ΔS	Soil water storage change
KRB	Karkheh River Basin	δ	Annual Mean Difference
n	Choudhury catchment characteristic parameter	ω	Fu catchment characteristic parameter
P	Precipitation	*obs*	Observed Value
P_e	Effective precipitation	*sim*	Simulated value
R_e	Nash-Sutcliffe Efficiency		
T	Temperature		
Q	Streamflow		
$\overline{Q_o}$	Average annual streamflow		
ε_{E0}	Evapotranspiration elasticity		

Chapter 1
Introduction

Assessment of catchment water balance provides fundamental information about the hydrologic cycle and water availability in the catchment. Analysing water balance components can track the hydrologic response of the given catchment to climate and land use change in long-term (i.e., decade scale) or water movement in short-term (i.e., monthly scales) (Mitchell et al. 2003, Chauvin et al. 2011). In the long-term studies, hydrological behaviour of the catchment and water balance components due to long term climate change and human activities may be investigated. Climate change, and more precisely global warming, changes quantity of precipitation and temperature which in return affects water resources (including streamflow and groundwater) (Jones et al. 2006; Schaake 1990; Wigley and Jones 1985, Teng et al. 2012). Humans, on the other hand, manipulate hydrological cycle by different activities such as, construction of dams, water withdrawals for industrial, domestic and agricultural purposes, as well as forestation and deforestation (Haddeland et al., 2014). Some studies show influences of regional human activities on water resources can be as effective, or even more destructive than the impacts of climate change (Guyennon et al., 2017; Haddeland et al., 2014). Studying impacts of climate change and human activities on water resources, provides critical information for authorities and decision makers to develop sustainable water resources management plans (Liu et al., 2017; Teng et al., 2012). The long-term water balance studies can also include prediction of water balance change under available climate scenarios, which provide useful information in areas such as water resources potentials, water distribution policies or agricultural water management (Yaseen et al., 2016).

Monthly scale water balance analysis, on the other hand, investigates the importance of water balance components under different hydrologic conditions. These studies are particularly important in fields such as seasonal anomalies assessment, seasonal water resources management, water supply or drought assessment (Mouelhi et al., 2006; Nasta et al., 2020).

Catchment scale water balance basically can be shown in the format of below Equation (Eq. (1.1))

$$Q = P - (E + \Delta S + \Delta G) \quad (1.1)$$

where Q is streamflow, P is precipitation, E is actual evapotranspiration , ΔS is change of soil water storage and ΔG is effective change of groundwater.

One of the critical components of this water balance equation is streamflow. Accurate estimation of streamflow, is vitally important for water infrastructure designing, flood control, domestic, industrial and agricultural water supply, controlling the impacts of climate change and human activities on water resources, and many more applications. Hence careful and accurate streamflow investigation is vital for sustainable water resources management of the catchment (Dey and Mishra, 2017; Li et al., 2019; Mohammadi et al., 2020).

Similar to water balance studies, streamflow analysis can be carried out in long-term scale and short term scale. Researchers employ numerous methods in order to study short and long-term streamflow variation (e.g., distributed hydrological modelling, conceptual hydrological modelling, statistical modelling and data-driven modelling) (Kazemi et al., 2021). Among these methods, conceptual hydrological models are commonly used because of computational efficiency, simple calibration process and easy parametrization of the models (Shahid, et al. 2018).

One of the most popular conceptual models is Budyko model, which was developed in 1974 and has proved to be successful in long-term streamflow analysis (e.g., Sankarasubramanian et al., 2001; Fu et al., 2007; Chiew et al., 2009; Hu et al., 2012; Teng et al., 2012; Hashemi et al., 2015). The Budyko model provides a link between the water balance components (i.e., streamflow, precipitation and evapotranspiration). The model assumes that in sufficiently long-term studies the values of ΔS and ΔG are negligible (McMahon et al. 2013; Du et al. 2016; Wang et al. 2016).These assumption makes the model unqualified for the short-term or monthly scale assessments where the soil and ground water storage changes are not negligible (Du et al. 2016; Mianabadi et al. 2020). Therefore, several versions of extended Budyko model were proposed to enable the model for short-term or monthly scale studies (e.g., Yokoo et al., 2008; Zhang et al., 2008; Wang, 2012 and Du et al., 2016).

Conceptual models including Budyko model usually presume some simplified assumptions (e.g., assuming constant catchment characteristic parameter during the study period, ignoring spatial distribution of climate stations, etc) (Shahid, Cong et al., 2018) to perform the estimation (Shahid et al., 2018). These assumptions may put the accuracy of the models in jeopardy. Since, input data for these models are in the time-series format, statistical models are competent tools to be coupled with conceptual modes and employ the times-series to improve the performance of the modes. Hence, a recently published paper (Fathi et al., 2019) developed a model using the original Budyko model and a statistical model to estimate streamflow variation in several catchments around the world. In viewing the above, this study

pursue the following scopes and objectives to develop a novel approach (a hybrid conceptual-statistical framework) to assess the long term as well as short term change of water balance components, particularly, streamflow, in several catchments with different climatological characteristics. The different physical (e.g., size, location, approximity to the sea or mountain) and climate (e.g., mean temperature and rainfall, precipitation patterns) features of the catchments show the approach is not limited to a certain environment or location and is applicable to other catchments regardless of their characteristics.

1.1 Scopes and Objectives

The study is carried out in two approaches; long-term (annual scale) and short-term (monthly scale). For the first approach (i.e., long-term scale) impacts of climate change and regional human activities on streamflow is assessed. The Budyko model is employed and the results are validated using other methods such as hydrological modelling and remote sensing technique. Moreover, the application of the Budyko model for prediction of streamflow change under two climatological scenarios (i.e., RCP4.5 and RCP8.5) for the near future (2045-2065) and late future (2080-2100) are investigated. To the best of the authors' knowledge, this study is the first study, the Budyko model is employed to predict streamflow change.

For the second approach (i.e. short-term scale), the application of the Budyko model in inter-annual and monthly scale is investigated. In this step, monthly water balance components (i.e., $Q, P, E, \Delta S$ and ΔG) are investigated intensively. Groundwater level (GWL) change is assessed to better understand the link between streamflow and groundwater level change. Soil water storage change and its importance in water balance equation is evaluated. In order to overcome the disadvantages of simplified assumptions in the conceptual models, and to investigate the competency of the models for inter-annual and intra-annual studies, the hybrid conceptual-statistical models are developed. This modules use information in the time series and the errors from previous predictions to improve the accuracy of the estimation (Raman et al., 2018). Accordingly, effectiveness and applicability of using conceptual models in monthly and annual streamflow estimation is further discussed throughout the thesis.

1.2 Thesis structure

This thesis is organised into nine chapters. The current chapter (i.e., Chapter 1) provides an introduction of the thesis and main scopes and objectives of the study. Chapter 2 proposes a background and literature review of water resources assessment using two different approaches (i.e., long-term and short-term scales). Chapter 3 explains the methodology, case studies and required data and their sources. Chapters 4 to 6, investigate application of the Budyko model for long-term streamflow analysis. In Chapter 4 the Budyko model assesses the streamflow changes in the Australian catchments and determines the attribution of climate change and regional human activities on the changes. In Chapter 5 the Budyko model application in streamflow analysis is compared with of the HBV hydrological model. Moreover, for the first time the Budyko model is applied to predict the streamflow variation under two future scenarios. Performance of the model is cross-validated with HBV model results. Chapter 6 discusses the land use change in the Iranian basin and quantitatively validates the Budyko model results according to the remote sensing technique.

In Chapter 7 and 8, streamflow variation in short time period (i.e., monthly scale) is investigated. Hence, Chapter 7 explores the groundwater level change and provides information necessary for inter-annual streamflow analysis. Chapter 8 explains the ultimate goal of this study which is application of the Budyko model in unsteady condition. The models use results of Chapter 7 and estimates the streamflow variation in the important Harvey Catchment in Western Australia. The results are compared with other conceptual models. And finally, it presents the development of the statistical-conceptual model and discusses the application of the model for short-term studies. Chapter 9 provides the main conclusions and recommendation for further studies.

Chapter 2

Literature review

Catchment water balance study provides crucial information for water management, policy making and agricultural activities. The long-term or short-term water balance studies are usually carried out by assessing hydrological components. Since accurate and uniform observation data for all components are not always accessible (Jalota and Arora, 2002, Oliveira et al., 2014) numerous methods are used to estimate the components in either temporal scales. The water balance equation (Eq. (1.1)) is a continuity equation based on the mass balance. Streamflow (Q) is one of the main components of this equation which guarantee access to freshwater for domestic, industrial and agricultural uses in many catchments. Streamflow information is of privileged importance for hydrologists and water system designers to propose optimal and sustainable water management and water allocation plans for economical and agricultural purposes (Mohammadi et al., 2020). To develop adaptation plans for future population and predict economic status streamflow estimation and forecasting is used which provide necessary data for drought and flood risk assessment, hydropower and reservoir operations (Noori and Kalin, 2016, Wang et al., 2018, Al-Safi et al., 2020).

In long-term studies impacts of climate change and human activities on streamflow may be investigated. Climate change, particularly global warming leads to precipitation reduction and temperature increase and accordingly streamflow change in many catchments around the world (Al-Safi et al., 2020). On the other hand, human activities (such as deforestation, land use change or excessive water withdrawal) can be as effective on streamflow variation. For instance, some studies found that one of the main factors which severely affect streamflow is soil water manipulation through land cover change (Zhang et al., 2014).

In short-term studies, impacts of inter annual and seasonal change of climate parameters (such as temperature and precipitation) on streamflow can be explored. Since evapotranspiration and soil moisture vary with the inter annual climate parameters, it can be assessed if their change affect the streamflow (Kahya and Kalaycı 2004).

To study the streamflow either in short-term or long-term scales, the most common methods may be categorized in two groups; data-driven modelling (e.g., statistical modelling, Regression modelling, Neural Network) and hydrological modelling, including distributed hydrological modelling and conceptual hydrological modelling.

Data driven models such as Artificial Neural network (ANN) have been widely used in hydrological studies. They can learn the linear or non-linear link between the training parameters as an input and output of the system without considering their physical correlations (Noori and Kalin, 2016). These models focus on the characteristics of the time-series and try to estimate the link between inputs and outputs of the models (Wang et al., 2018). Noori et al 2016 used a hybrid data driven (ANN) and hydrological model to estimate daily streamflow of an ungagged catchment. The ANN alone is not applicable to an ungauged catchment because in these catchments the observed training dataset is unavailable. Therefore, the semi-distributed Soil and Water Assessment Tool (SWAT) model was used to estimate the streamflow for the near catchment for the regionalization purpose. Hence, ANN worked as an optimizer to improve the simulated streamflow. Noori et al applied this hybrid model to 29 watersheds near the city of Atlanta, USA. It was shown that the model has a better performance during warm months. Moreover, the accuracy of the model decreases where the portion of forested area to the catchment size increases which shows the developed model's performance is better in urban areas (Noori and Kalin, 2016).

Another popular data driven model to simulate hydrological variables and their temporal change is the time series/ statistical model. Modarres et al (2013) compared linear time-series model with non-linear model to estimate daily streamflow of the Matapedia River, Quebec, Canada. The nonlinear time series model, Generalized Autoregressive Conditional Heteroscedasticity (GARCH), was compared with linear ARIMA (Autoregressive Integrated Moving Average). Their result showed the non-linear model outperform the linear statistical model (Modarres and Ouarda, 2013). Wang et al (2018) used the ARIMA model in combination with a decomposition approach (Empirical Mode Decomposition (EMD) and Ensemble Empirical Mode Decomposition (EEMD)) to develop EMD/EEMD-ARIMA to forecast long-term streamflow variation in the upper stream of the Yellow River. The model was able to successfully forecast the streamflow using comprehensive information derived from the time series (Wang et al., 2018). Mohammadi et al (2020) developed three data-driven models by coupling the multi-layer perceptron (MLP) with three optimization algorithms, (i.e., particle swarm optimization (PSO) and coupled particle swarm optimization-multi-verse optimizer (PSOMVO) and a time series model (bi-linear (BL)). The daily streamflow of the Grand River, Canada and Ocmulgee and Umpqua rivers, United States were used for this study. They compared performance of the developed hybrid models with the original MLP

and BL and showed the hybrid models outperformed the original ones to simulate daily streamflow (Mohammadi et al., 2020).

Data driven models are usually simple models which work considering link between the parameters that may not be able to explain the detailed interconnection between them (Noori and Kalin, 2016, Shahid et al., 2018). The main concern in the data driven models, however, is to select the best combinations of input parameters. The application of data-driven models are highly dependent on the availability of data such that without sufficient observed data the outcome is unreliable (Sahoo et al., 2006). Moreover, the models are not able to perform realistically if the range of the investigated parameters are beyond the training range (Noori and Kalin, 2016). Therefore many researchers prefer to use hydrological modelling for streamflow estimation, to have a better understanding of the physical interaction between parameters. For instance, Sahoo et al (2006) used MIKE SHE distributed hydrological model to estimate high frequency streamflow in mountainous Hawaii region for short time frame (interval of 15 minutes) to investigate the storm and flood occurrence. The challenge is MIKE SHE is a sophisticated distributed model which needs large data sets of parameters (e.g., distribution of topography, soil and vegetation types, and geology) to physically characterize the watershed and spatially represent the physical and meteorological variability of the catchment. The model, however, provided consistent streamflow values and responded to the land use variation and climatological parameters change (Sahoo et al., 2006). Fan et al (2010) used the distributed hydrological approach (SWAT model) to analyse contribution of climate change and human activities impacts on runoff variation in Mian River Basin in North China, where the results indicated human activities have the dominant influence on runoff variation rather than climate change. In another example, Du et al (2012) coupled HEC-HMS (a distributed hydrologic model) and CA-Markov model (a dynamic land-use change model) to assess impacts of urbanization and land use change on Qinhuai River annual runoff in China. The HEC-HMS model used various urbanization scenarios provided by CA-Markov as an input to estimate streamflow under different conditions. It was shown that because of urbanization, flood volume and daily runoff peaks have increased during 1988 to 2009. It was also motioned that the runoff is more sensitive to urbanization in dry years comparing to wet years (Du et al., 2012).

Almost all distributed hydrological modelling need to be calibrated prior to application. The large and complex data set, range of the parameters and interaction between the values make the calibration process complicated, time-consuming and expensive (Noori and Kalin, 2016).

The large amount of spatial and temporal data requirement makes the models performance highly sensitive to the quality of data. By optimizing each parameter usually the other pre-calibrated parameters should be changed again. Moreover, increasing the number of calibration parameters increases requirement for field data and time for calibration. Last but not least, there is no guarantee the proposed variables is the optimum set (Sahoo et al., 2006). The conceptual hydrological models on the contrarily, are computationally efficient and easy to calibrate and parametrize (Shahid et al., 2018). These conceptual models using mathematical equations, estimate streamflow based on hydrological cycle of the catchment (Noori and Kalin, 2016).

2.1 The Budyko model

The Budyko model is one of the most popular conceptual models, developed by Budyko (1974) based on the water balance equation (Eq. (1.1)) (Budyko 1974), and since, has been successfully applied for streamflow modelling in numerous catchments around the globe (Dooge, 1992; Sivapalan et al., 2003; Yang et al., 2007; Zhang et al., 2008; Oudin et al., 2008; Zheng et al., 2009; Donohue, et al., 2011; Roderick and Farquhar, 2011; Alimohammadi, 2012; Zhang and Chiew, 2012; Hu et al., 2012; Li et al., 2012; Xu et al., 2014; Tang et al. 2014, Zeng et al., 2015; Huang et al., 2016; Liu et al., 2017).

Budyko (1974) suggested there is a link between the mean annual evapotranspiration ratio (*E/P*) and the drought index (i.e., mean annual potential evaporation ratio (E_0/P)) in a catchment (Alimohammadi, 2012; Budyko, 1974):

$$E = f(P, E_0) \tag{2.1}$$

where E_0 is the potential evapotranspiration (mm/day) and P represents precipitation (mm/day). Budyko (1974) later proposed his famous Equation (2.2) (McMahon et al. 2013; Wang et al. 2016):

$$\frac{E}{P} = \left[\frac{E_0}{P}\tanh\left(\frac{P}{E_0}\right)^{-1}(1-\exp(-\frac{E_0}{P}))\right]^{0.5} \tag{2.2}$$

Later, Fu (1981) and Choudhury (1999) proposed their popular equations (i.e., Eq. (2.3) and (2.4), respectively) based on the Budyko model (Li et al., 2013). These equations estimate mean annual evapotranspiration using an empirical parameter called the "catchment characteristics parameters" (Wang et al., 2016):

$$\frac{E}{P} = 1 + \frac{E_0}{P} - \left[1 + \left(\frac{E_0}{P}\right)^{\omega}\right]^{\frac{1}{\omega}} \quad (2.3)$$

$$\frac{E}{P} = \frac{\frac{E_0}{P}}{\left(1+\left(\frac{E_0}{P}\right)^{n}\right)^{1/n}} \quad (2.4)$$

where ω and *n* are catchment characteristic parameters representing soil properties, slope, land use, and climate seasonality (Liang et al., 2015). There is also a theoretical relationship between these two empirical parameters, (i.e., Eq. (2.5)) (Li et al., 2013; Yang et al., 2008).

$$\omega = n + 0.72 \quad (2.5)$$

An optimised *n* or ω for the catchment can be derived using a curve fitting procedure by minimising the mean squared errors between the calculated and observed annual evapotranspiration to precipitation ratios (*E/P*) (Eq. (2.6)) (Li et al. 2013):

$$n = min \sum_i \left\{ \frac{Ei}{Pi} - \left\{ \frac{1}{\left(1+\left(\frac{Pi}{E_0 i}\right)^{n}\right)^{1/n}} \right\} \right\}^2 \quad (2.6)$$

Higher values of the characteristic parameter represents higher actual evapotranspiration (*E*) for a given *P* and E_0, and, consequently lower streamflow (*Q*) (Xu et al., 2014b).

Zhange et al (2008) used the Budyko framework to model water balance of 265 Australian catchments in daily, monthly, annual and mean annual scales. The input data for the model was daily precipitation, potential evapotranspiration, and streamflow. They suggested for finer time scales (e.g., monthly or daily), the model should be improved or extended to consider more parameters such as soil water storage to perform reliably. The framework showed for the long-term analysis, climate parameters like average precipitation and potential evapotranspiration are the main affecting factors on streamflow, while for the shorter time frame other parameters such as soil-moisture dynamics should be taken into account which increase the complexity of the model (Zhang et al., 2008). In another example, Zhou et al (2012) compared the application of global land surfaces models with the Budyko model in annual runoff simulations for several catchments around the globe. The results showed superiority of the Budyko model in the case studies such that although both models provided consistent mean annual runoff but the estimated values by LSMs were more biased comparing to the Budyko-type models' (Zhou et al., 2012). Wang et al (2013) successfully employed the

Budyko model to separate impacts of climate change and human activities on runoff in the Haihe River basin in China where it was concluded that human activities were responsible for more than 50% of the runoff reduction in the basin (Wang et al., 2013). Patterson et al (2013) also used the Budyko equation to study the impact of both climate and human activities on the mean annual streamflow in the South Atlantic region in the USA. Human activities were found to be responsible for streamflow change in 27% of basins in South Atlantic where experiencing agricultural land expansion and dam constructions which has significantly affected runoff (Patterson et al., 2013). In the Yanhe Basin in China, the Budyko model was used to examine runoff reduction. The model suggested that runoff reduction in the Yanhe River basin was dominantly related to the climate change rather than human interaction. Climate change was estimated to account for 46.1%–60.8% (mean 54.1%) of the total decrease in runoff, whereas human activities accounted for 39.1%–53.9% (mean 45.9%) (Wu et al., 2017). In another study in several river basins across China, Liu et al (2017) used the Budyko model and found, until recently, climate change was a controlling factor affecting streamflow, however, it has given up its superiority in favour of human activities during the last decade (Liu et al., 2017). They compared the performance of the Budyko model with hydrological models from literature and advised to assess impacts of climate change and human activities on streamflow, the Budyko-type models and hydrological models perform comparably. However, the fact that Budyko model does not require complicated parameterization and large input data, makes it more efficient to quantify impacts of the influencing factors on streamflow (Liu et al., 2017). In a more recent study, Shahid et al (2018) successfully used two conceptual models (ABCD and Budyko) to determine the role of climate change and human activities on streamflow variation in Soan Basin where climate parameters variation (i.e., decrease in precipitation and increases in potential evapotranspiration) reduced streamflow in the basin by 68% (Shahid et al., 2018).

Several studies believe that hydrological modelling is a better choice to investigate the hydrological responses of a catchment at shorter time frame, such as daily or monthly scales, while the Budyko model is proved to be a competent alternative model for the longer temporal scales (Dooge, 1992, Zheng et al., 2009, Hu et al., 2012, Li et al., 2012, Xu et al., 2014, Zeng et al., 2015, Huang et al., 2016, Liu et al., 2017).

The Budyko model states that over a sufficiently long period and in a steady condition, where change in water storage (ΔS and/or ΔG) is negligible mean annual evapotranspiration ratio (E/P) is a function of drought index (E_0/P), where E_0 is potential evapotranspiration (Eq. (2.2))

(McMahon et al., 2013; Du et al., 2016; Wang et al., 2016; Kazemi et al., 2019). This condition, however, is not valid in many catchments, under unsteady condition, where the study includes finer time-scales or for unconfined catchments. Therefore, the application of the original Budyko model is limited (Du et al., 2016, Mianabadi et al., 2020). Accordingly, many researchers proposed modified versions of the equation to be suitable for fine time-scales. For example, Zhang et al. (2008), Yokoo et al. (2008) and Wang (2012) believed that the impact of inter-annual water storage changes, especially for fine time-scale, should not be neglected. Hence, they added water storage change in the original Budyko model, and successfully extended the equation to inter-annual or monthly scales (Yokoo et al., 2008, Zhang et al., 2008, Wang, 2012). Han et al (2011) believed that irrigation can be a significant source of available water for evapotranspiration in the water balance equation. Therefore they added contributed irrigation parameter to extend a Budyko-type model (i.e., Fu model). They successfully applied the extended version to 26 sub-catchments in the Tarim Basin, Northwest China to estimate mean annual and inter-annual streamflow variations (Han et al., 2011). Greve et al (2016) believed that human activities such as land use change or soil moisture change can provide extra sources of water for evapotranspiration and therefore they should be included in the water balance equation and accordingly the Budyko model. They modified the Fu model and proposed a new boundary condition for the model to be applicable for short-term studies. The modified Fu model was successfully applied to several catchments across the world for monthly streamflow estimation (Greve et al., 2016).

Some other studies introduced new parameters to make the Budyko model suitable for unsteady conditions. For instance, Wang (2012) and Chen et al (2013) introduced the effective precipitation parameter (Pe) to the equation to make it more applicable for inter and intra annual time-scales. The parameter is defined as (P-ΔS), based on the idea that soil water storage change can be a potential water supply for evapotranspiration (Wang and Zhou, 2016). Du et al (2016) extended the Budyko model (hereafter called Budyko-Du model), for unsteady condition using effective precipitation as follow (Du et al., 2016):

$$\frac{E}{P_e} = 1 + \frac{E_0}{P_e} - [1 + \left(\frac{E_0}{P_e}\right)^{\omega} + \lambda]^{1/\omega} \qquad (2.7)$$

where ω and λ are two non-dimensional parameters (Du et al., 2016, Mianabadi et al., 2020). Introducing the effective precipitation parameter (P_e) made soil water storage change as an additional source of water for evapotranspiration. Negative soil water storage change (ΔS) means drained water from soil makes an additional source for evapotranspiration, and positive

ΔS means part of rainfall penetrates into the soil and therefore less water is available for streamflow and evapotranspiration (Wang and Zhou, 2016).

The drawback of using P_e is the lack of available observed historical water storage data for many catchments. Therefore, Wang and Zhou (2016) used ABCD model to estimate the annual and monthly soil water storage data for the Heihe River basin (HRB) in China. The ABCD model is one of the most widely-used conceptual models to estimate soil water storage in a catchment. The simplicity of this conceptual model, developed by Thomas (1981), and its limited data requirement made it one of the most widely used models in hydrological studies (e.g. (Martinez and Gupta, 2010; Du et al., 2016; Wang and Zhou, 2016; Chen et al., 2020; Li, Huang et al. 2020; Wang et al., 2020)).

2.2 The ABCD model

The model uses precipitation and potential evapotranspiration as an input and provides actual evapotranspiration, streamflow and soil and groundwater storage. There are four parameters in the model (i.e., a, b, c, and d) to be defined and calibrated prior to simulation (Du et al. 2016). In this model, initial soil water storage (S_{i-1}) and precipitation in a month (P_i) are defined as available water. Equation (2.8) describes the correlation between available water (W_i) and evapotranspiration opportunity (Y_i). The parameter of evapotranspiration opportunity (Y_i) is a combination of soil water storage at the end of the month (S_i) and actual evapotranspiration (E_i) (Du et al., 2016; Wang and Zhou, 2016; Wang et al., 2020):

$$Y_i(W_i) = \frac{W_i+b}{2a} - \sqrt{\left(\frac{W_i+b}{2a}\right)^2 - \frac{W_i b}{a}} \quad (2.8)$$

The groundwater discharge (base flow) is calculated as:

$$G_i - G_{i-1} = cR_i - dG_i \quad (2.9)$$

where G_{i-1} and G_i are initial and end of the month groundwater storage. The monthly streamflow (Q_i) from direct runoff (R_i) and groundwater discharge is estimated as:

$$Q_i = (1-c)R_i - dG_i \quad (2.10)$$

Soil water storage at the end of the month can be derived as:

$$S_i = Y_i \exp(-E_{0i}/b) \quad (2.11)$$

Therefore, actual evapotranspiration of the month (E_i) can be obtained by deducting S_i from evapotranspiration opportunity (Y_i).

Using ABCD model, Wang and Zhou (2016) showed that water storage change in monthly scale is significant and if ignored, results in inaccurate streamflow estimation.

While most of the previous studies explain the significance of soil water storage in the Budyko models, the importance of groundwater-dependent evapotranspiration is almost ignored (Wang and Zhou, 2016). To study the importance of groundwater change in a surface water balance, Wang and Zhou (2016) extended the ABCD model to estimate groundwater-dependent evapotranspiration. It is believed that shallow groundwater areas in the catchment can actively be involved in evapotranspiration process. The new ABCD-GE model uses monthly precipitation and potential evapotranspiration as inputs and estimates effective groundwater change and soil water storage change, simultaneously (Wang and Zhou, 2016).

2.2.1 ABCD-GE model

As suggested by Wang et al (2016), two parameters, "i.e., G and E" are added to ABCD model to estimate the possible groundwater-dependent evapotranspiration based on the depth of water table. ABCD-GE, has 6 parameters (i.e., *a*, *b*, *c*, *d*, *g* and *k*) to be defined and calibrated prior to simulation where *a* is a dimensionless parameter, *b* is the upper limit of available water, *c* and *k* are groundwater recharge and groundwater recharge rate and *d* is groundwater discharge coefficients and *g* is responsible for groundwater dependent evapotranspiration (Wang and Zhou 2016). The study area is divided into two zones, zone-1 or deep groundwater and Zone-2 or shallow groundwater. In ABCD-GE model, actual evapotranspiration from zone-1(E_{1i}) is as described in section 2.2. E_2 is effective groundwater dependent evapotranspiration from zone-2 and is calculated as:

$$E_{2i} = gG_iE_{0i} \tag{2.12}$$

The parameter G_i is derived as:

$$G_i - G_{i-1} = (1-\alpha)kV_i + \alpha(cP_i - E2_i) - dG_i \tag{2.13}$$

where α is the ratio of area of zone-2 to the whole catchment area; V_i is value of storage in the transition vadose zone and is estimates using equation (2.14):

$$V_i - V_{i-1} = cR_i - kV_i \tag{2.14}$$

where V_{i-1} is the value of initial storage in the month. Hence, the total streamflow is estimated as:

$$Q_i = (1-\alpha)(1-c)R_i + \alpha(1-c)P_i + dG_i \quad (2.15)$$

By adding monthly E_2 and E_1, the total evapotranspiration of a catchment is:

$$E_i = (1-\alpha)E_{1i} + \alpha E_{2i} \quad (2.16)$$

The catchment is divided into two zones, based on the accessibility to water table for evapotranspiration. In many cases, groundwater depth of 2m is the limit beyond which groundwater dependent evapotranspiration is assumed to be zero (Yin et al., 2015; Wang and Zhou, 2016). For the Harvey catchment, this limit is 3m based on a study conducted by Antao (Michelle, 2015). Accordingly, the value of α is calculated as the ratio of shallow groundwater area (i.e., area with groundwater depth less than 3m) to the whole catchment area. Monthly groundwater level data for each grid point of the catchment is calculated using Rkriging method, adopted from Chapter 7. Therefore instead of calibrating and choosing one value for α for the whole study period, the monthly α (α_i) is used.

2.3 The ARIMA model

To develop the Budyko models some simplification assumptions should be made (e.g., assuming constant catchment characteristic parameter or ignoring spatial distribution of climatological stations) (Shahid et al., 2018). Therefore, Fathi et al (2019) suggested to employ the capabilities of streamflow time-series and improve the model's accuracy for monthly scale. They combined the Budyko-Du model with the statistical ARIMA model (Auto Regressive Integrated Moving Average) in view of taking advantage of the streamflow time-series (Fathi et al., 2019).

The ARIMA model is a common traditional approach for time-series analysis which assumes the trend in the observed time-series continues from the past to the future. It learns from the errors between the estimated streamflow and observed values to improve performance of the model (Raman et al., 2018). The ARIMA model was first developed by Box and Jenkins (1970) for time series analysis (Fathi et al., 2019). The model estimates parameters based on two main factors of prior information in the time series (*AR*) and the errors from previous predictions (*MA*). These factors makes ARIMA model more robust confronting rapid changes, and capable of producing more accurate estimation. When ARIMA is extended to include

independent regressors (exogenous variables), the model is called ARIMAX. The exogenous variables are the influencing external factors, although it increases the complexity of the model, it also increases the accuracy of estimation (Andrews et al., 2013).

2.3.1 SARIMAX model

As most of the hydrological parameters in this study have significant seasonal variation, SARIMAX model is used for this study. SARIMAX or seasonal auto-regressive integrated moving average is the seasonal version of ARIMAX which considers seasonality of the parameters and regressors (Raman, Mohanty et al. 2018).

The SARIMAX model usually is shown as ARIMA (p, d, q)(P, D, Q)s. where *p, d* and *q* are orders of auto regression (*AR*), differencing (*I*) and moving average (*MA*), respectively; and *P, D* and *Q* are orders of seasonal *AR*, seasonal differencing and seasonal MA, respectively; and seasonality is shown with s. The model can be written as equation (2.17) using *B* as the back shift operator ($BY_t = Y_{t-1}$) (Andrews et al., 2013, Raman et al., 2018; Fathi et al., 2019).

$$\emptyset_p(B)\Phi_P(B^s)(1-B)^d(1-B^s)^D Y_t = \mathrm{c} + X_t\beta + \theta_q(B)\Theta_Q(B^s)\varepsilon_t \qquad (2.17)$$

where ε_t is random error with zero mean and constant variance X_t is the input (independent) time-series and Y_t is the dependent time-series at time t. The terms $\emptyset$ and Φ are autoregressive and seasonal autoregressive coefficients, θ and Θ are the moving averages and seasonal moving averages coefficients, respectively, β is the regression coefficients and *c* is a constant parameter.

The proposed Budyko-ARIMA model by Fathi et al (2019), using the time-series' capabilities and considering interconnection between precipitation and potential evapotranspiration from previous months, was able to, accurately, estimate the monthly streamflow variation in the catchment. Their results suggested ignoring ΔS in monthly scale, introduces errors into the streamflow estimation (Fathi et al., 2019).

In the view of above and considering Table 2.1, this study is carried out following two approaches (i.e., Long-term and short-term), examining water balance of the several catchments with various physical and hydrological characteristics using the Budyko conceptual model as the main model. The Budyko model is modified to be applicable for the non-steady condition with concentrating on the importance of the groundwater change in the case studies. Finally the statistical model is couple with the modified Budyko model to

increase its performance for short-term studies. The results are cross validated with other models including conceptual, hydrological, statistical models and remote sensing technique.

To carry out the study for the long-term period, some assumptions should be made. Similar to literature (e.g., Zeng et al., 2014; Zhang et al., 2016; Wu et al., 2017), it is assumed that no human activity is involved in the streamflow variation during the pre-change period. In other words, the human activities in the pre-change period are considered negligible and the hydrological processes are assumed to be natural. It is also assumed that climate change and human activities are two independent variables, while in reality they are tied together and can amplify or amend each other (Kim et al., 2013; Dey and Mishra, 2017). In this study, the climate change is defined as a combination of variability in the climate parameters, as well as global-scale human-induced effects that cause a worldwide greenhouse gas emission. Human activities, on the other hand, are defined as the regional impacts of human considering the fact that dam construction and land use change, including urbanization and agricultural activities, etc., are intimately embedded in the human impact.

Table 2.1 Pros and Cons of the proposed models and their combinations in estimating streamflow change

Model	**Pros**	**Cons**
Budyko	User friendly Low data requirement Suitable for long-term studies	Not suitable for short-term studies
ABCD	User friendly Low data requirement Suitable for long-term studies	Not suitable for short-term studies
HBV	Suitable for short-term and long-term studies Competent approach for different climate characteristics Freely available	Relatively complicated Relatively higher data requirement Might suffer from uncertainty
Budyko-Du	User friendly Low data requirement Suitable for short-term and long-term studies	Might suffer from oversimplification
ABCD-GE	User friendly Low data requirement Suitable for short-term and long-term studies	Might suffer from oversimplification
Hybrid conceptual statistical	User friendly Low data requirement Suitable for short-term and long-term studies Using time-series capabilities to perform with higher accuracy	Relatively complicated comparing to other conceptual models

Chapter 3

Methodology and study area

In view of the literature, this study investigates application of conceptual models and most specifically the Budyko model to assess water balance of hydrological systems in catchment scale. Several catchments with different climatic conditions and biophysical characteristics are used to study the water resources change and most specifically, streamflow variation in long-term and short-term scales. Figure 3.1 presents the flowchart of the implemented methodology.

For the long-term study, the Budyko model is used to track the streamflow variation during the last decades and determine the role of climate change and regional human activities on these changes. The results are compared with a widely used hydrological model (the HBV model). In this phase of the study, the competency of the Budyko model to predict streamflow under future climate change scenarios is also compared with the HBV modelling. Then the remote sensing technique is integrated to qualitatively validate the competency of the Budyko modelling.

For the short-term phase of the study, applications of the Budyko type models are compared with other widely used conceptual models (i.e., ABCD type models). In this step, the importance of groundwater change and soil water storage change are investigated. Later, the models are coupled with the statistical component, developing a hybrid conceptual-statistical model to increase the accuracy of the assessment.

Figure 3.1 presents the activities implemented in the study and the integration of the approach.

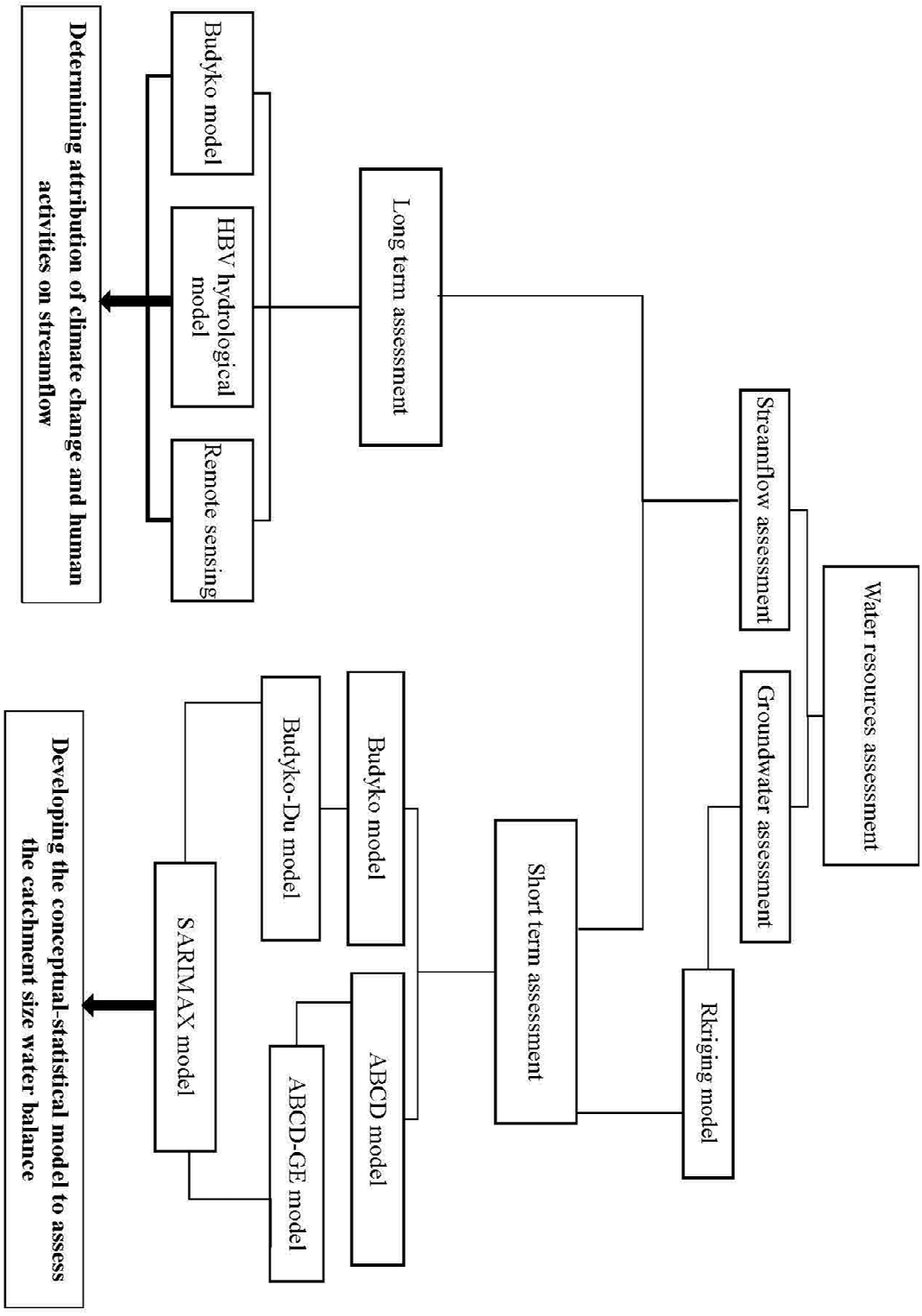

Fig.3.1 Flowchart of the implemented methodology

3.1 Study areas

The Budyko based water balance approach has been successfully applied for five different catchments to represent different climatological regions and different hydro-environments. Five selected catchments, including four catchments in Australia and one in Iran, representing a range of climatic conditions and biophysical characteristics (e.g., latitude, longitude, elevation, land use type and soil type) are selected for this study.

Two of these catchments are associated with Harvey River (i.e., at Dingo Road station and Forrest station) are located in Western Australia. Beardy catchment and Goulburn catchment are in New South Wales as shown in Fig.3.2 and the Karkheh basin is located in Western Iran.

3.1.1 The Australian catchments:

Beardy and Harvey Rivers basins support biodiversity of environmental and ecological communities. Harvey and Goulburn Rivers represent the main tributaries of the surface water supply system in their catchments. Hence, assessing the impacts of future climate changes and human activities on the hydrological system of these rivers is a significant task to draw efficient and sustainable water management strategies in their contributing catchments.

Figure 3.2 shows the locations of the catchments and associated weather and streamflow stations.

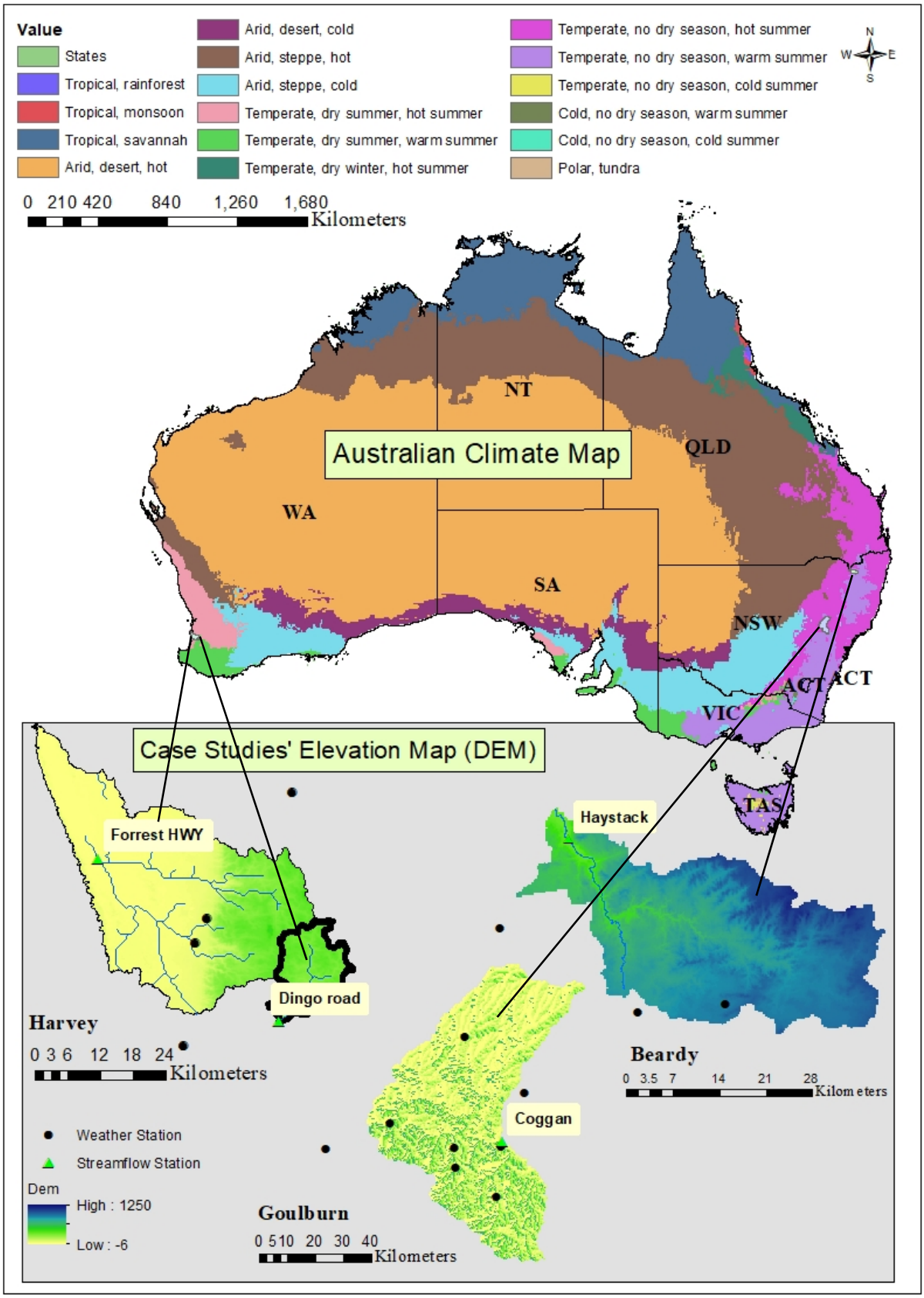

Fig.3.2 Australian climate map and the Australian case studies' DEM

Harvey catchment

Harvey is one of the fastest developing areas in Western Australia. Rapid urbanisation is also taking place, especially in areas close to the ocean and estuaries, which accordingly has led to an extensive change in land cover of the catchment (Belinda and Shakya, 2011).

Although the Harvey River Basin supports the biodiversity of unique environmental and ecological communities, few studies concerning potential hydrological responses of the catchment to human activities and future climate change exist.

The main Peel Harvey catchment (including the Harvey River Catchment at Dingo road (hereafter called Harvey-Dingo) and Harvey catchment at Forrest station (hereafter called Harvey-Forrest) is located 130 km south of Perth, Western Australia, between latitudes 32.55º-33.05ºS and longitudes 116.02º-116.26ºE.

The catchment has a temperate climate with a summer season tend to be hot-dry, the average daily minimum and maximum temperature fluctuates between 18°C–28°C and sometimes reaches 40°C and a winter season tends to be cool-wet, with an average daily minimum and maximum temperature range between 10°C and 18°C (Peel-Harvey Catchment Council, 2012). The period between April and October nearly holds 90% of the total annual rainwater with an approximate annual mean rainfall of 900 mm (Peel- Harvey Catchment Council report, 2012). The annual mean potential evaporation (*E*) across the catchment is normally going above the annual mean precipitation and it approximately reaches 1,460 mm (Australian Bureau of Meteorology, 2018). Harvey River drains directly to the Peel-Harvey estuary. The Peel-Harvey estuarine system has a considerable ecological, recreational, commercial and scientific importance in south Western Australia. Its fringing environment comprises ecologically important wetlands and lakes that have been placed on the list of wetlands of international importance (Environmental Protection Authority, 2008). The estuary is an internationally important habitat for waterbirds and migratory wading birds, in which tens of thousands of waterbirds gather annually with more than 80 species (Environmental Protection Authority, 2008). The depth of the Peel-Harvey estuarine system is relatively shallow (up to 2 m for the deepest point) and more than 50% of its area has a depth of only 0.5 m (Kelsey et al., 2010).

Beardy catchment

Beardy River, which is an important perennial river that is part of the Murray–Darling basin, is located in the New England region of New South Wales, Australia. The Murray–Darling basin is a large geographical area in the interior of south-eastern Australia. The basin, which drains around one-seventh of the Australian land mass, is one of the most significant agricultural areas in Australia (Pigram, 2007).

Beardy catchment is located in the far northeastern part of New South Wales with the latitude of 29.11° to 29.30°S and longitude of 151.18° to 151.50° E and area of 908 km^2. The actual vegetation cover of the catchment is mainly evergreen broadleaf forest, shrublands, woody savannas, croplands and natural vegetation mosaic (USGS, 2011). The climate of the catchment is temperate with a relatively warm dry summer, the temperature approximately ranges between 27°C–30°C and cool moderate winter, and temperature nearly ranges between 19°C–20°C (Commonwealth Scientific and Industrial Research Organisation and Australian Bureau of Meteorology, 2007). The rainfall distribution over the catchment is extremely seasonal in which the summer season holds the maximum rainwater volumes due to the activity of summer storm, while the other seasons of the year hold the minimum amounts of rainfall. The average monthly summer precipitation is around 100 mm and it decreases to 40–50 mm during the period between April and September (Green et al., 2012). The annual mean potential evaporation in the catchment is higher than the annual mean precipitation with a spatial variation over the catchment ranged between 1,200 and 2,000 mm (Green et al., 2012).

Goulburn catchment

The Goulburn catchment extends over 3,402 km^2 area (Bureau of Meteorology, 2017) (the majority are national parks, forest and wasteland areas). It forms the whole western part of the Hunter River catchment (the largest coastal catchment in NSW). The Goulburn River is a major branch of the Hunter River which drains around 50% of the Hunter catchment and donates nearly quarter of the mean Hunter River flow (NSW Department of Infrastructure, Planning and Natural Resources, 2002). The Goulburn River catchment stretches from 31°48` to 32°51` Southern latitude and from 149°40` to 150°36` Eastern longitude. The climate of the catchment is sub-humid to temperate and varies with elevation and ocean proximity (Krogh et al., 2013). As the Goulburn River catchment is relatively located far away from the ocean, it receives the lowest annual rainfall (around 620 mm) compared to the eastern part of the Hunter catchment which receives around 1,600 mm. The rainfall in the catchment is

seasonally distributed in which the summer is the wettest season in the year (December to February) and the annual potential evaporation normally exceeds the annual rainfall to reach more than 1,300 mm and it varies with temperature variations (Krogh et al., 2013). Figure 3.3 shows statistical characteristics of mean monthly precipitation in the study areas, such as the first and third quartiles, and mean maximum and minimum precipitation.

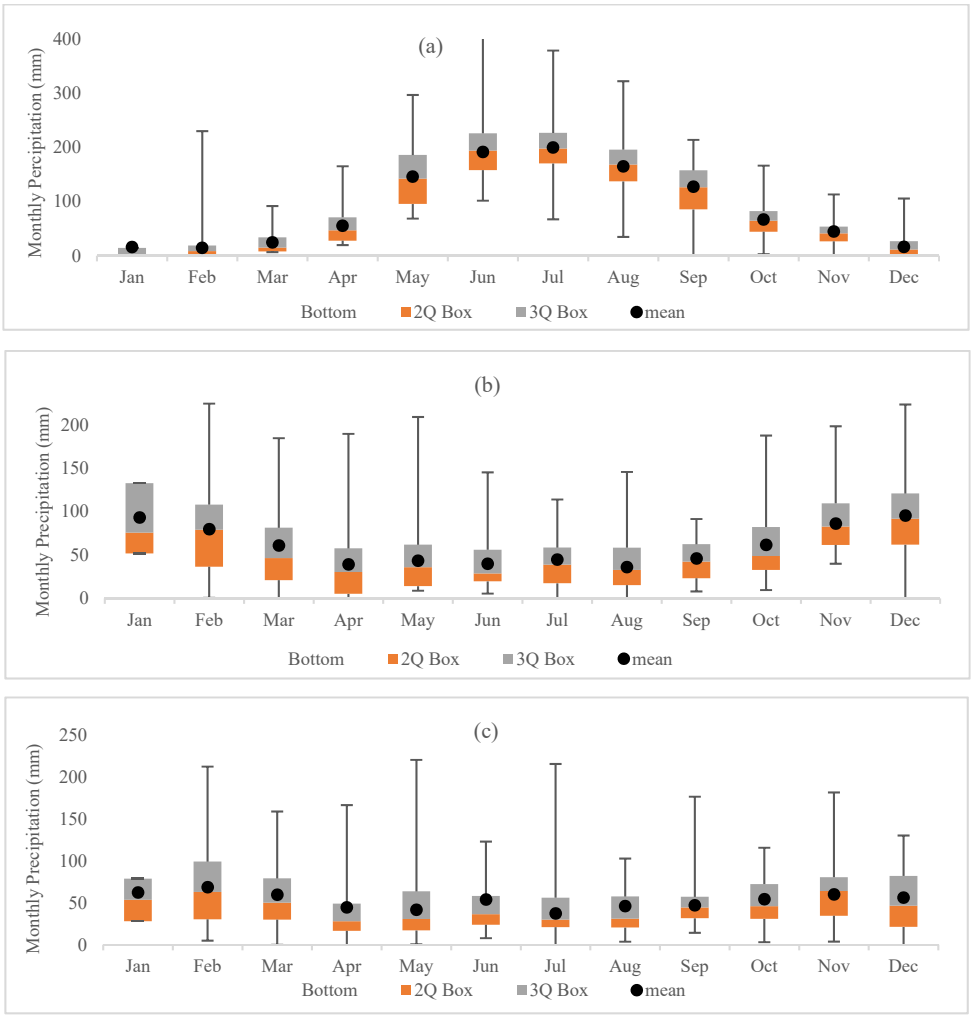

Fig.3.3 Statistical characteristics of mean monthly precipitation (mm) in the study areas: a) Harvey, b) Beardy and c) Goulburn catchments

3.1.2 The Karkheh Basin (the KRB)

The Karkheh River Basin (the KRB), with an area of 43,000 km^2 stretching over seven provinces and 32 districts, is located in the western part of Iran between 30° and 35° N latitude and 46° and 49° E longitude (Fig. 3.4). Five major rivers flow through the KRB, and the basin is divided into five main sub-basins named Gamasiab, Qarasou, Kashkan, Seimareh, and Upper Karkheh (Ahmad and Giordano, 2010). The basin is a primary source of wheat production in Iran and encompasses 9% of the total irrigated area of the country (Muthuwatta et al., 2010). It plays a key role in food production in Iran, hence, any hydrological changes in the basin directly affect the livelihoods of farmers as well as urban consumers at both the basin and country levels. Figure 3.4 illustrates the location of the KRB in Iran and the location of the climatology stations in each sub-basin. The Upper Karkheh sub-basin is located upstream of the Karkheh dam. The flow that reaches the Upper Karkheh outlet is drained from the entire study area.

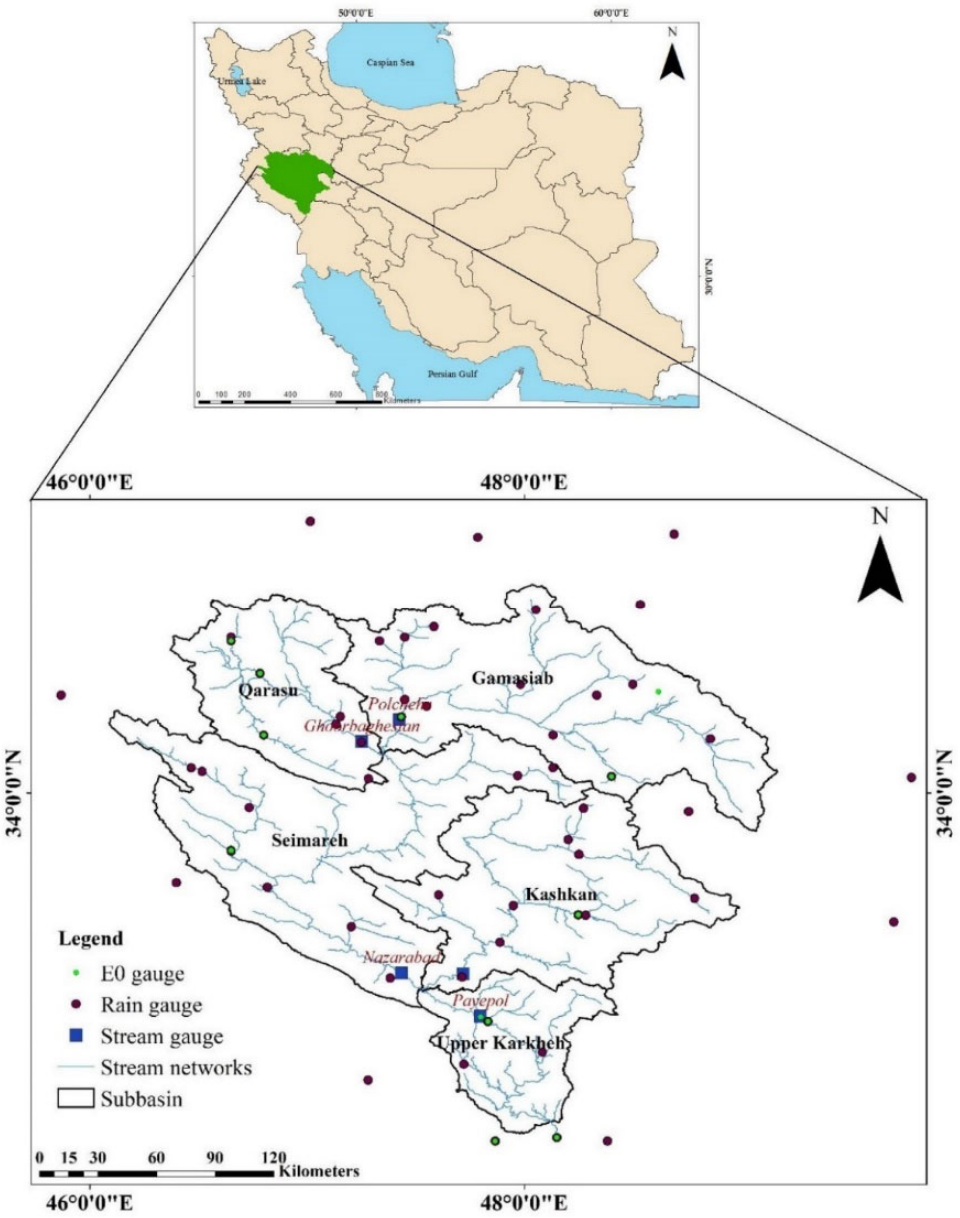

Fig.3.4 Location of the Karkheh River Basin in Iran and the associated sub-catchments.

The KRB is relatively populated, accommodating 5% of Iran's population, which makes it the third most populated basin in the country. It has 3.5 million residents, from which 40% live in urban areas. Figure 3.5, shows the rural and urban population of each studied sub-basin. It should be noted that there is no official population record based on the catchment division, and values are approximated based on the data of the smallest available countrywide division. The population is mostly concentrated in Qarasou sub-basin, which occupies 17% of the KRB area and houses 30% of the population. The southern parts of the KRB basin, with almost 11%

of the area, are home to 5% of the population (JAMAB consulting, 1999; JAMAB consulting, 2006; Marjanizadeh et al., 2010).

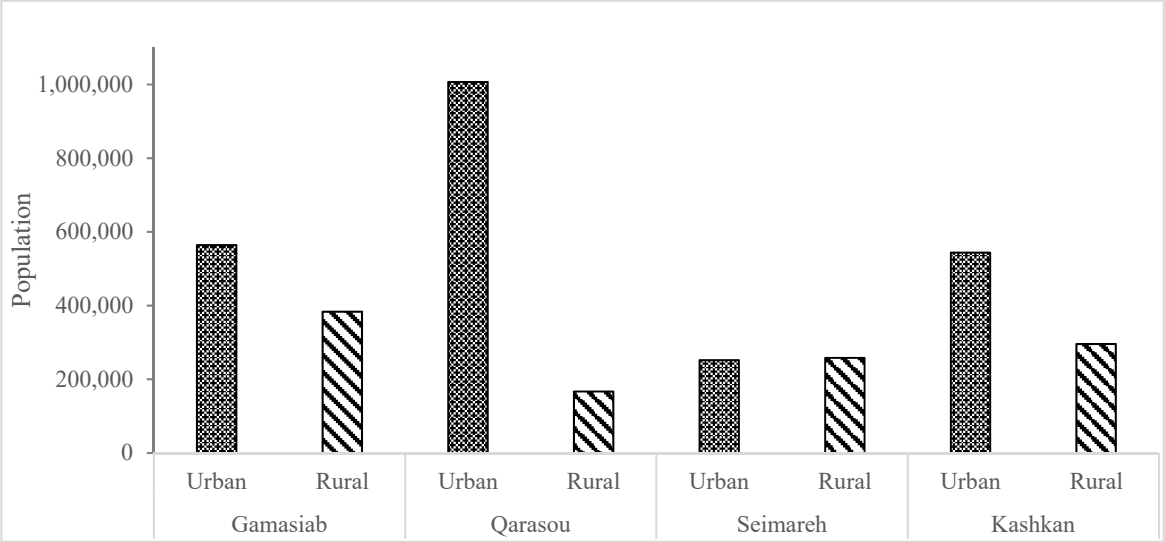

Fig.3.5 Approximated population distribution in the KRB based on the 2015 national record

The altitude of the basin varies from less than 10 m in the south to more than 3,500 m above mean sea level in the north. Mean annual precipitation ranges from 150 mm in the south to 750 mm in the northern region (see Table 3.1). The maximum summer temperature varies between 35 and 45°C across the basin. Range and pasture, rainfed agriculture, forest, irrigated agriculture, and urban area are the dominant land uses (Muthuwatta et al., 2010).

Table 3.1 Karkheh sub-basins' physical and climate characteristics

Sub-basin	Area (km^2)	Mean altitude (m amsl)	Mean precipitation (mm/year)	Mean streamflow (mm/year)
Qarasou	5,508	1,559	424	111
Gamasiab	11,512	1,856	461	81
Kashkan	9,524	1,611	477	158
Seimareh	12,350	1,179	412	97
Upper Karkheh	3,995	795	422	114

In the basin, spring water is, traditionally, used for irrigation, however, due to the frequent droughts and subsequent surface water scarcity, the pumping of groundwater and river water diversions have become widespread in recent decades. The competition between irrigated agriculture and the wetland ecosystems over water has led to a low water productivity,

increasing salinity, and reduced surface water availability in the lower parts of the basin (Muthuwatta et al., 2010).

During the twentieth century, the KRB remained mainly unregulated. The first dam constructed in the area was the Karkheh dam, which was completed in 2001 and was the first large multipurpose dam in Iran, with a total storage of 5,600 MCM (Table 3.2). Its reservoir is designed to irrigate 320,000 ha of agricultural land in the Upper Karkheh basin. The Seimareh dam was built in 2013 and there are a few smaller reservoirs under operation with several other small scale dams and irrigation schemes either under construction or under planning, all of which could impose extra burden on the streamflow of the study area (Muthuwatta et al., 2010).

Table 3.2 Locations and characteristics of major dams in the KRB

Name	Longitude ºE	Latitude ºN	Storage-normal level (BCM)	Purpose	Operation date
Karkheh	48.1506	32.4208	5.6	Irrigation, hydropower generation, flood control	2001
Seimareh	47.1908	33.3183	2.8	hydropower generation	2013

3.2 Data

3.2.1 The Australian catchments

The climate data, including daily rainfall were collected from the SILO Data Drill (Scientific Information for Land Owners). SILO Data Drill was also used to provide daily potential evapotranspiration using Morton's equation. High-quality streamflow data with missing data less than 5% were obtained from the Bureau of Meteorology (Hardwinarto and Aipassa, 2015; Teng et al., 2012; Vaze and Teng, 2011).

Future temperature and rainfall data were derived from a multi-model ensemble of eight-GCMs of the CMIP5. A Statistical Downscaling Model developed by the Australian Bureau of Meteorology (BoM) was applied to downscale the data, with spatial and temporal resolutions of the 5x5 km (approximately $0.05^{o} \times 0.05^{o}$) and 24 hours, respectively (Timbal and Jones, 2008).

The monthly groundwater data were collected from the Bureau of Meteorology (BOM) of Australia's website (Australian Bureau of Meteorology (BoM), 2020), from monitoring wells for the period of 1982 to 2017, where the reference point is the mean sea level.

3.2.2 The Karkheh Basin

Daily precipitation data for the study period were acquired from a well-distributed gauge network across the basin. The Thiessen method was used to determine the weight of each station for the total precipitation of the sub-basins.

The potential evapotranspiration (E_0) stations are not spatially representative of the basin, though these stations (hereafter called reference stations) have a sufficiently long period of recorded temperature and E_0. The temperature stations, however, are relatively well-distributed in the basin and provided a long period of recorded temperature, but no E_0 data. To extend the E_0 estimation throughout the basin, the temperature stations were classified based on their altitude and their distance from the reference stations (Lambert and Chitrakar, 1989). Accordingly, for each year, a monthly relationship between observed E_0 and temperature in the reference stations was developed to calculate E_0 at the temperature stations of the same altitude class. For instance, in 1995, for the Polchehr reference station (Fig. 3.4), there is a high correlation between monthly E_0 and monthly mean temperature, T ($R^2 = 0.95$) (see Fig. 3.6):

$$E_{0(P)} = 15.103 \, . \, T_{(P)} - 20.929 \qquad (3.1)$$

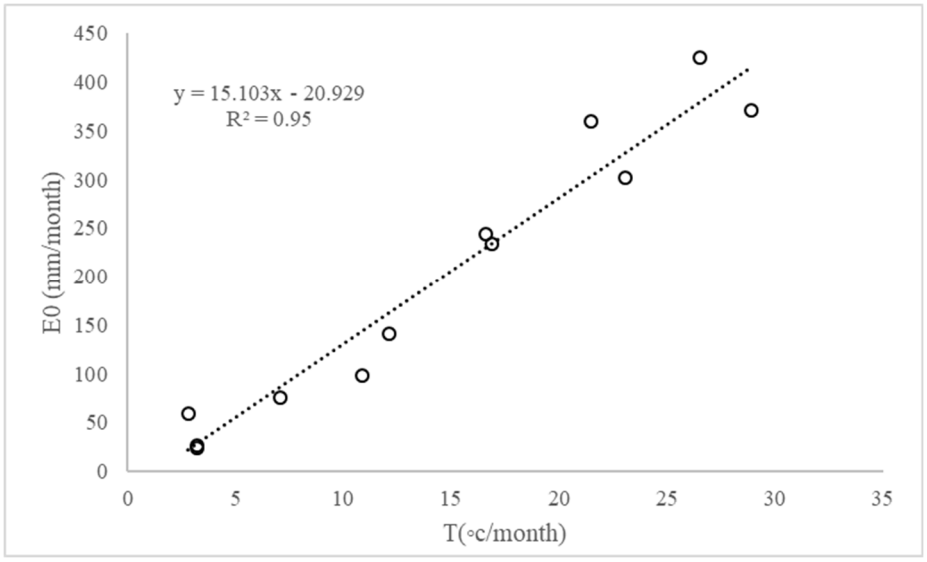

Fig.3.6 The goodness of fit between monthly evapotranspiration (E_0) and average temperature (T) for the Polchehr reference station in the KRB, 1995

where T is temperature. Given that the Kermanshah temperature station is located at the same altitude and has a significant correlation with Polchehr station (i.e. 0.94), $T_{Kermanshah}$ was substituted in Eq. (3.1) to estimate E_0 for the Kermanshah station.

Similarly, for each year of the study period and each temperature station, a relationship was derived to provide spatially distributed E_0 data throughout the basin. Table 3.3 shows the temperature stations that are correlated with the E_0 reference stations.

Table 3.3 E_0 reference stations in the KRB and the associated temperature stations

Reference E_0 station	Altitude (m)	Temperature station	Altittude (m)
Chamanjir	1140	Khorramabad	1147
		Koohdasht	1190
Dasht Abbas	161	Dehloran	232
Abdolkhan	40		
Hamidieh	22		
Chamgaz	350	Darreshahr	670
Doab	1310		
Varayeneh	1760	Hamedan	1741
		Borujerd	1630
Kheirabad	1763	Malayer	1778
		Eyvan	1200
		Kangavar	1468
		Nahavand	1680
Ravansar	1388	Kamyaran	1404
Mahidasht	1360	Eslamabad	1349
Holeilan	950	Ilam	1340
Dartoot	703		
Polchehr	1280	Kermanshah	1306

Regarding streamflow data, five discharge stations located at the outlet of the sub-basins, namely Polchehr at Gamasiab River, Ghoorbaghestan at Qarasou River, Poldokhtar at Kashkan River, Nazarabad at Seimareh River, and Payepol at Upper Karkheh River, were selected considering their locations, period of records, and quality of data (Fig.3.4 and Table 3.4). The Payepol station is located downstream of the Karkheh dam and receives a cumulative discharge from the upstream sub-basins. Thus, it can provide useful information about the impact of the reservoir on the main river flow.

Table 3.4 The KRB streamflow stations, their locations, recorded length and streamflow characteristics

Sub-basin	Station	Long. ºE	Lat. ºN	Elev. (m)	Record length	Annual P (mm)	Mean streamflow (mm/year)	Streamflow Coefficient	Standard deviation (mm/year)
Qarasou	Ghoorbaghestan	47.25	34.23	1300	1975–2011	452	111	0.25	49.0
Gamasiab	Polchehr	47.43	34.33	1306	1970–2011	429	81	0.19	38.9
Kashkan	Poldokhtar	47.72	33.17	650	1980–2011	512	158	0.31	63.2
Seimareh	Nazarabad	47.43	33.17	559	1979–2011	406	97	0.24	41.2
Upper Karkheh	Payepol	48.15	32.42	90	1974–2011	422	114	0.27	49.2

To calculate the equivalent depth of streamflow of each sub-basin in millimetres, the mean annual flow at the discharge station was divided by the area of the sub-basin. However, as the Seimareh sub-basin receives a part of its streamflow from the two upper sub-basins, i.e., Qarasou and Gamasiab, the mean annual flow was divided by the summation of the three sub-basins. Likewise, for the Upper Karkheh sub-basin, which receives water from the upper sub-basins (Masih et al., 2011), the entire drainage area was considered while calculating the mean annual flow.

3.3 Criteria

Several criteria and commonly used mathematical equations have been employed to assess the competency, fitness and applicability of the models.

3.3.1 Stationarity

Augmented Dickey-Fuller (ADF) test is used to check the stationarity of the streamflow times-series. The ADF which is a unit root test, is one of the main test for stationarity of a time-series. It checks the null hypothesis that α is equal to one in Eq. (3.2).

$$Y_t = \alpha Y_{t-1} + \varepsilon_t \quad (3.2)$$

Where Y is the data, α is coefficient of the first lag on Y and ε_t is white noise. If the value of α is 1, a unit root exists in the time-series (Y_t) and accordingly (Y_t) is not stationary. In this

test, since the null hypothesis is based on (α=1), to reject the null hypothesis, the P-value should be less than the significance level (in this study = 0.05) (Wang et al., 2005, Prabhakaran, 2020).

3.3.2 Correlation and White noise tests

To make sure the time-series are uncorrelated ACF (Auto Correlation Function) and PACF (Partial Auto Correlation Function) plots are used. To check if the time-series follow the white noise, the Ljung-Box (Q statistics) test is employed (Raman et al., 2018, Fathi, et al., 2019) as:

$$Q = T\,(T+2)\sum_{k=1}^{m}[r_k^2/(T-k)] \qquad (3.3)$$

where T is the sample size, rk is the autocorrelation of lag k of the residuals and m is the number of residual autocorrelations. If the P-value (the probability values) is less than 5%, it rejects the null hypothesis that the time-series follows a white noise.

3.3.3 Choosing the fittest model

The Akaike Information Criterion (AIC) is used to select the fittest SARIMAX model. AIC is an estimator of out-of-sample prediction error and employs the maximum likelihood of the model to measure its fitness. Since, model with the maximum likelihood fits the time-series the best, the model with the least AIC value performs the best (Eq. (3.4)).

$$AIC = -2 \times Ln(L) + 2 \times k \qquad (3.4)$$

where L is the value of the likelihood and k is the number of estimated parameters (Mohammed et al., 2015, Zajic, 2019).

3.3.4 Performance of the fittest model

To check the efficiency of the models estimated monthly and annual streamflow are compared with observed values. The model assessment criteria (coefficient of determination (R^2), Volume Ratio (VR) and Kling-Gupta efficiency (KGE)) are used to show the models' performances (Eqs. (3.4, 3.5 and 3.7)) (Kazemi et al., 2019).

$$R^2 = \frac{\sum(obs-\overline{obs})^2 - \sum(sim-obs)^2}{\sum(obs-\overline{obs})^2} \quad (3.51)$$

$$VR = \frac{\sum sim}{\sum obs} \quad (3.6)$$

$$KGE = 1 - \sqrt{(r-1)^2 + (\alpha-1)^2 + (\beta-1)^2} \quad (3.7)$$

Where r is linear correlation, α is standard deviation and β is bias between observed (*obs*) and simulated values (*sim*) (Gupta et al., 2009; Santos et al., 2018, Knoben et al., 2019).

Approach 1:

Long-term streamflow analysis

Chapter 4
Evaluation of Streamflow Changes due to Climate Variation and Human activities using the Budyko model

4.1 Background and method

The Budyko method is employed to precisely assign the influences of human-activities and climate-change on the runoff variations. The case studies are the three unregulated catchments of the Australian-Hydrologic-Reference-Stations (HRSs) namely Harvey- Dingo catchment in Western-Australia and Beardy and Goulburn catchments in New-South-Wales (Al-Safi et al., 2020). These catchments have experienced significant streamflow reduction during the last decades due to climate change and human activates.

4.1.1 Change detection

The total change in streamflow (ΔQ) can be assumed as a result of streamflow changes due to climate change (ΔQ_c) and human activities (ΔQ_h) (Li et al., 2012; Ye et al., 2013; Liang et al., 2015; Al-Safi et al., 2019; Kazemi et al., 2019).

$$\Delta Q = \Delta Q_c + \Delta Q_h \quad (4.1)$$

In order to determine climate change and human activities influences on streamflow change, the first step is to find the breakpoint/s in the temporal trend of streamflow during the period of study (Dey & Mishra, 2017; Xu et al., 2014). To determine the breakpoint in a time-series, the Mann- Kendall statistic (MK) test is used which is one of the most popular methods to define the breakpoint in a trend (Ashofteh et al. 2016; Fan et al. 2017; Li et al. 2012; Liu et al. 2017). The detected breakpoint divides the streamflow time-series into a pre- and post-change period. In the pre-change period, also called the natural period, it is assumed that human's impacts on the streamflow was not considerable. For the period after the breakpoint, the post-change period, both climate change and human activities are considered to affect the streamflow (Fan et al., 2010; Zeng et al., 2014; Zhang et al., 2016; Dey and Mishra, 2017; Wu et al., 2017).

4.1.2 The Budyko model

As mentioned in Chapter 2, the Budyko model assumes the water storage change is negligible on a long time scale. Hence, the water balance equation (Eq. (1.1)) can be written as Eq. (4.2) (Xu et al. 2013).

$$Q = P - E \quad (4.2)$$

Total variation of streamflow (ΔQ) is calculated using Eq. (4.3), where $\overline{Q_o}$ is average annual streamflow. Subscript 1 denotes the pre-change period and 2 represents the post-change periods.

$$\Delta Q = \overline{Q_{o2}} - \overline{Q_{o1}} \quad (4.3)$$

To define the influence of climate change and human activities on streamflow variation, Schaake (1990) proposed the Analytical Elasticity equation based on the Budyko model (Fu et al., 2007; Sankarasubramanian et al., 2001; Schaake 1990; Yang and Yang, 2011). In the Analytical Elasticity equation the sensitivity of streamflow change to the variation of P and E_0 is calculated (Liang et al. 2015; Wu et al. 2017; Yang and Yang 2011). In this method, streamflow variation induced by climate change can be addressed using Eq. (4.4) (Liang et al., 2015; Yang and Yang, 2011):

$$dQ_C = \frac{\partial f}{\partial P} dP + \frac{\partial f}{\partial E_0} dE0 \quad (4.4)$$

Taking to account the definition of elasticity ($\varepsilon_X = \frac{dQ/Q}{dX/X}$), Eq. (4.4) can be rewritten as (Liang et al., 2015; Yang and Yang, 2011):

$$\frac{dQ_C}{Q} = \varepsilon_P \frac{dP}{P} + \varepsilon_{E_0} \frac{dE_0}{E_0} \quad (4.5)$$

where ε_P and ε_{E_0} represent P elasticity and E_0 elasticity of Q, respectively. The values of ε_P and ε_{E_0} are calculated using Eq. (4.6 and 4.7), respectively.

$$\varepsilon_P = \left\{1 - 1/\left[1 + (\frac{P}{E_0})^n\right]^{1+1/n}\right\} / \left\{1 - 1/\left[1 + (\frac{P}{E_0})^n\right]^{1/n}\right\} \quad (4.6)$$

$$\varepsilon_{E_0} = -\frac{1}{\left[1+\left(\frac{E_0}{P}\right)^n\right]^{1+\frac{1}{n}}} \cdot \frac{1}{\frac{1}{E_0/P}\left[1+\left(\frac{E_0}{P}\right)^n\right]^{\frac{1}{n}}} \quad (4.7)$$

Consequently, changes in streamflow due to climate change can be calculated using Eq. (4.8); and Eq. (4.9) determines the impact of human activities on streamflow variation, as follow:

$$\Delta Q_c = \varepsilon_P \frac{\Delta P}{\bar{P}} \bar{Q} + \varepsilon_{E_0} \frac{\Delta E_0}{\bar{E_0}} \bar{Q} \quad (4.8)$$

$$\Delta Q_h = \Delta Q - \Delta Q_c \quad (4.9)$$

4.2 Defining the dominant factor affecting streamflow in the Australian catchments

4.2.1 Streamflow change

The Mann-Kendall test with a statistical significance of α=0.05 shows 1993 and 2000 are the changing years for Harvey and Beardy catchment, respectively. The period of study for these catchments is from 1971-2015. While at Goulburn catchment, for a period of (1951-2015), the year 1978 is the point in which changing of streamflow trend happened (Fig.4.1 and Table 4.1). These years are also stated as the breaking points by the Australian Bureau of Meteorology (Australian Bureau of Meteorology (BoM), 2018).

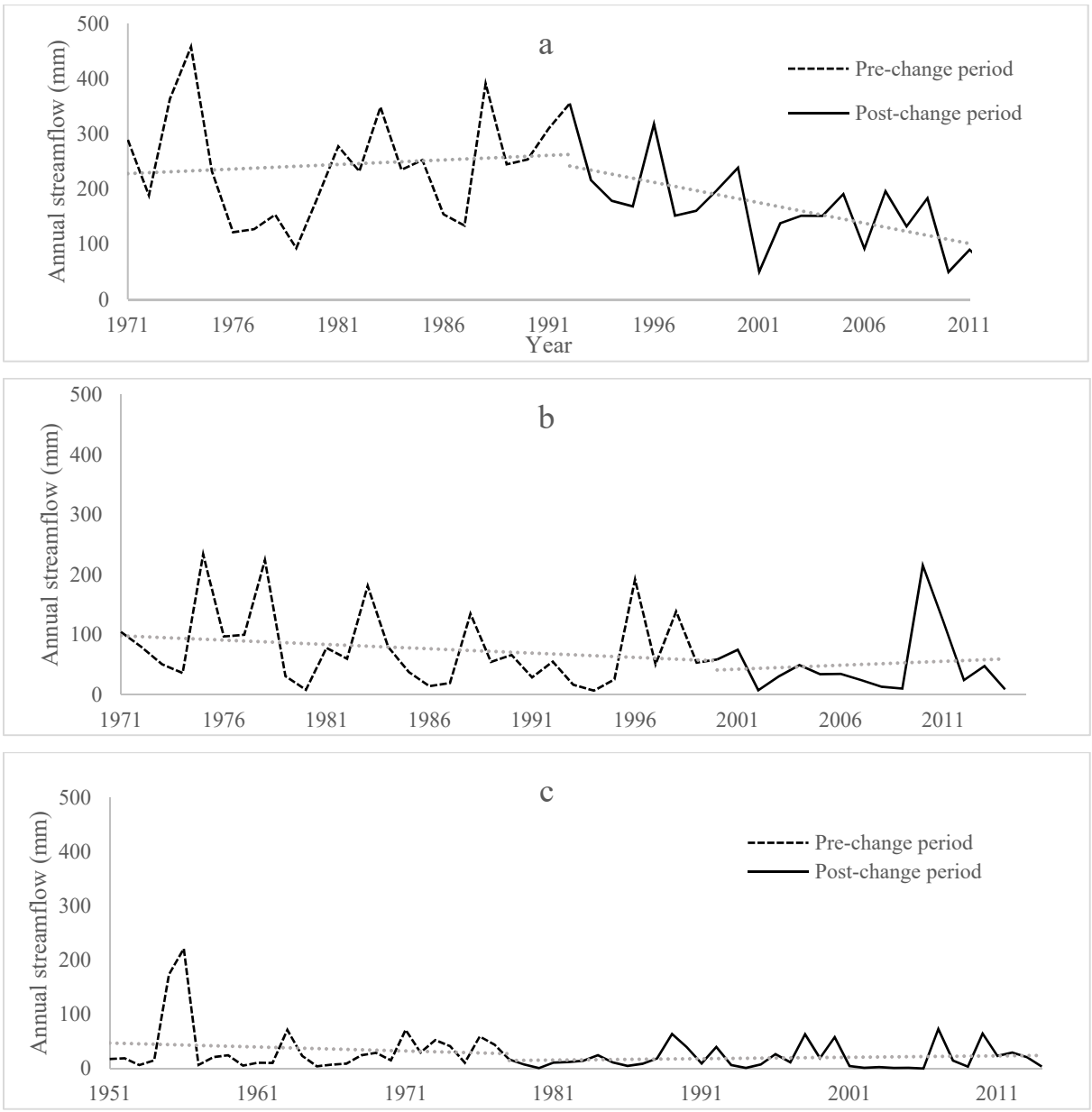

Fig.4.1 Annual streamflow variation and the breakpoint in the time series trends a) Harvey-Dingo Catchment, b) Beardy Catchment and c) Goulburn Catchment

Table 4.1 Climate parameters variation during the base period and the second period in the Australian catchments

	Variables	1971-1993 (mm)	1994-2015 (mm)	Changes (mm)	Rate of Change
Harvey-Dingo	Annual $\overline{Q}$	244	148	-96	-39%
	Annual $\bar{P}$	1124	1017	-107	-9.5%
	Annual $\overline{E_0}$	1758	1804	46	2.6%
	Variables	1971-2000 (mm)	2001-2015 (mm)	Changes (mm)	Rate of Change
Beardy	Annual $\overline{Q}$	77	50	-27	-35%
	Annual $\bar{P}$	740	700	-40	-5%
	Annual $\overline{E_0}$	1641	1668	27	2%
	Variables	1951-1978 (mm)	1979-2015 (mm)	Changes (mm)	Rate of Change
Goulburn	Annual $\overline{Q}$	41	20	-21	-51%
	Annual $\bar{P}$	723	615	-108	-15%
	Annual $\overline{E_0}$	1305	1298	-7	-0.5%

Based on Figure 4.1 and Table 4.1, the annual runoff in all catchments has experienced a significant reduction during the last decades (35 to almost 40%). The precipitation has also suffered a considerable decrease from the pre-change period to the post-change period, while the values for evapotranspiration did not experience a dramatic fluctuation.

Further analysis of the streamflow changes shows the significant difference between the minimum streamflow statistics (Q25), mean streamflow statistics (Q50) and maximum streamflow statistics (Q75) of the pre-change period comparing to the post-change period in all catchments (Table 4.2). The Q25s in all catchments have decreased by more than 33%, Q50s have almost reduced by 54% and Q75s have experienced a significant reduction between 36% -68%. For the Harvey catchment, the zero-flow frequency was 6%, which almost never happened in the first period. The values of zero frequency for Beardy catchment are 6% for the base period, which has increased to 14% of the days in the second period. Goulburn catchment did not experience days with the zero-flow frequency.

Table 4.2 Mean monthly streamflow statistics during the pre-change period and the post-change period in the Australian catchments

	Variables	1971-1993 (mm)	1994-2015 (mm)	Rate of Change
Harvey-Dingo	Q25	30	20	-33%
	Q50	12.36	5.63	-54%
	Q75	4.8	1.5	- 68%
	Variables	1971-2000 (mm)	2001-2015 (mm)	Rate of Change
Beardy	Q25	7.2	4.7	-34%
	Q50	1.3	0.7	-48%
	Q75	0.2	0.13	-36%
	Variables	1951-1978 (mm)	1979-2015 (mm)	Rate of Change
Goulburn	Q25	2	1.3	-35%
	Q50	0.83	0.4	-51%
	Q75	0.4	0.1	-68%

4.2.2 Determining attribution of climate change and human activities on the streamflow

The parameters of precipitation elasticity and evapotranspiration elasticity for each catchment are calculated by applying annual rainfall and annual potential evapotranspiration for the study period. The values of ε_p and ε_{E0} which suggest the streamflow variation sensitivity to precipitation and evapotranspiration are derived based on Eqs. (4.6 and 4.7). As presented in Table 4.3, the values of precipitation elasticity are higher comparing to the evapotranspiration elasticities', which means that the runoff change is more sensitive to rainfall than to E_0.

The impacts of Climate change and human activities mentioned in Table 4.3 are estimated using Eqs. (4.4 to 4.9). The results suggest that the main factor of streamflow reduction in each catchment is different. In Harvey catchment, the impacts of climate change and human involvement were not that much different although the climate change had a higher share in this reduction. Beardy catchment, on the other hand, was most affected by human activities. In the Goulburn catchment, human activities were responsible for only 30% of the decrease in streamflow. Considering the location of the Goulburn catchment, which has been less manipulated by human activities, suggests we should have expected such a result.

Table 4.3 Contribution of climate change and human activities on streamflow reduction in the case studies based on the Budyko model

Catchment	$\Delta Q(mm)$	ε_P	ε_{E0}	$\Delta Q_C\ (mm)$	$\Delta Q_h\ (mm)$	$\Delta Q_C\ (\%)$	$\Delta Q_h\ (\%)$
Harvey-Dingo	96	2.3	-1.3	52	44	55	45
Beardy	27	2.65	-1.65	12	15	44	56
Goulburn	21	3.73	-2.73	14.5	6.5	69	31

The results of the current study suggest that streamflow in the study areas has been significantly influenced by climate change and human activities due to land use and land cover change, water management projects and development and excess usage of groundwater which manipulate the water resources. At Harvey River catchment, the expected streamflow decline, measured at Dingo Road gauging stations, would possibly reduce the flows received by the Peel-Harvey Estuary. The Harvey River discharges directly to the Harvey Estuary, therefore any reduction in the flow amount of the River will badly affect the quantities of water received by the Estuary. As the depth of the Estuary is quite shallow (up to 2m for the deepest point), and more than 50% of its area has a depth of only 0.5m (Kelsey et al., 2010), this will affect the aquatic life, habitat of waterbirds and the environmental status of the lagoon. The growing environmental and economic importance of the estuary (such as water demands for drinking and agricultural production, parasite control, commercial fishing, foreshore development and access, boat use and moorings and jetties) have placed additional burdens on the estuarine system. Furthermore, the projected reduction in the flow amount of the Harvey River would also reduce the quantities of water received by the Stirling and Harvey Reservoirs which represent the main water supply sources to the Perth Metropolitan (Al-Safi and Sarukkalige, 2018). As the population and the economic development in Perth and its outskirts is in continuous growth, this would increase the competition for the currently available water resources in the area. Therefore, options for additional water supply sources in the future would be necessary to support the economic and population development in the area.

For the Beardy River region which is rich in rare flora and fauna, the expected streamflow reduction would adversely impact the environmental and ecological communities of the Beardy River system particularly the Beardy River Hill Catchment. On the other hand, the Goulburn River is the right bank tributary to the Hunter-River in NSW, Australia. It drains approximately 50% of the Hunter catchment and contributes nearly quarter of the mean Hunter River flow. Water in the Hunter basin is the main source for power generation, irrigation and agriculture, stock manufacturing, coal mining and public water supplies. The streamflow

reduction in this catchment would impose further limitations on the surface water supply systems in the Hunter River basin.

4.3 Conclusion

The Budyko elasticity method was applied to understand the distribution between climate change and human interventionsof the hydrological variations in the catchments. The elasticity approach, by using the hydrological parameters and their variation during the recent decades, suggested not only the climate change had impacts on runoff, but also human activities have significantly contributed to the runoff reduction. Climate change and human activities played almost the same roles in Harvey and Beardy catchments. However, for the Goulburn catchment, climate change was responsible for almost 70% of runoff decrease. The results were predictable as the Goulburn area is mostly covered by national parks and forests and has been less affected by human activities.

The hydrological results of this study will provide a theoretical basis to the local management authorities to make scientific and rational control measures and response plans which allow them to manage the usage of future water resources in the study area.

Chapter 5
Budyko model vs hydrological model to assess streamflow changes

5.1 Background and method

In this chapter application of the Budyko model in assessing streamflow variation is cross validated with HBV hydrological model. In order to reduce the time required for manual calibration, a hybrid simulation-estimation algorithm (ANN-PSO) was used to auto-calibrate the HBV model. To determine the impact of climate change and human activities, other than the analytical elasticity equation, the statistical elasticity equation is used to calculate the precipitation and evapotranspiration sensitivities of the streamflow. The case study is Harvey-Dingo catchment in Western Australia and the period of the study is from 1971 to 2015. Figure 5.1 shows the temporal rainfall and streamflow variation in this catchment.

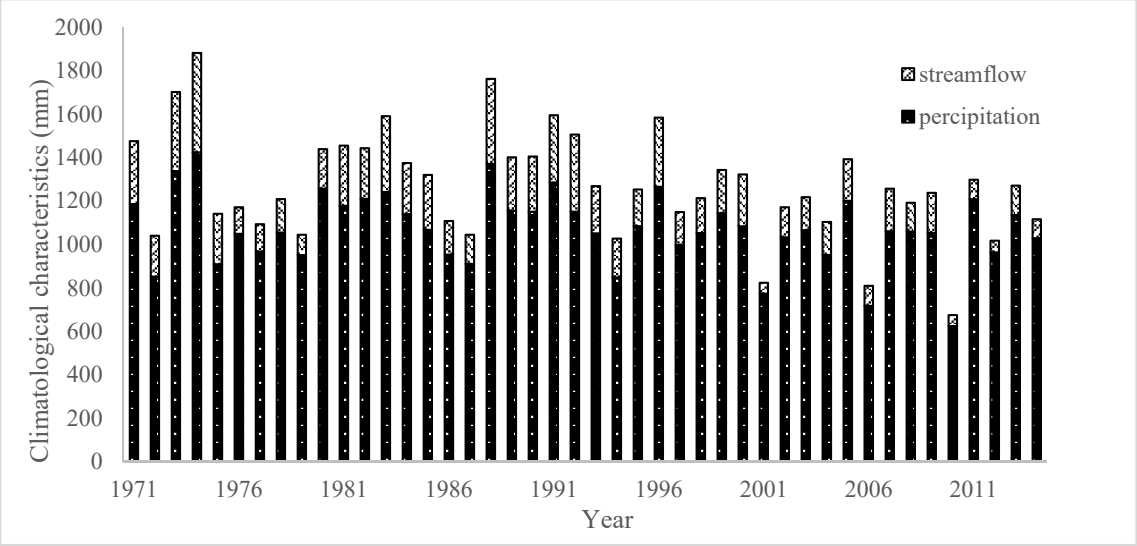

Fig.5.1 Annual rainfall and streamflow variation in the Harvey-Dingo Catchment, WA

5.1.1 Statistical Elasticity

The statistical elasticity equation, ε (either ε_{E0} or ε_P), is estimated using the definition of 'elasticity' presented in Eq. (5.1), where *t* represents time (Fu et al. 2007; Sankarasubramanian et al. 2001; Xu et al. 2014b; Yang and Yang 2011):

$$\varepsilon_P = median\left(\frac{\bar{Q}_t - \bar{Q}}{P_t - \bar{P}} \times \frac{\bar{P}}{\bar{Q}}\right) \quad (5.1)$$

$$\varepsilon_P = \frac{\bar{P}}{\bar{Q}} \frac{\sum(P_i - \bar{P})(Q_i - \bar{Q})}{\sum(P_i - \bar{P})^2} \quad (5.2)$$

Consequently, the share of human activities and climate change in streamflow variation can be calculated as described in Chapter 4 (Eqs. (4.4 to 4.9)).

5.1.2 Hydrological modelling

Same as the Budyko model, the first step to use the hydrological model for assessing the streamflow is to determine the breakpoint in streamflow trend. The pre-change period is divided into calibration and validation sub-periods and the model is calibrated and validated, accordingly. Then it simulates the streamflow for the post-change period, adopting the pre-change parameters. Accordingly, ΔQ_c is calculated by deducting the mean annual simulated streamflow of the post-change period and that of the pre-change period. ΔQ_h is calculated as the difference between the mean annual simulated and observed streamflow, both from the post-change period (e.g., Fan et al., 2010; Hu et al., 2012; Zeng et al., 2014; Zhang et al., 2016; Chang et al., 2016; Dey and Mishra, 2017; Wu et al., 2017). In this way, it is possible to quantify the impact of climate change and regional human activities for the post-change period.

The selected hydrological model for this study is the HBV model. The model is user-friendly and needs comparatively few input data. It has been employed in several hydrological studies to simulate, forecast and predict streamflow (Al-Safi and Sarukkalige, 2018; Li and Zhou, 2016; Li et al., 2016) and proven to be a competent model (Al-Safi and Sarukkalige, 2017; Lindström et al., 1997).

The HBV model was developed by Swedish Meteorological and Hydrological Institute (SMHI) (HBV-manual 2013). The HBV is a semi-distributed conceptual model used to simulate daily streamflow at a catchment outlet (Seibert, 2005). Input data for this model are daily precipitation, air temperature, potential evapotranspiration and mean monthly evapotranspiration (HBV-manual, 2013). It operates using three main segments: precipitation

routine, soil moisture routine and response routine (Seibert 2005). To simulate streamflow, these three segments need characteristic parameters as inputs (i.e., *β, ecorr, K4, KHQ, FC, LP, MAXBAS, PERC,* and *rcfc*). The parameters of *FC*, *β* and *LP,* provide data on wetness and soil moisture storage for a catchment as input for soil moisture routine. Parameter *FC* refers to maximum soil-storage capacity in a basin; and parameter *β* represents the relative participation of rainfall to streamflow at a given soil moisture deficiency. The shape of the potential evapotranspiration curve is controlled by parameter *LP*. Parameters *KHQ* and *K4* are recession coefficients for the response routine and *PERC* represents a constant percolation rate. Parameter *MAXBAS* is the transformation function and calculates outflow from the catchment, *rcfc* is the rain fall correction factor, and *ecorr* denotes the general evaporation correction factor (Al-Safi and Sarukkalige, 2018; Lindström et al., 1997; Seibert, 2005). All parameters are set to a one-day time-step (HBV-manual, 2013).

5.1.2.1 Calibration of the HBV model using an optimisation-estimation algorithm

A hybrid optimisation-estimation algorithm was developed to avoid the time-consuming process of manual calibration. This hybrid algorithm contains two modules: a simulator module and an optimisation module (Afshar and Kazemi, 2012). In this study, the hybrid FNN-PSO (Feedforward Neural Network – Particle Swarm Optimisation) algorithm automatically calibrated the HBV model. Both codes for the optimisation module (PSO) and estimator module (FFNN) were written in Matlab.

Optimisation module: Particle Swarm Optimisation (PSO)

The PSO algorithm, which is a population-based evolutionary algorithm, was selected due to its fast–convergence capabilities, because it is easy to understand and also because it circumvents local optimums (Afshar et al., 2011). Similar to other evolutionary algorithms, standard PSO is established using a random population called a “swarm”, where each particle in the population carries a candidate solution for the problem (Afshar et al., 2011). In this study, a population of 100 particles was selected for PSO. Upon completion of the algorithm, all particles converge on the best solution, and provide the HBV model with a set of calibration parameters.

Estimation module: The Feedforward Neural Network (FNN)

The simulator module in the current study was a feedforward neural network (FNN). In this algorithm, information flows through the input layer to the hidden layers to be acted on by the training functions. Subsequently, information flow through to the output layer for final calculations (Brilliant.org 2018). For the FNN presented, in addition to an input and an output layer, two hidden layers with 20 neurons were selected.

FNN utilise the outcome of HBV-PSO model for training. A trained FNN acts as a substitute for the HBV model and estimates its behaviour in a more convenient and efficient manner. In other words, rather than the HBV-PSO couple, PSO produces decision variables (calibration parameters) for the FNN until it reaches the least objective functions and provides the fittest set of parameters (Afshar and Kazemi, 2012).

The characteristic parameters for the calibration of the HBV and their ranges (suggested by HBV manual, 2013) are presented in Table 5.1.

Table 5.1. Suggested and calculated values for the HBV calibration parameters

Characteristics parameters	Units	Description	Suggested domain	Best match
beta	-	Exponent in formula for drainage from soil	1-4	1.5
ecorr	-	General correction factor for potential evaporation	<= 1	0.9
K4	[Unit day^{-1}]	Recession coefficient for lower response box	0.001-0.1	0.04
fc	mm	Field capacity	100-1500	700
khq	[Unit day^{-1}]	Recession coefficient for the upper box	0.005-0.5	0.25
lp	-	Limit for potential evaporation	<= 1	0.8
maxbaz	-	Number of days in the transformation routine	0-7	0.07
perc	[mm/day]	Percolation capacity	0.01-6	1.1
rfcf	-	Rain fall correction factor	0.8-1.3	0.8

In this study, a fourteen-year period (i.e., from 1971 to 1986) was selected for the calibration of the HBV model and the validation period was from 1994 to 2015. A comparison of the simulated and observed daily hydrographs of the streamflow (as presented in Fig.5.2 and Table 5.2) justifies the capability of the HBV model to assess the hydrological behaviour of the Harvey Catchment.

Table 5.2. The HBV model performance in estimating the Harvey River streamflow variation for the calibration and validation periods

Calibration (1971-1986)		Validation (1994-2015)	
VR (%)	R^2	VR (%)	R^2
92	0.9	101	0.89

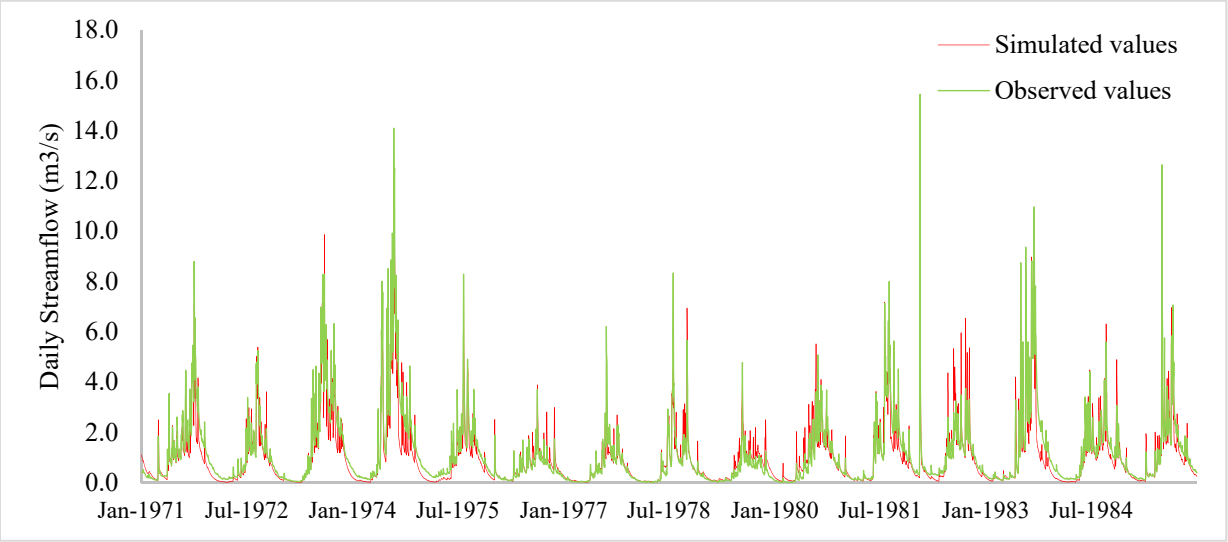

Fig.5.2 Calibration of the HBV model for the period 1971-1986

For the analysis, the HBV model was calibrated using the pre-change data. Once calibrated, the HBV model simulated the streamflow for the post-change period (Chang et al. 2016). Accordingly, as explained in chapter methodology, Eqs. (5.3- 5.5) were applied to derive the impacts of climate change and human activities on the streamflow of the catchment (Chang et al., 2016; Hu et al., 2012; Sun et al., 2014):

$$\Delta Q = Q_{o2} - Q_{o1} = \Delta Q_c + \Delta Q_h \quad (5.3)$$

$$\Delta Q_c = Q_{s1} - Q_{s2} \quad (5.4)$$

$$\Delta Q_h = \Delta Q - \Delta Q_c \quad (5.5)$$

where Q_s is HBV-simulated streamflow based on parameters of the pre-change period in which catchment characteristics are constant and human activities are negligible; Q_o is observed streamflow, and h and c denote human activities and climate change, respectively; and subscript 1 and 2 denote the pre-change and post-change period, respectively.

5.1.3 Streamflow prediction

The literature suggested Australian local watersheds may experience severe changes in precipitation, temperature, and evapotranspiration (Donohue et al., 2010, Al-Safi et al., 2019). They also predicted extreme weather events would occur in the future. These changes threatens physical and biological life in the study area (Donohue et al., 2010). Hydrological modelling is a popular approach for investigating future changes of hydrological characteristics in a catchment. In this section, for the first time, the Budyko model is used to predict streamflow change in the Harvey-Dingo catchment. Thus, the study implies a significant novelty, as per the literature there is lack of evidences to show that the Budyko model has been applied to predict the future impacts of climate change. The two most popular Budyko models (i.e., Fu and Choudhury) are employed to predict the streamflow trends in the Harvey-Dingo Catchment. The catchment characteristic parameter (ω or n) is the same as catchment characteristics for the current period (1971-2015), which are adopted from Chapter 4.

The results then is validated with the HBV model, for two periods: the near future (2045-2065) and late future (2080-2100), under the two climatological scenarios (i.e., RCP4.5 and RCP8.5). The HBV model is, also, calibrated using the same catchment parameters for the current period. Using daily values for temperature, evaporation and precipitation parameters as input data, the HBV model simulated the streamflow in the Harvey-Dingo Catchment under two scenarios: RCP4.5 and RCP8.5 for the periods near future (2046–2065) and late future (2080–2099).

5.2 Performance of the Budyko and HBV models in estimating streamflow variation

In this section, the proposed methods are employed to provide a deeper understanding of the hydrological response of the system due to climate change and human activities.

Previous studies on the Harvey Catchment suggest the catchment has experienced extensive changes over recent decades; Natural catchments have been cleared to develop agricultural and urban areas, dams have been constructed, and artificial drainage networks have been built

to prevent flooding and store water for irrigation (Belinda and Shakya, 2011). Human activities including land use and change in land cover, water conservancy projects, and the development and usage of groundwater, place additional pressure on water resources. Figure 5.3 analyses the change in the Harvey Catchment population with regard to streamflow variation during the study period and shows the constant population increase in the study area, which may have contributed to additional withdrawals of water from the Harvey River.

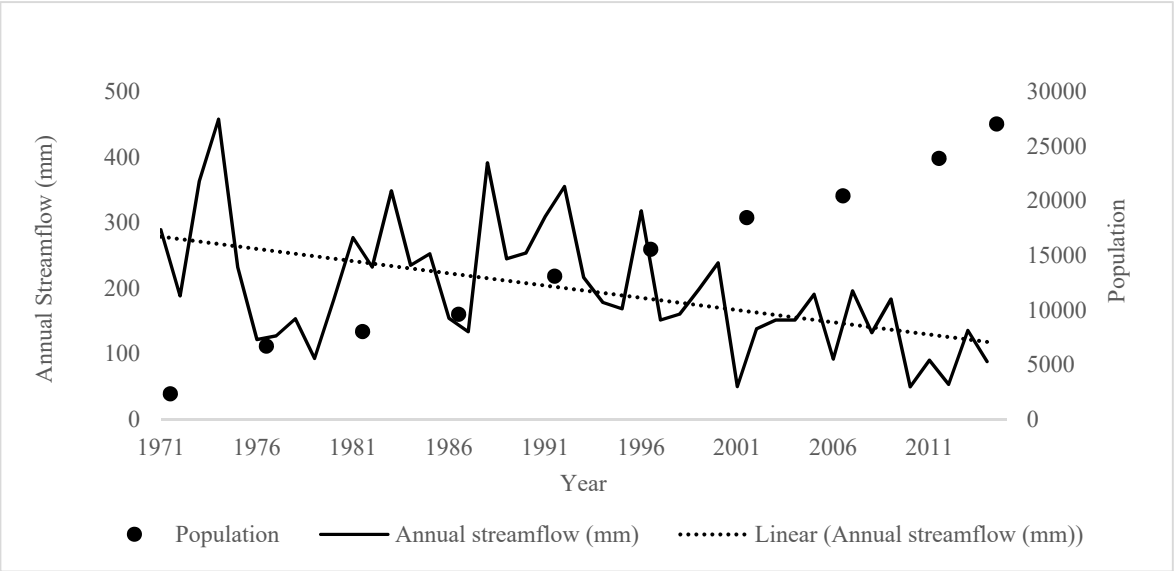

Fig.5.3 Population and streamflow change during the study period in the Harvey Catchment, WA

The Flow Duration Curves (FDCs) of the Harvey-Dingo streamflow illustrates a significant difference between the pre-change and post-change periods (Fig.5.4). The high flow (Q5) and low flow (Q95) for the period 1994–2015 decreased by 26% and 87% compared with the period 1971-1993. It also illustrates that the mean monthly observed streamflow of the Harvey River reduced significantly during the post-change period. Figure 5.5 represents the mean monthly streamflow values for the two periods. It shows during some months in the post-change period, the streamflow dropped to zero (frequency of zero flow is 6%), while zero flow rarely happened during the pre-change period.

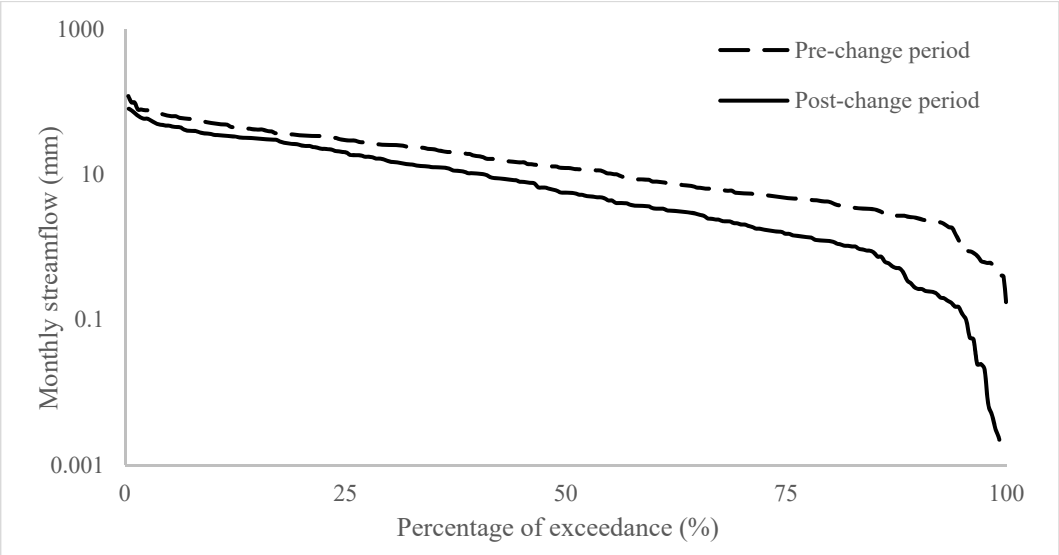

Fig.5.4 monthly observed streamflow FDCs variation in the Harvey River during pre-change and post-change periods

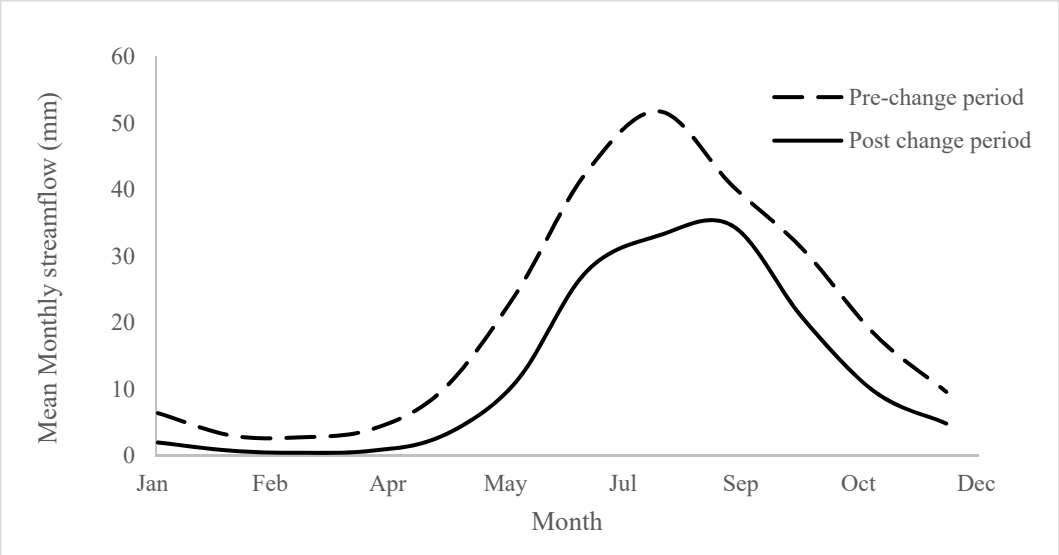

Fig.5.5 Mean monthly observed streamflow in the Harvey River during pre-change and post-change periods

5.2.1 The Budyko model

The value 1.71 for n and 2.43 for ω for Choudhury and Fu equations were derived respectively, using Eq. (2.6), which confirms with the correlation between the two parameters (Eq. (2.5)). The statistical elasticity and analytical elasticity equations were used to determine the sensitivity of streamflow change to precipitation (ε_P) and evapotranspiration (ε_{E0}) (Table 5.3). For both methods, the precipitation elasticity is higher than the evapotranspiration elasticity. This means that streamflow variation in the Harvey-Dingo Catchment is more sensitive to precipitation than evapotranspiration.

Table 5.3 Values of elasticity parameters for Harvey-Dingo Catchment, WA

method	εp	ε_{E0}
Statistical	2.3	-2.8
Analytical	2.3	-1.3

5.2.2 The HBV method

The HBV model was employed to calculate the climate change and human activities quotas in the streamflow variation. The simulated annual streamflow presented in Fig.5.6 fits well with the observed data for the pre-change period (1971–1993); however, there is a remarkable difference between the observed streamflow and simulated streamflow during 1994-2015. This means non-climate factors and more specifically, human activities, probably contributed to changes in the hydrological behaviour of the study area (Hu et al., 2012).

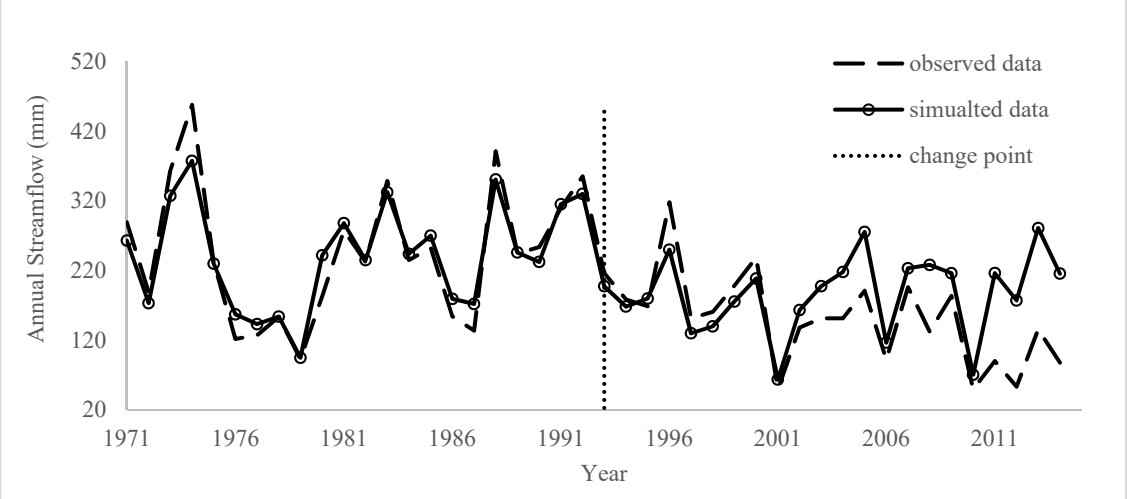

Fig.5.6 Harvey River annual streamflow estimation using the calibrated parameters of the pre-change period

The HBV model indicates that 56% of the streamflow reduction results from climate change, which means that share of human involvement in this change is 44% or 42 mm (Table 5.4). The two Budyko Elasticity equations (the Analytical Elasticity and Statistical Elasticity) indicate that 55% and 63% of the total drop in streamflow in this study area is due to climate change, respectively.

Table 5.4. Contribution of climate change and human activities on streamflow reduction in the Harvey-Dingo Catchment based on the HBV and Budyko models

method	ΔQ	$\Delta Q_C\,(mm)$	$\Delta Q_h\,(mm)$	$\Delta Q_C\,(\%)$	$\Delta Q_h(\%)$
HBV		-54	-42	56	44
Statistical	-96	- 60	- 36	63	37
Analytical		- 52	- 44	55	45

The outcomes of the Budyko Elasticity Equations are very similar to those of the HBV simulation, demonstrating the capability of this method in attributing streamflow reduction to the impacts of climate change and human activities.

5.2.3 Predicting streamflow changes under the two future scenarios

Table 5.5 presents the current mean annual data and downscaled mean annual data for precipitation and temperature under the two selected climate scenarios. The future mean annual potential evapotranspiration values were calculated using Morton's equation.

Table 5.5. The Harvey-Dingo catchment climat parameters compared with the current period

variable	current Period	Period/ scenario			
		2046-2065		2080-2100	
	(1971-2015)	RCP 4.5	RCP 8.5	RCP 4.5	RCP 8.5
P (mm/year)	1073	907	897	912	774
T (˚c)	16.4	24	25.02	25.07	25.5
E_0 (mm/year)	1780	1955	1985	1985	2004

As presented in Figure 5.7, the influence of climate change on streamflow is obvious. A comparison of future streamflow trends with the current period suggests a considerable streamflow reduction in the catchment, especially during the latter half of the century, for the chosen scenarios.

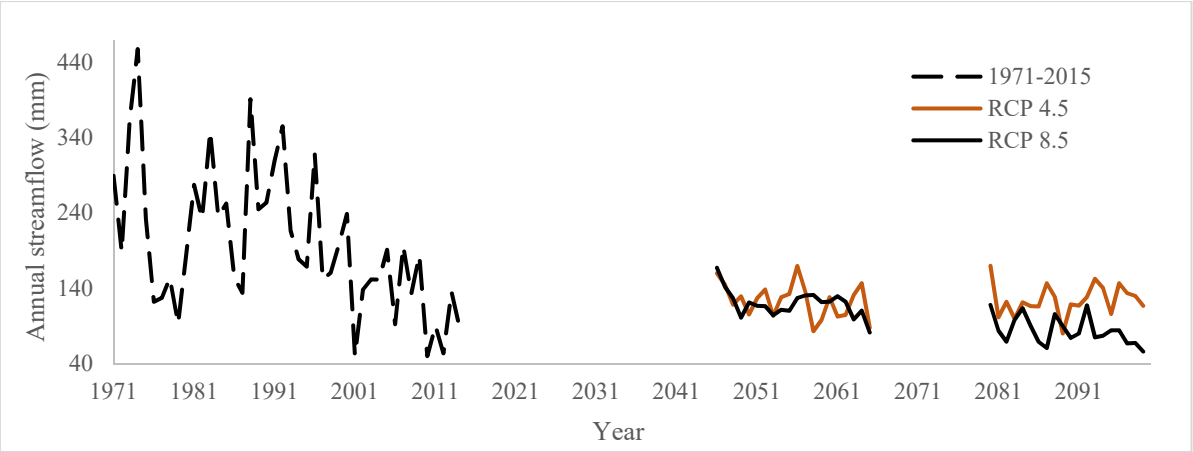

Fig.5.7 Annual streamflow prediction for the near future and late future periods, using the HBV model under the two climate scenarios (RCP4.5 and RCP8.5)

Figure 5.8 compares the results from the Fu and Choudhury methods versus the HBV model output for both the RCP4.5 and RCP8.5 scenarios. The coefficient of determination (R^2) value is represented in Table 5.6 to illustrate the level of fitness of the Fu and Choudhury equations against the HBV model.

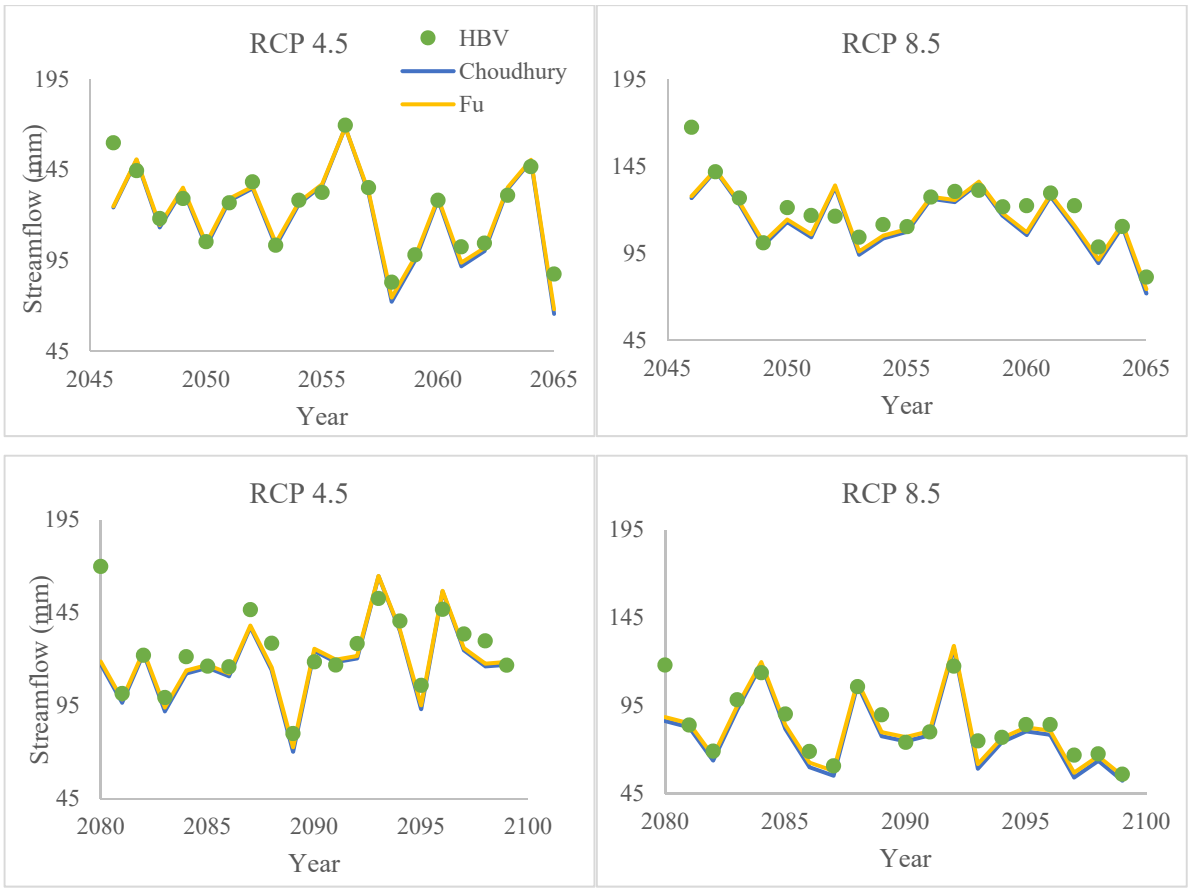

Fig.5.8 Harvey River streamflow prediction using the Fu and Choudhury models for the near (2045-2065) and late (2080-2100) future periods under the two climate scenarios and comparison of the results with the HBV model's

Table 5.6. The Budyko model Performance (R^2) compared to the HBV model

Method	2046-2065		2080-2100	
	RCP 4.5	RCP 8.5	RCP 4.5	RCP 8.5
Fu	0.96	0.82	0.89	0.94
Choudhury	0.97	0.83	0.89	0.94

All methods predicted a significant reduction in streamflow for both future periods. Considering the value of 198 mm for mean annual streamflow for the current period, Table 5.7 illustrates the expected mean annual streamflow for the future timeframes in this study. For the near future, for both scenarios, the models predicted a 38% reduction in streamflow. For the period of 2080-2100, under RCP4.5, all the models confirmed almost the same 38% reduction in streamflow; however, the suggested value based on scenario RCP8.5, shows 58% decrease in streamflow.

Table 5.7. The estimated mean annual streamflow (mm) for Harvey-Dingo catchment under the two climate scenarios

Method	1971-2015	2046-2065		2080-2100	
Scenarios	-	RCP 4.5	RCP 8.5	RCP 4.5	RCP 8.5
HBV		121	117	122	82
Fu	198	121	114	119	80
Choudhury		119	112	118	78

In all scenarios, a decrease in mean annual rainfall and an increase in potential evapotranspiration is anticipated. The 9-12% potential evapotranspiration increase in these scenarios could be a consequence of the expected rise in mean annual temperature in the future. The aggregated effects of the decrease in precipitation and increase in potential evapotranspiration can result in streamflow reduction across the catchment in the future (Alsafi et al., 2017).

Figure 5.9 presents the boxplot for the future streamflow estimations. To avoid an overcrowded diagram, only the results from the HBV model and Fu equation are shown and compared with the current period (1971-2015). The parameter Q1 (Q25%), which represents minimum streamflow statistics, showed a 20-25% decrease for the near future and a 20–50% decrease for the late future period, for the two scenarios. Similarly, the maximum streamflow statistics Q3 (Q75%) are anticipated to decline more than 50% in the near future and between a 45%-65% decrease in the late future for both scenarios.

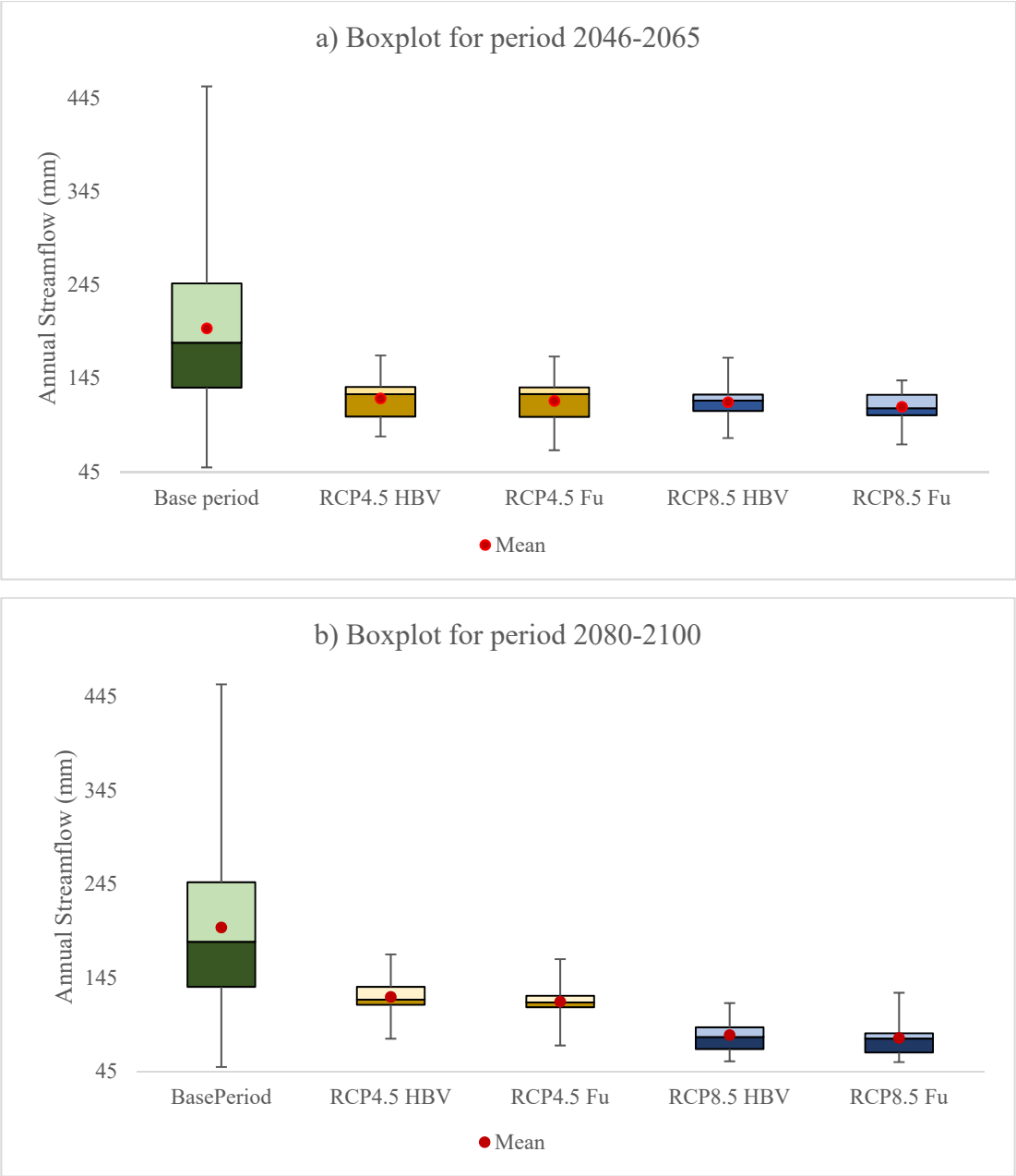

Fig.5.9 Harvey River streamflow Boxplot for a) near future (2046-2065) and b) late future (2080-2100) periods under the two climate scenarios

The Peel- Harvey Estuary, which is a recipient of the river flow from the Harvey River, is shallow and reaches up to two meters at its deepest point. Its depth is a mere 0.5 meters in most areas. The estuary is predicted to experience extra water stress due to agricultural, environmental and economic growth. It may experience an increase in drinking and agricultural water demands, parasite control, commercial fishing, foreshore development and access, boat use, and moorings and jetties (Belinda and Shakya, 2011). Therefore, a reduction in streamflow could possibly affect the estuary and, consequently, disturb the quantity and

quality of water received by the estuary. It can lead to greater vulnerability as a result of this change for aquatic life, the habitat of water-birds and the environmental status of the lagoon. The results support previous studies conducted on other South-West Australian catchments, all of which predicted a decline in future streamflow for the region (Al-Safi and Sarukkalige, 2018; Durrant and Byleveld, 2009; Al-safi et al., 2017; Islam et al., 2014; McFarlane et al., 2012; Silberstein et al., 2012). The estimated decrease in the streamflow of the Harvey River, will likely be felt by the Stirling and Harvey reservoirs, which form the main supplies for Perth Metropolitan (Al-Safi et al., 2018, Al-Safi et al., 2019). Perth city and the surrounding area is experiencing continuous economic and population growth, which in turn will put extra pressure on the available water system.

The outcome of this study will provide recommendations to the state and local water resource management authorities to consider scientific and rational control measures and response plans in their decision making process. Careful attention and effort should be given to future water resource management and ecosystem planning in the study regions. If this does not occur, the impacts of climate change and human activities may put the stability of the ecosystem at risk. The finding of the current study are useful for authorities such as the Peel-Harvey Catchment Council (PHCC) and other organisations in developing of water resource management plans, urban and rural development plans, ecological restoration and conservation projects; regulating water for irrigation, domestic use and industry; and for evaluating ecological engineering and the sustainable management of the Harvey River Catchment.

5.3 Conclusion

The Harvey River catchment in Western Australia recorded sever reduction in streamflow over the past decades. The catchment has experience significant land use change and precipitation reduction. Therefore, to investigate the attribution of climate change and human activities in the change of streamflow, two different methods (the Budyko model and HBV hydrological model) were used to assess the impacts of climate change and human activities on streamflow in the Harvey-Dingo Catchment in Western Australia. To enhance the accuracy and to avoid the time-consuming process associated with calibration of the HBV model, the auto-calibration method (hybrid estimation-optimisation – [ANN-PSO]), was proposed to prevent human errors and to reduce the required time of calibration. The results demonstrate that streamflow has decreased by almost 40% during the last two decades. This reduction has

occurred due to both climate change and human influences. The results from both methods indicate that climate change was responsible for about 55% of streamflow reduction for the period of 1971-2015 in the catchment.

To predict streamflow change under the two future scenarios (i.e., RCP4.5 and RCP8.5), the Budyko was used. The results were then compared with HBV model results to assess the applicability of the Budyko model in predicting streamflow variations. Both models illustrated that the catchment will experience another significant reduction in streamflow (more than 38%) in the future. It is expected that future climatological alterations of precipitation, temperature, evapotranspiration and the frequency of extreme weather events will affect many physical and biological processes in many Australian local watersheds (McVicar et al., 2010). Consequently, this can alter the amount and spatial and temporal distributions of water that flows into downstream rivers and estuaries. The results is consistent with the previous research suggesting streamflow reduction in the Harvey-Dingo Catchment and a decreasing rainfall-runoff trend for the future. It proves the capability of the Budyko approach in assessing water resources using limited data and with higher accuracy. The Budyko model proved to be a very reliable, simple and user-friendly tool for predicting future streamflow patterns.

Chapter 6
Validating the Budyko model using remote sensing technique

6.1 Background and method

This chapter introduces a novel framework that combines mathematical, hydrological, and remote sensing methods to separate the contribution of climate change and regional human activities (such as land use/land cover change) to streamflow changes of the large river basins in the data-scarce areas. The study area is the Karkheh River Basin (KRB), called "the food basket of Iran", which is one of the most important agricultural basins in Iran. Irrigated farmland in the basin produces wheat for the entire country, while non-irrigated areas yield grain and livestock products (Ahmad and Giordano, 2010). The KRB is equally essential for hydropower production. Nonetheless, due to frequent droughts, massive agricultural activities, and dam construction programs, the KRB has experienced significant streamflow reduction in recent decades (Ahmad and Giordano, 2010). Enduring streamflow reduction in the basin may put the sustainability of food production for the nation as well as downstream environments in jeopardy. Therefore, it is of vital importance to investigate the primary cause of the streamflow reduction to be able to develop an alternative management plan (Falkenmark, 2001; Masih et al., 2011).

The Budyko model and the HBV model are used to analyse the mean annual streamflow variation of the studied region, during the last three decades (from 1980 to 2012) and quantify the impact of climate change vs. regional human impacts. Furthermore, trend analysis to detect the breakpoints in the observed streamflow was carried out using the newly developed Detecting Breakpoints and Estimating Segments in Trend (DBEST) algorithm (Jamali et al., 2015). The newly developed DBEST method is a user-friendly algorithm for analysing time-series with two main application domains of generalizing trends to main features, and detecting and characterizing trend changes. It uses a novel segmentation algorithm that simplifies the trend into linear segments, using the number of changes or a threshold for the magnitude of changes of interest for detection. In addition to detecting trend changes and estimating the statistical significance of the trend, DBEST determines the timing, magnitude, number, direction, and type (abrupt or gradual) of the detected changes (Jamali et al., 2015; Dey and Mishra, 2017). Applying the DBEST algorithm in the hydrological studies, for the

first time here, offers a systematic improvement for the segmentation of the streamflow time-series. The remote sensing technique is employed to provide multiple land use maps of the basin area over the studied period for quantification of the impact of human-induced changes. To carry out the study, some assumptions are made. The catchment characteristic parameter is assumed to be constant during the study period, while, this value is subjected to change by changing LULC and also is dependent on other climate parameters, such as climate parameter seasonality, mean storm depth (Yang et al., 2014), vegetation coverage (Li et al., 2013; Yang et al., 2009), and/or effective rooting depth and plant root characteristics (Cong et al., 2015; Donohue et al., 2012). To calculate this parameter, per literature suggestion (e.g., Hu, Liu et al., 2012; Liang et al., 2015), we simultaneously modelled E using Eq. (2.4) and minimized the difference between the calculated E and observed long-term E.

To summarize, the developed framework mainly comprises i) quantification of the impact of human activities and climate variability on streamflow reduction, ii) evaluation of the results of the Budyko method with the HBV model, and iii) validation of the findings using remote sensing and image classification techniques. Although, such a hybrid framework will provide a basis to discuss the reliability of the results depending on the agreement among different individual methods' outcome, sensitivity and uncertainty analyses are included as supplementary to the framework to emphasize reliability of the results based on modelling, which is a way to conceptualize reality.

6.1.1 The Budyko model

As mentioned, the Budyko model investigates the link between precipitation as an input of the hydrological system, and evapotranspiration and streamflow as the outputs of the system. Hence, in the equation the water storage change (ΔS) is insignificant when the water balance system is steady (Xu et al., 2013).

In the current chapter, in order to validate the steady state condition for the KRB, the ABCD model was employed. The ABCD model is a popular conceptual model to estimate water storage change in catchments. This conceptual model, developed by Thomas (1981), is especially applicable for data-scarce regions (Du et al., 2016; Wang and Zhou, 2016; Wang et al., 2020), such as the KRB.

6.1.2 The ABCD model

The ABCD model code is written in R, and the embedded genetic algorithm (GA) provides the best set of parameters (i.e., a,b,c and d) for the model. The objective function for GA is Kling-Gupta efficiency (KGE) between monthly observed streamflow and monthly estimated streamflow.

After confirming the steady state condition of the KRB, one of the most popular Budyko-type Equation, i.e., the Choudhury equation (Eq. (2.4)), is employed to calculate the effects of climate change and regional human impact on streamflow at the basin level (Wang et al., 2016).

6.1.3 The hydrological HBV-light model

Different versions of the HBV model have been successfully applied in several basins across the world to simulate streamflow changes, including snow-influenced areas as well as semiarid climates at both local and regional scales (e.g., Lindström et al., 1997; Merz and Blöschl, 2004; Lidén and Harlin, 2000; Götzinger and Bárdossy, 2007; Love et al., 2010; Masih et al., 2010; Li and Zhou, 2016; Li et al., 2016; Al-Safi and Sarukkalige, 2018; Al-Safi et al., 2019). The latest version of the model, HBV-light, is selected for this study, due to its simple yet flexible structure. Simplicity and flexibility of the model is an important feature for a model to simulate a basin like Karkheh, which covers a large space from high mountainous terrain to low land areas at the sea level. In this version, the basin area can be subdivided into different elevations and vegetation zones, suitable for the KRB, which is characterized by extensive elevation and vegetation range (Masih et al., 2010). The model simulates streamflow at daily time steps using daily climate variables such as potential evapotranspiration, precipitation, and temperature. The HBV-light uses the warming-up period for initialization of parameters. An embedded Genetic Algorithm (GA) is a helpful feature for auto calibration, which is provided in this version. To assess the performance of the calibration, the model provides several common yet informative measures such as Annual Mean Difference (δ), Nash-Sutcliffe Efficiency (R_e), and Kling Gupta Efficiency (KGE). The calibration parameters (Table 6.1) are adapted according to the manual, catchment characteristics, and literature (Lindström et al., 1997; Seibert, 1999; Uhlenbrook et al., 1999; Uhlenbrook and Leibundgut, 2002; Masih et al., 2010; Al-Safi et al., 2019; Kazemi et al., 2019).

Table 6.1 The HBV Manual suggested range for the parameters for the HBV model calibration

Parameter	Unit	Description	Range
TT	˚c	Threshold temperature	-2.5 - 2.5
CFMAX	mm ˚c^{-1} d^{-1}	Degree-day factor	1-6
SFCF		Snowfall correction factor	0.5-1.25
FC	mm	Maximum of storage in soil box	50-500
LP		Threshold of reduction of evaporation	1-6
Perc	mm d^{-1}	Maximum flow from upper to lower box	0.1-6
UZL	mm	Threshold of Q_0 outflow in upper box	10-100
K0	d^{-1}	Recession coefficient	0.05-0.5
K1	d^{-1}	Recession coefficient	0.01-0.15
K2	d^{-1}	Recession coefficient	0.0001-0.05
MaxBAS	d	Routing, length of weighting function	1-6

The pre-change period is divided into calibration and validation periods. After calibration and validation of the model for the pre-change period, the HBV-light is used to simulate the flow for the post-change period, adopting the same parameters. Accordingly, ΔQ_c and ΔQ_h are calculated as explained in section 4.2.2.

6.1.4 Analysing Land Use–Land Cover change during the study period

Given the scarcity of land cover information in the KRB, Multispectral Landsat satellite imagery were used to investigate the likely relationship between the land cover change and streamflow variation in the basin, and to obtain a spatio-temporal Land Use/Land Cover (LULC) information of the study area (Muttitanon and Tripathi, 2005; Ghobadi et al., 2012; Jafari and Hasheminasab, 2017). Landsat 5 Thematic Mapper (TM) was selected for this study because it offers high-resolution images (120 m) and complete spatial coverage of the study basin from 1980 to 2012.

Cloud-free Landsat images are acquired from Landsat 5 TM C1 Level-1 for three years of 1987, 1995, and 2012 (different months) representing the pre-change or natural period, transition period, and the post-change period, respectively. The images are, then, projected to the UTM (zone 38) and WGS 84 datum reference system. Also, the ground truth data are collected using the Global Positioning System (GPS) and ground control points from the Google Earth application to provide a signature for each land use type. These data are applied for classification and overall accuracy assessment of the classified images. The image classification processing is performed in ENVI 4.8 environment, employing a supervised

classification technique with the maximum likelihood algorithm for generating the land use map. The maximum likelihood classifier (MLC) is a commonly used statistical technique for image classification and for evaluating the standard LULC (Zaidi et al., 2017). Due to the complexity of the land use types in the basin, overlaps among different land use types, and lack of sufficient number of historical ground truth data, an optimum threshold was determined to simplify the LULC classification of the study area.

6.1.5 Uncertainty analysis

Application of hydrological models to discriminate the climate change vs. human activities is a common approach (e.g., Li et al., 2004; Wang et al., 2009; Montenegro and Ragab, 2010). However, if the model is not well calibrated, it can lead to uncertain results (Legesse et al., 2003; Hu et al. 2012). One of the main sources of uncertainty arises from non-uniqueness of the model parameters, which means that different combination of parameters may result in the same streamflow prediction (Beven, 2001; Masih et al., 2010). Hence, the non-uniqueness of the model parameters was investigated. For this the ten-best sets of calibration parameters values produced by Genetic Algorithm (GA) are selected for each sub-basin to simulate the streamflow for the pre- and post-change periods. Then, the impacts of climate change and human activities are separated, accordingly.

For the case of Budyko method, the results can be affected by the noisy historical climate data (Hu et al., 2012). In this study, the sensitivity of the Budyko equation to the precipitation and evapotranspiration input data is investigated using Eq. (5.1) proposed by Yang et al. (2014). The equation derives the possible error of estimating streamflow due to climate parameter change:

$$dQ = \varepsilon_a \frac{da}{a}.Q \qquad (6.1)$$

where Q is flowrate (mm/year), ε is streamflow elasticity, and a is a climate parameter.

6.2 Quantitative and qualitative analysis of streamflow change

For each sub-basin, the DBEST method detected a breakpoint in the streamflow time series at the 0.05 statistical significance. Abrupt changes were detected for all the sub-basins, which occurred during 1994–95 (Fig. 6.1).

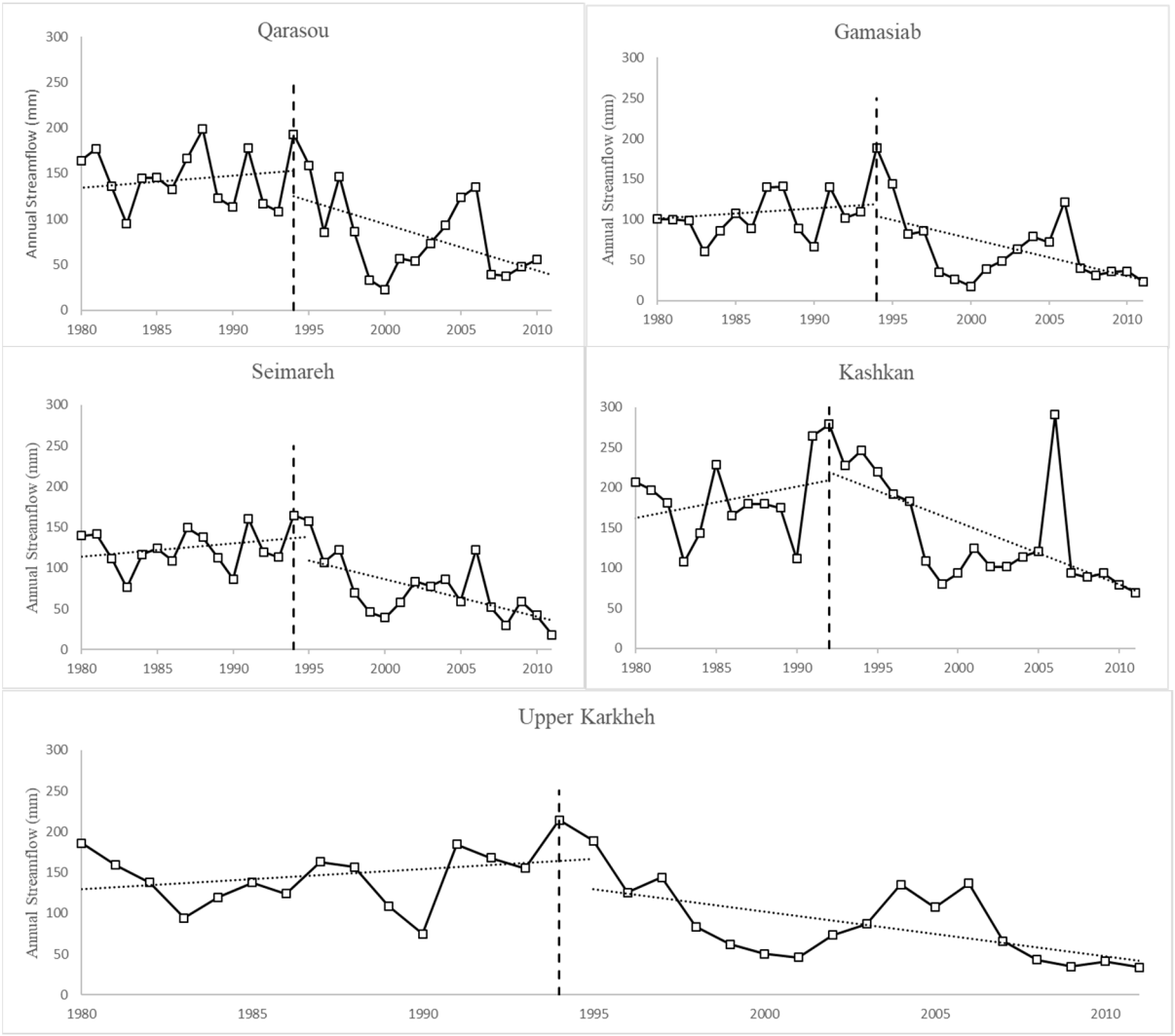

Fig.6.1 Streamflow trends in the KRB sub-basins, and the detected breakpoints

In the sub-basins, the annual streamflow experienced a dramatic decrease from the pre-change period (1980-1994) to the post-change period (1995–2012). Table 6.2 illustrates the detected breakpoints for all sub-basins, as well as the quantified changes in streamflow.

Table 6.2 Mean streamflow variation in the pre-change (Q1) and the post-change periods (Q2) and the magnitude of the change for the KRB sub-basins

Sub-basin	Break-point	Q1 (mm/year)	Q2 (mm/year)	ΔQ (mm/year)	ΔQ (%)
Qarasou	1995	146	77.9	- 68.1	-47%
Gamasiab	1995	107.8	57.7	- 50.1	-47%
Kashkan	1993	186.2	138.5	- 47.7	-26%
Seimareh	1995	124.2	72.3	- 51.9	-42%
Upper Karkheh	1995	145.4	85.6	- 59.8	-41%

As presented in Table 6.3, all the sub-basins experienced a reduction in precipitation and an increase in evapotranspiration from the pre- to post-change period. The Qarasou sub-basin showed the most severe decline in average annual precipitation (-19%) while, the Kashkan sub-basin experienced minimum change in precipitation (+1%) relative to other sub-basins.

Table 6.3 Observed E_0 and P during the pre- and post-change periods. Number 1 and 2 denote pre-change and post-change period, respectively

Sub-basin	E_{01}(mm)	E_{02} (mm)	ΔE_0	P_1 (mm)	P_2 (mm)	ΔP
Qarasou	2098	2206	+5%	473	381	-19%
Gamasab	2021	2277	+13%	494	432	-13%
Kashkan	2202	2597	+18%	480	474	+1%
Seimareh	2073	2240	+8%	446	382	-14%
Upper Karkheh	2138	2344	+9%	454	393	-13%

6.2.1 The Budyko model

In order to confirm the steady state condition for the Budyko model, it was investigated if long-term water storage change in the case study is negligible. The ABCD model code was developed in R, and the embedded genetic algorithm (GA) provided the best set of parameters (i.e., a, b, c and d) for the model. The objective function for GA were Kling-Gupta efficiency (KGE) and Nash-Sutcliffe Efficiency (R_e), between monthly observed streamflow and monthly estimated streamflow (Table 6.4).

Table 6.4 The ABCD model performance for the KRB (Upper Karkheh sub-basin)

	KGE	Re
ABCD model	0.76	0.63

The ABCD model showed that the average amount of water storage change (ΔS), over the study period, is negligible (-0.17 mm) confirming that the steady state condition for the KRB is applicable (Fig. 6.2).

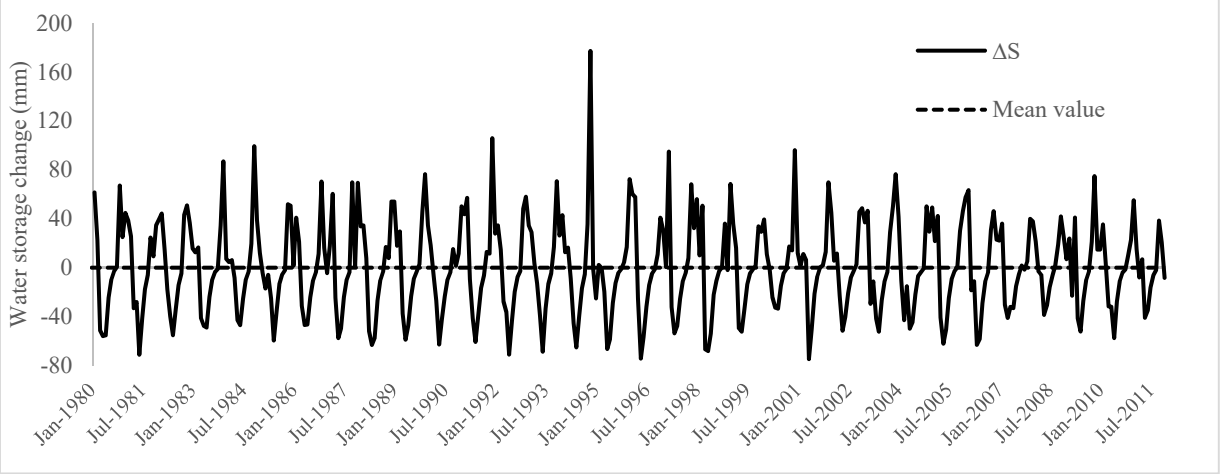

Fig.6.2 Estimated monthly water storage change in the main KRB using ABCD model

Consequently, the parameters of precipitation elasticity (ε_P) and evapotranspiration elasticity (ε_{E0}) were calculated using Eqs. (4.6 and 4.7) (Table 6.5). The higher values of ε_P in comparison to ε_{E0} for all sub-basins suggest that the hydrological responses of the sub-basins are more sensitive to the variation in precipitation than evapotranspiration. The negative ε_{E0} indicates that evapotranspiration and streamflow are oppositely related.

Table 6.5 Values of elasticity parameters for the KRB sub-basins

Basins	ε_P	ε_{E0}
Qarasou	1.61	-0.61
Gamasab	1.81	-0.81
Kashkan	1.50	-0.50
Seimareh	1.65	-0.65
Upper Karkheh	1.60	-0.60

6.2.2 Hydrological modelling

The evaluation indices presented in Table 6.6 implies that the HBV model was well calibrated for the pre-change period with the poorest performance observed for the Kashkan sub-basin ($R_e = 0.57$), which seems to be a result of observed data quality.

Table 6.6 The HBV model Calibration performance for the KRB sub-basins

Basin	Qarasou	Gamasab	Kashkan	Seimareh	Upper Karkheh
R_e Calibration	0.77	0.75	0.57	0.77	0.68
δ (mm/year)	2.0	-8.0	11.0	5.0	0.0
KGE	0.88	0.88	0.68	0.82	0.79

The HBV modelling result for the ΔQ_c and ΔQ_h is presented in Table 6.7. It is shown that for all sub-basins with the exception of Kashkan, the streamflow reduction is mostly caused by the climate change. For the case of Kashkan, the streamflow reduction due to regional human activities (ΔQ_h) is significantly higher than ΔQ_c. As can be seen in the table, the ΔQ_c and ΔQ_h from the HBV model and the Budyko method varied between the sub-basins, but for any given sub-basin the results were compatible.

Table 6.7 Comparison between Budyko and HBV model for estimating streamflow changes in the KRB sub-basins

Basins	Breakpoint	ΔQ (mm)	Budyko		HBV	
			ΔQ_c (mm/year)	ΔQ_h (mm/year)	ΔQ_c (mm/year)	ΔQ_h (mm/year)
Qarasou	1995	68.1	41.8	26.3	40.6	27.5
Gamasab	1995	50.1	27.7	22.4	25.9	24.2
Kashkan	1993	47.7	15.3	32.4	14.4	33.2
Seimareh	1995	51.9	29.6	22.3	28.9	23.0
Upper Karkheh	1995	59.8	32.2	27.6	30.9	28.9

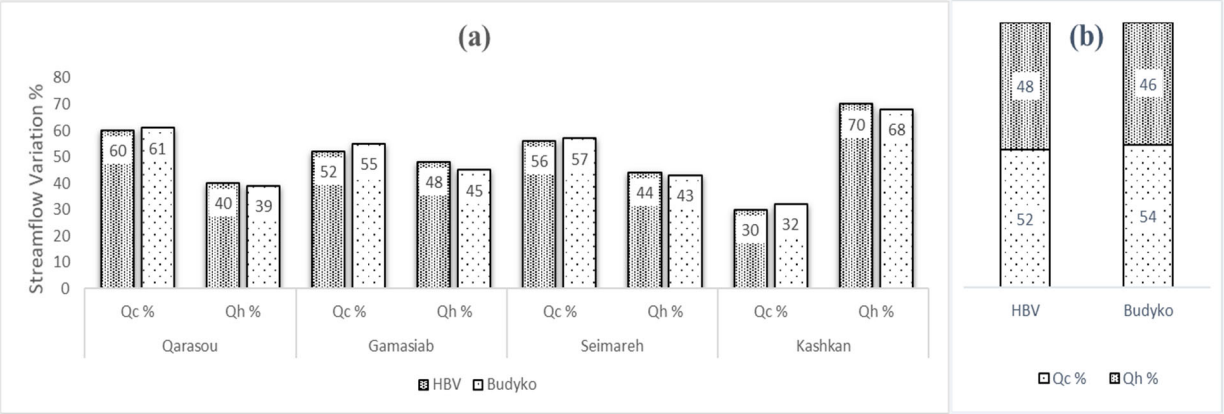

Fig.6.3 a) Streamflow changes for all sub-basins due to climate variability and human activities. b) Streamflow variation (%) for the entire KRB due to climate variability and human impacts. Qc and Qh denote climate change and human activities, respectively

Figure 6.3 (a and b) provides a visual comparison between the implemented methods. Results for the Seimareh sub-basin are the cumulative response of the two upper sub-basins, Qarasou and Gamasiab, and Seimareh. These findings indicate that both climate change and human activities have strong influence on streamflow changes in the sub-basins. However, the impact of climate change on the stream flow changes is observed to be more substantial than that of human activities in most of the sub-basins.

6.2.3 Land use change

The land cover change during the study period was investigated using Landsat 5 TM as it is the only satellite mission that provides images dating back to the 1980s. Three years of 1987, 1995, and 2012 were selected to present the land use condition of KRB representing three phases of pre-change, transition, and post-change periods, respectively. Five types of land use were detected in the study area encompassing i) irrigated (merged with about 5–10% rangelands and pasture area), ii) rainfed (merged with about 10–20% irrigated and rangeland and pasture area), iii) range and pasture, iv) forest (merged with about 10–20% rangeland and pasture area), and v) urban (includes buildings and orchards).

Figure 6.4 shows a noticeable expansion of irrigated farmlands in the basin during the three investigated years. Before the breakpoint, the majority of rainfed and range and pasture were located in the mountainous region of the basin (mainly in northern parts of the KRB). Forests, mainly, covered the middle and south eastern parts of the basin, while irrigated areas were scattered in the northern parts (Fig. 6.4a). By 2012, after the breakpoint as presented in Figure

6.4c, a noticeable portion of rainfed farmland has been converted to irrigated farmlands throughout the basin.

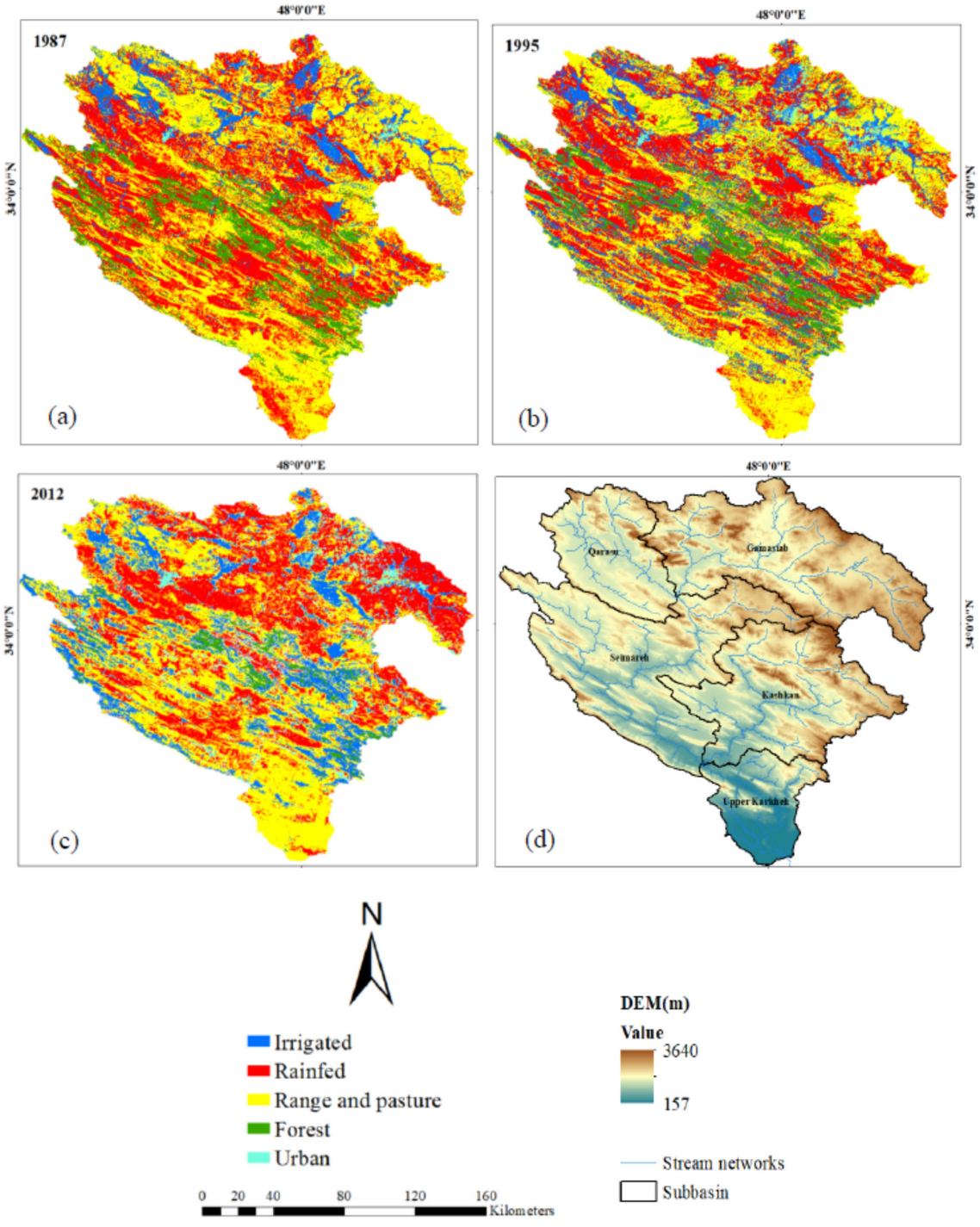

Fig.6.4 Land use maps for the KRB, (a) before breakpoint (1987), (b) transition (1995), and (c) after breakpoint (2012), and (d) the digital elevation map

The LULC maps show that the KRB was initially covered predominantly by range and pasture and rainfed farms. Although the basin is still covered, mostly, by the same land use types, the area of the classes has changed since 1980s (Table 6.8).

According to Tables 6.8 and 6.9, land use change (~70% reduction in dense forest area and 100% increase in irrigated farms), accompanied with a 13% decline in rainfall, led to more than 40% streamflow reduction for the entire basin implying impacts of both climate change and human activities. The present study suggests that all sub-basins in the KRB experienced a major abrupt change of streamflow during the 1994–1995 period, which coincides with the period of dam construction in the basin.

Table 6.8 Percentage of land use class change in the five KRB sub-basins in the three selected years 1987 (before breakpoint), 1995 (transition), and 2012 (after breakpoint)

Sub-basin	Land use Type	1987 (%)	1995 (%)	2012 (%)
Seimareh	Irrigated	1.37	4.49	6.88
	Rainfed	11.84	10.91	8.39
	Range and pasture	10.71	9.81	12.24
	Forest	4.77	3.42	1.08
	Urban	0.09	0.17	0.24
Qarasou	Irrigated	2.29	2.66	2.98
	Rainfed	5.02	5.55	4.92
	Range and pasture	4.87	4.07	4.61
	Forest	0.57	0.41	0.13
	Urban	0.11	0.15	0.19
Gamasiab	Irrigated	4.28	5.11	5.91
	Rainfed	7.62	8.09	13.00
	Range and pasture	14.16	11.41	6.73
	Forest	0.32	0.89	0.04
	Urban	0.46	1.35	1.12
Kashkan	Irrigated	1.12	2.82	6.80
	Rainfed	9.12	8.33	5.58
	Range and pasture	7.81	7.09	8.50
	Forest	4.10	3.85	1.15
	Urban	0.05	0.11	0.23
Upper Karkheh	Irrigated	0.09	0.90	1.08
	Rainfed	2.09	1.59	0.85
	Range and pasture	6.34	6.40	7.15
	Forest	0.74	0.37	0.07
	Urban	0.05	0.05	0.12

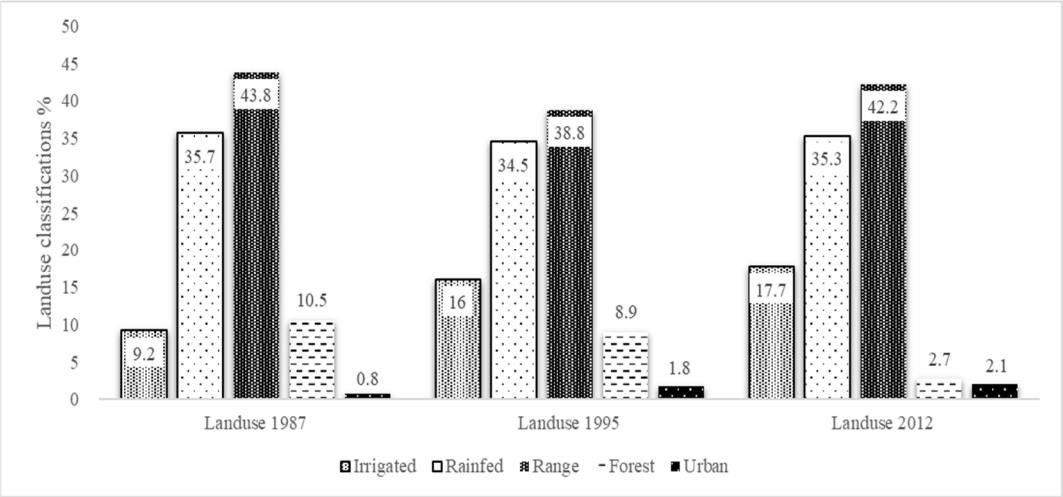

Fig.6.5 From left to right, the KRB land use classifications before breakpoint (1987), transition (1995), and after breakpoint (2012) periods

Table 6.9 Total percentage of Land use classes for the KRB basin during the three selected years

Land use class	Year		
	1987	1995	2012
Irrigated (%)	9.2	16.0	17.7
Rainfed (%)	35.7	34.5	35.3
Range and pasture (%)	43.9	38.8	42.3
Forest (%)	10.5	8.9	2.7
Urban (%)	0.8	1.8	2.1

Figure 6.5 and Table 6.9 show that the forest area significantly decreased from 1987 to 2012, while the size of both irrigated areas and urban areas increased noticeably during the study period. Deforestation occurred in the south-eastern part of the basin, in the Kashkan sub-basin. Increasing urban area can influence the hydrological cycle of a basin dramatically by decreasing infiltration, vegetation cover, and changing the water consumption (Dey, 2017). On the other hand, urbanization and deforestation result in decreased groundwater recharge and groundwater level. The spatial decline of groundwater level can have a major impact on the surface water flow through surface water-groundwater interaction.

The calculated land use map, together with the results from the Budyko and HBV methods, suggests that the streamflow decrease in Kashkan sub-basin is mainly related to human activities rather than climate change. In the case of Upper Karkheh sub-basin, in addition to the cumulative response of the upstream sub-basins, the Karkheh dam plays a major role in streamflow reduction. Based on a study conducted by Ahmad et al. (2010), annual actual evapotranspiration varies from 41 to 1,681 mm/year throughout the basin, with the highest

rate for the Karkheh dam (Ahmad and Giordano, 2010), which indicates the substantial impact of the dam on basin-wide water balance.

6.2.4 Uncertainty analysis

The use of hydrological models is usually accompanied with uncertainty estimation related to the input of observed data or model structure. In order to adequately simulate a hydrological response at the basin level, accurate data such as climate variables (precipitation, E, etc.) and the basin's physical characteristics (topography, land coverage, vegetation, etc.) are vital. In climate change related studies, in which the study period is on the scale of decades, it is often difficult to obtain uniformly distributed and accurate data sets (Kapangaziwiri et al., 2009). In the KRB, specifically, part of the uncertainty may arise from observed rainfall, potential evapotranspiration, and streamflow data. The weather gauges are usually not uniformly distributed in the entire basin. Moreover, elevation and topography of the basin can introduce bias to the observation time series, which can subsequently affect the runoff simulation (Rientjes et al., 2013). In order to investigate uncertainty, we used 10 best GA-produced parameter-sets to simulate the streamflow. For each set, we calculated the separate impacts of climate change and human activities. If the results for the sub-basins remain consistent, despite the change in parameters, the uncertainty is not significant and can be ignored (Masih et al., 2010). Table 6.10 shows that the streamflow change due to climate change and human activities, does not vary significantly. The highest range of change is less than 3.5% of the streamflow for all sub-basins.

Table 6.10 The HBV model responses to the changes in the calibration parameters

Sub-basin	min ΔQ_c (mm/year)	max ΔQ_c (mm/year)	min ΔQ_h (mm/year)	max ΔQ_h (mm/year)	Variation%
Qarasou	39.8	40.6	27.5	28.3	1.0
Gamasab	25.9	27.6	22.5	24.2	3.3
Kashkan	14.4	16.2	31.4	33.2	3.5
Seimareh	28.9	29.5	23.0	22.4	1.1
Upper Karkheh	30.9	32.5	28.9	27.3	2.7

While the Budyko method is more convenient and efficient, the potential evapotranspiration and precipitation can introduce uncertainty to the results. Precipitation measurement was calculated by using Thiessen method within the sub-basins, which is, basically, a simplification of the spatial variability of the input water to the system. Due to the lack of

uniformly distributed E_0 stations, a regression method was used for the case of E_0 data, which again can introduce possible error to the modelling result. To address these issues, a sensitivity analysis of the Budyko equation with respect to the precipitation and evapotranspiration inputs was carried out. Table 6.11 presents possible sources of error in the streamflow estimation, as a result of a 10% alternation in Budyko parameters (i.e., P, E_0, n), for each sub-basin. For instance, the results suggest that a 10% change in the input precipitation data leads to a 3–5% error in streamflow estimation. On the other hand, the results indicate that the streamflow is not as sensitive to the possible error in evapotranspiration data.

Table 6.11 The KRB Streamflow changes due to 10% error in the Budyko parameters

Basins	ε_p	ε_{E0}	n	$\bar{Q}$ (mm/year)	$\bar{P}$ (mm/year)	$\overline{E_0}$ (mm/year)	$dQ_p\%$	$dQ_{E0}\%$	$dQ_n\%$
Qarasou	1.61	-0.61	0.8	111	424	2155	4.3	-0.32	2.3
Gamasab	1.81	-0.81	0.99	81	461	2157	3.3	-0.32	2.7
Kashkan	1.50	-0.50	0.7	158	477	2437	5	-0.32	1.3
Seimareh	1.65	-0.65	0.83	97	412	2162	3.9	-0.3	2.1
Upper Karkheh	1.60	-0.60	0.77	114	422	2248	4.5	-0.32	2.0

Most climate studies in the region have investigated the future hydrological response of the KRB basin under different climate scenarios (Abbaspour et al., 2009; Jamali et al., 2013; Emam et al., 2015). A handful of studies investigated water availability in the basin (Masih et al., 2010; Masih et al., 2012) and displayed significant decrease in streamflow of KRB during the recent decades. For illustrating streamflow changes, the Flow Duration Curves (FDCs) and mean monthly flow for the pre- and post-change periods are provided in Figures 6.6 and 6.7.

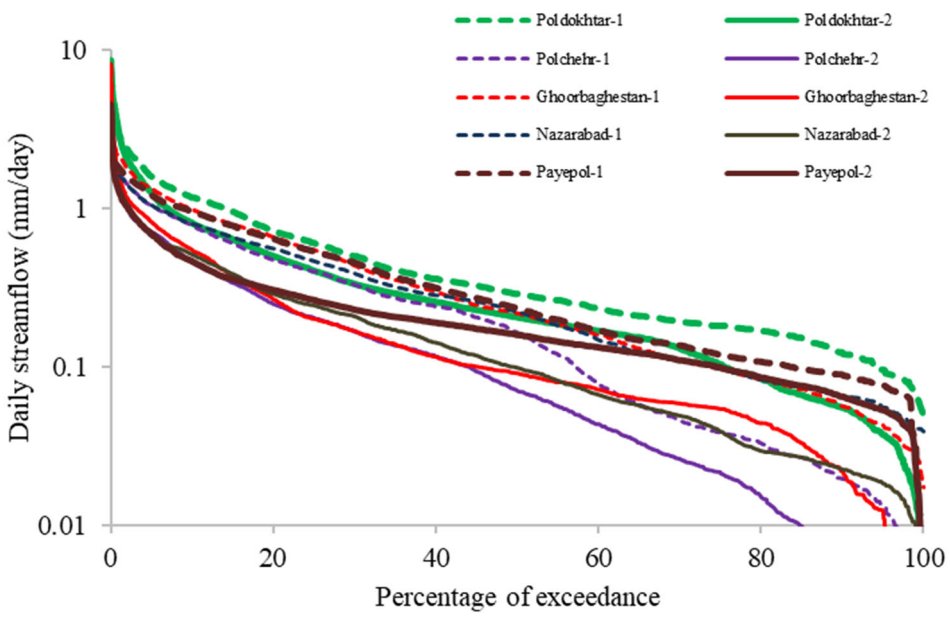

Fig.6.6 FDCs of the studied sub-basins in the KRB for pre-change (1) and post-change (2) periods

Whilst the findings of this study confirm the streamflow reduction in all sub-basins, a closer look at the flow duration curve (FDC) revealed significant reduction in both high flow (i.e., streamflow with the exceedance probability of 5% (Q5)) and low flow (i.e., streamflow with the exceedance probability of 95% (Q95)) (Fig.6.6). For instance, the mean daily streamflow decreased by one-third during 50% of the of exceedance probability in the Payepol station (Fig. 6.6). The mean monthly flows in the sub-basins also experienced a major reduction for all months (Fig.6.7), with the exception of the Payepol station, in which the streamflow showed an increase in the summer months (June-August) in the post-change period.

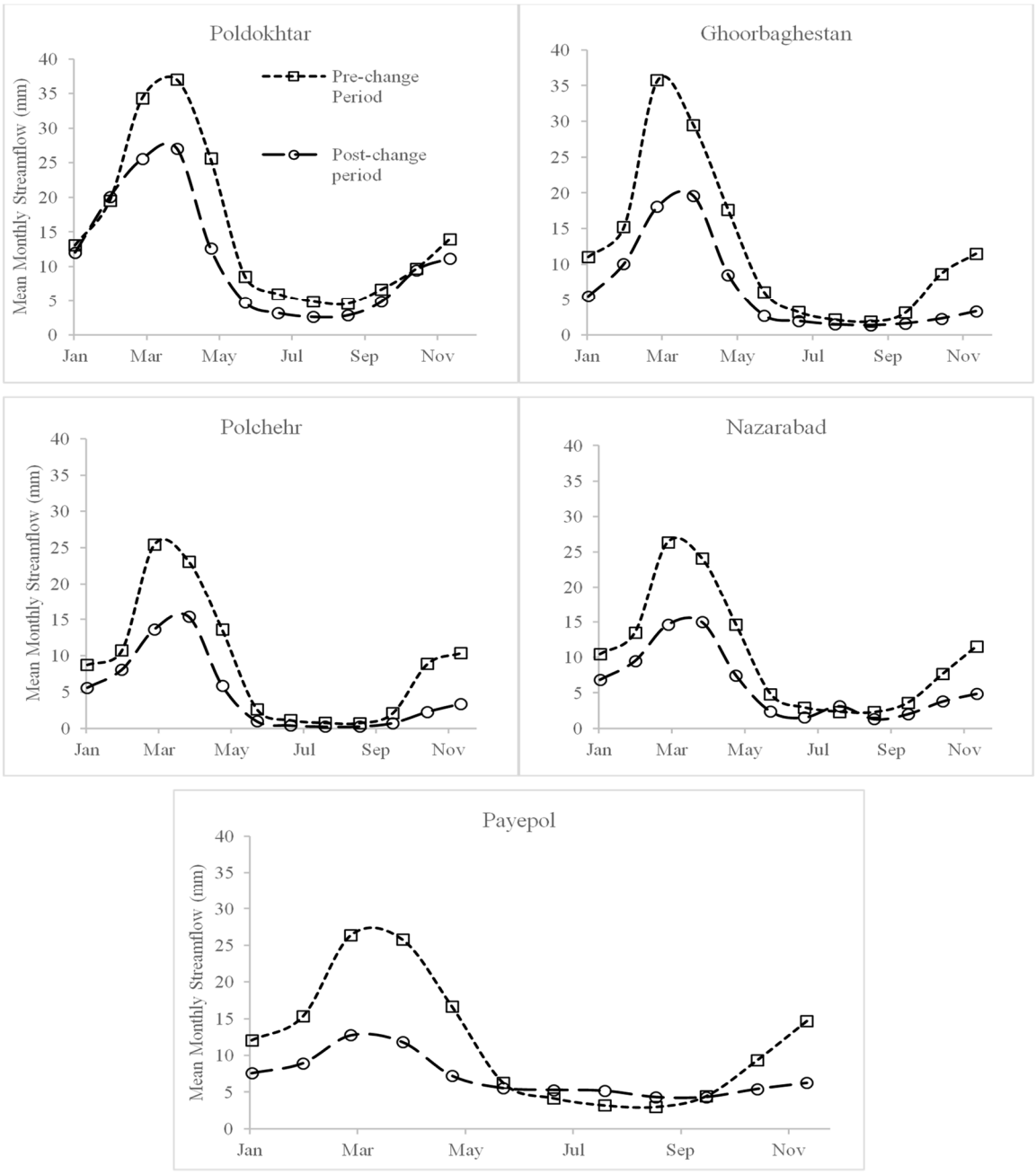

Fig.6.7 Mean monthly streamflow of the studied sub-basins in the KRB during pre-change (1) and post-change periods (2)

This might be the result of river flow regulation due to the operation of the Karkheh Dam since 2001. The reservoir water, which is stored during abundance, is released in the summer season. Therefore, an increase in summer flow does not necessarily mean an increase in natural streamflow throughout the basin. Moreover, for the Kashkan sub-basin, the difference between streamflow in the pre- and post-change periods, during late autumn and winter (October-February) was less than that of the other sub-basins. For the summer months (June-August), on the contrary, largest differences between pre- and post-change period streamflow

was observed in Kashkan sub-basin (Fig.6.7). It can be postulated that intensive agricultural activities in the area led to a higher actual evapotranspiration and, therefore, the larger difference between the streamflow during the two periods.

A handful of studies that investigated the small-scale sub-basins hydrological processes of the KRB, revealed notable land use changes during the 1990's. For instance, Karimi et al. (2018) observed dramatic increase of irrigated farms and urban areas during the 1992-2015 period in the Ravansar basin within the Qarasou sub-basin. Based on personal discussions with local authorities in Kashkan sub-basin, there was a substantial investment in expanding agricultural lands in this basin during the 1990s. The primary purpose of this investment was to create jobs for locals. Kashkan, with a rural population of almost 300,000 is the most densely populated sub-basin in the KRB. The population density and development of agricultural lands are in line with the result of this study, suggesting that human influence is a dominant factor in streamflow reduction in this specific basin. The Seimareh sub-basin also experienced extensive agricultural development during the study period (Table 6.8).

Developing water distribution systems and the construction of reservoirs in the KRB have improved food production and provided easier lives for the residents of the area. However, it has dramatically disturbed the water cycle in the basin. The KRB is considered a semiarid to arid region, which is vulnerable to water scarcity. Increasing human population, agricultural and industrial activities, and urbanization demands, combined with the governmental policy of being self-sufficient in food production, have put additional pressure on the water resources in the area (Ahmad et al., 2009; Masih, 2011). Any change in LULC can lead to significant change in the basin-wide water balance by impacting, for example, groundwater storage, soil infiltration, and actual evapotranspiration (Mekonnen et al., 2018; Hashemi et al., 2013).

The population of the KRB is predicted to increase to 4.8 million by the year 2025, out of which 75% will live in urban areas. Urbanization in the northern sub-basins will increase the strain on water resources in the basin, while in the southern part of the basin, dam constructions and 300,000 ha planed irrigation programs would be overwhelming for the groundwater and surface water resources (Marjanizadeh et al., 2010). Accordingly, policymakers should carefully follow any change in the quality and quantity of the available freshwater and changes in the hydrological behaviour of the stream flows. We believe the implemented method in this study is easy to replicate and does not need extensive observed data, which makes it a competitive approach to adapt, especially in the basins with limited data. Despite the timescale differences considered in the calculations (annual timescale for

Budyko method and daily timescale for hydrological modelling), the results of both methods, were highly consistent, with a minimum underestimation of climate change by the HBV model compared to the Budyko method.

6.3 Conclusion

This paper introduces a new framework for analysing and separating contributions of climate change vs human activities to streamflow changes in the large and data-scarce basins. It relied on a relevant case study in a semi-arid climate of Iran for validating the methodology. A new element used in the framework was the recently developed DBEST method for detecting significant breakpoints in the historic hydrological time-series. Observable impacts of human activities in the form of land use change, obtained from satellite remote sensing, were additionally used for verification of the results of Budyko and HBV. Sensitivity and uncertainty analyses were applied to these two methods, respectively. It was shown, by both Budyko and HBV that in most of the studied sub-basins, climate change and human activities (i.e., agriculture, deforestation, and water diversion) were more or less equally responsible for the streamflow reduction. Land use maps based on Landsat 5 TM images suggested significant changes in land cover throughout the basin for the study period between 1980 and 2012. While it might be difficult to locally manage the impact of climate change (as it is likely to be affected by the global scale changes), existing knowledge of the regional scale anthropogenic impacts on water quantity, as suggested by the framework, can provide an insight that leads to informed management plans, such as improved irrigation techniques, nature based solutions, and urbanization control, to limit the adverse impacts of human activity on streamflow. This in turn can compensate the adverse impact of climate changes by adapting to a changing climate. On the other hand, the lack of such framework in the hydrological studies may result either in wrongly condemning climate change as the only important factor contributing to the most hydro-agricultural and environmental problems or in confusing the regional policymakers to cope with the problem efficiently based on the less likely assumptions. Therefore, the outcomes of this study can also be used to assist policymakers and water professionals in proposing a proper water management plan to prevent the further reduction of streamflow. More specifically, for the KRB, where the contribution of regional scale human activities are almost equal to the impact of climate change, it can help to offer appropriate urban and rural development plans, ecological restoration, conservation projects, regulation of water for irrigation, and sustainable management based on regional decisions in the basin

and even sub-basin scales. In the case that the current water management and ecosystem planning remains unchanged, the impacts of climate change and human activity may severely damage the stability of the ecosystem of the entire basin.

Approach 2:

Short-term streamflow analysis

Chapter 7
Integrating groundwater change into the Budyko model

7.1 Background

As discussed so far, the Budyko model is a useful method to track streamflow change, however, because it is based on the steady state assumption of catchment water balance, the model is not suitable for inter-annual studies where water storage change is not negligible. Therefore, in the second approach, the monthly and inter-annual performances of the extended version of the Budyko model (i.e., Budyko-Du) is employed. To be able to perform the analysis, it is necessary to investigate and understand the groundwater level change in the study area.

Groundwater produces almost 30% of known freshwater resources worldwide and almost 96% of non-solid freshwater (Green et al., 2011). As groundwater is less sensitive to the immediate climate change, it is a great water source to overcome droughts and mitigate climate change impacts on limited freshwater resources. However, excessive groundwater discharge and lack of enough recharge threaten the existence of these precious freshwater systems (Green et al., 2011). Three main recharge mechanisms affecting groundwater system are direct recharge (e.g., infiltration resulted from precipitation), indirect recharge (e.g., infiltration from surface water), and localized recharge (e.g., concentrated surface water such as lakes and agricultural area) (De Vries and Simmers, 2002). In the case of Harvey catchment, where studies show the precipitation has decreased during the last decades, sandy soil structure of the area makes precipitation infiltration the only reliable means to replenish the water table. Groundwater consumption routine, on the other hand, has changed dramatically, from a very limited percentage during the 1960s to almost equal as surface water in 1985. Nowadays, more than 75% of water originates from groundwater in the area. Excessive water withdrawal for domestic, agricultural and industrial purposes, has affected the GWL, and therefore, has manipulated the dependent ecosystem (Ali et al., 2012; CSIRO, 2009).

Regularly monitoring program is usually conducted to understand the changing pattern of groundwater and help proposing effective groundwater management and decision-making plans. However, due to the costs and accessibility, only limited sites are monitored, resulting in sparse data series over the catchments, and even more seriously, discontinuous sites and missing observations within sites. The lack of regular measurements, which result in spatial

and temporal data gaps, can disturb our understanding of the catchment (Ruybal et al., 2019; Varouchakis and Hristopulos, 2013).

7.2 Spatiotemporal modelling

To better understand the status and changing patterns of groundwater levels for both management and research purposes, uniformly distributed groundwater levels are necessary but only can be achieved by filling the gaps (that is, estimating the missing values) through interpolation methods (Varouchakis and Hristopulos, 2013). Due to the changing environment, geohydrological parameters, such as groundwater, is subjected to change with time and space (Varouchakis and Hristopulos, 2019). To accurately take account of these changes, the employed method should consider the interdependency between temporal and spatial aspects of the parameters. From modelling perspectives, simultaneously use of both the irregularly sampled spatial and temporal data can best use the available information. One of the popular interpolation methods is spatiotemporal kriging which has been applied to variables in different catchments and is used for this purpose. In spatiotemporal interpolation kriging, the variability of the parameter in space and time is modeled by adding the temporal element to the spatial domain. In kriging method, spatial and temporal dependency of the parameter is modeled with variograms. Hence, selecting optimal variograms is the first step and one of the most important steps for producing an accurate spatiotemporal model. Variogram models spatial, temporal and spatiotemporal correlation with the regressors, and also provides essential parameter values (i.e., sill, nugget and range) for spatiotemporal kriging. In spatiotemporal kriging, the temporal and spatial variograms are not necessary the same. Even a simplest anisotropy in the spatiotemporal parameter might lead to mismatching variograms (Pebesma and Heuvelink, 2016; Voss et al., 2016). Earlier variograms were built of separate spatial and temporal elements and then joined together by addition or multiplication to form the final spatiotemporal variogram. These separable models are simpler but based on unrealistic assumptions (Varouchakis and Hristopulos, 2019). Therefore, non-separable variograms have been developed and used in many fields including hydrogeology. In this study both separable and non-separable variograms are used and their performances are compared.

In this chapter, the Spatiotemporal Regression Kriging method (Rkriging) is adopted to derive a spatiotemporal pattern for Harvey-Forrest Catchment in Western Australia, using the limited groundwater data in the catchment, where the historical observed data were spatially and

temporally irregular. This catchment is selected as a case study because of its importance, size, location and level of groundwater. The temporal and spatial availability of the data is highly non-uniform in the catchment. As presented in Fig.7.1, monitoring wells are unevenly scattered through the catchment. In the south-eastern part of the catchment, for instance, there are very few wells available.

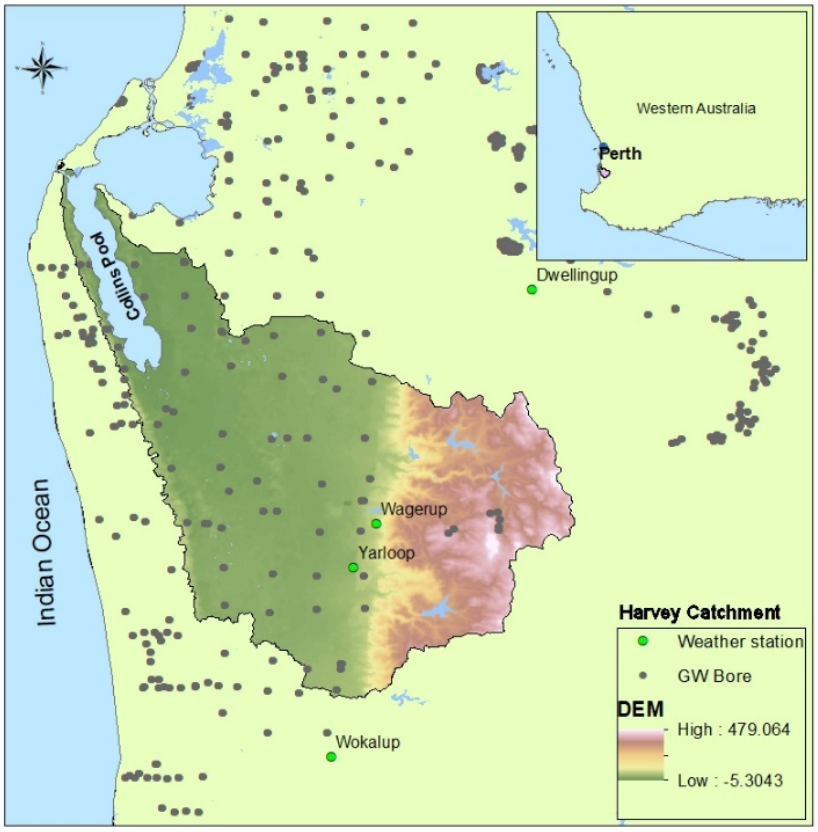

Fig.7.1 Locations of groundwater bores and weather stations in the Harvey Catchment, WA

The temporal distribution of the data is also not uniform. Many wells were operating only for limited years, some of the wells provide annual data and some monthly data (Fig.7.1). As presented in Fig.7.2, very few information is available in some years (e.g., 2000-2008). In this study, it is assumed that the temporal trend within the study period is continued and not affected by dramatic human-induced changes.

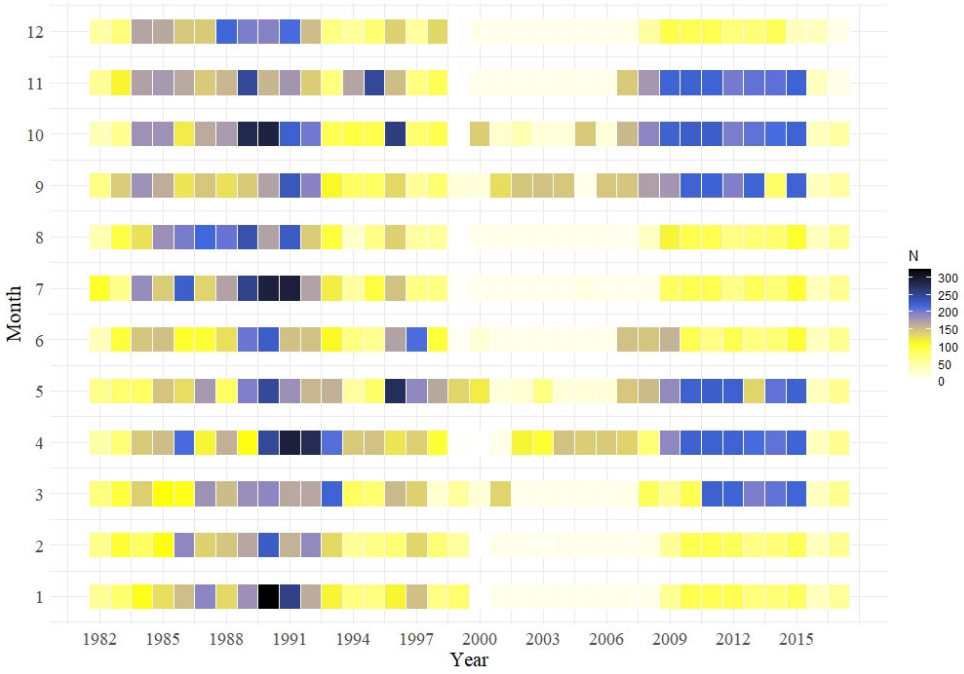

Fig.7.2 Heatmap of the available data showing non-uniform temporal distribution of the GWL information in the Harvey Catchment. N is number of available data in a month

The accuracy of the estimation is investigated using the Leave-One-Out Cross-Validation approach. Time-series analysis (i.e., auto-correlation and cross-correlation) is then employed to provide a better understanding of the estimated groundwater level change over time. To gain insight into the change of groundwater levels, the correlation between groundwater level (GWL) and rainfall pattern with possible time-lag is explored.

The Rkriging method produces spatiotemporal maps for the Harvey-Forrest catchment to track the groundwater change during the study period (1982-2017). To choose the best spatiotemporal variogram (STvariogram), for a given sample set, several variograms are compared and to find the optimum number of spatial and temporal observations, different spatiotemporal sampling sizes are investigated. The whole catchment is divided into fine grids and for each grid a monthly timetable is provided to overcome non-uniformity due to the temporal and spatial gap in the observed data.

As the catchment information (such as location and elevation) can be highly corrected, direct use of this data may make the model too sensitive. Correlated covariates can manipulate the significance of the variables and their interdependence. It can make the estimation sensitive to minor changes and introduce imprecise regression coefficients and high errors to the model. Therefore, Principal Component Analysis (PCA) is performed to prevent multi-collinearity in the covariates and to avoid information overlapping. The PCA is a common method that

transforms the covariates into orthogonal and uncorrelated components. It removes less important covariates and reduces them to a limited number of variables, which explain most of the variance (Ruybal et al., 2019). The stepwise regression algorithm is, also, used to select the most significant regressors. The accuracy of the Rkriging method is examined by the Leave-One-Out-Cross validation technique.

After studying GWL change in the catchment, it is interesting to explore the possible reason behind the change. Although rainfall is one of the main factors affecting groundwater level, its impact on GWL is not fully understood (Kotchoni et al., 2019), mainly due to lack of enough GWL information and complicated structure of groundwater. Time-series analysis (i.e., cross-correlation and auto-correlation) is a common approach to investigate correlation between hydrological time-series (Cai and Ofterdinger, 2016; Duvert et al., 2015; John and John, 2019; Kim and Lee, 2017; Lee et al., 2006; Lehmann and Rode, 2001; Shi et al., 2019). The cross-correlation analysis provides useful information regarding the significance and the first response of the groundwater resources to rainfall. Auto-correlation analysis, on the other hand, reveals structure of the time-series and impact of memory effect. In this paper, the correlation between the estimated groundwater and observed rainfall time-series with possible lags is examined at a randomly selected number of points, to investigate the interdependency between groundwater level and rainfall time-series, and detect any possible time-lag.

Spatiotemporal Regression Kriging (Rkriging) predicts the spatial and temporal links between observed values. In this method, the regression (deterministic) and residual (stochastic) parts of the model are analyzed separately (Eq. (7.1)).

$$Z(s,t) = m(s,t) + \varepsilon(s,t) + r \qquad (7.1)$$

where Z(s, t) is the observed groundwater level at space and time, m(s, t) is the trend (deterministic) component, ε(s, t) is residual (stochastic) component of the model, which is the spatiotemporally auto-correlated residual for every (s, t) ∈ S × T , and r is the uncorrelated noise (Hu et al., 2017; Ruybal et al.,2019). The regression method is applied to predict the values on a fine grid. This part of the analysis, which called trend analysis, gives a rough estimation for each grid. Then, the residuals are extracted by deducting the trend from the observed data. For the residual part, the best spatiotemporal variogram (STvariogram) is fitted and the interpolated residuals for all grid values are calculated. Finally, the two components (trend and residual) are added back, to provide the final estimation of the GWL (Hu et al., 2017). All of the analysis and codes are performed in Rstudio platform.

7.2.1 RKriging of the residuals

The sample spatiotemporal variogram (STvariogram) is produced using the residuals as follow (Hu et al., 2017):

$$\gamma(h,u) = \frac{1}{2.N(h,u)} \sum_{i=1}^{N(h,u)} [\varepsilon(s,t) - \varepsilon(s+h, t+u)]^2 \quad (7.2)$$

where h is the separation distance for points in space, u is the separation in time, and $N(h, u)$ is the number of paired observations separated by lag (h, u). After defining the sample STvariogram, a model is fitted. Among the several models to estimate STvariogram, separable models, product sum model, and the sum-metric are the most common (Hu et al., 2017; Ruybal et al., 2019; Varouchakis and Hristopulos, 2019). The separable model, belongs to the separable covariance models, assumes that space and time domains of the variogram are separate and treats them independently, while product-sum and sumMetric models, belong to the non-separable covariance models, consider the interaction between space and time components. The advantages of the separable models are computationally fast with few parametrization, however these models cannot fully grasp the complicated interaction between the spatial and temporal components (Hengl et al., 2012, Geniaux, 2017, Varouchakis and Hristopulos, 2019). Therefore, in the current study, models from both separable and non-separable groups are selected and the results are compared to choose the best fit for the sample (empirical) spatiotemporal variogram.

7.2.2 Leave-One-Out Cross-Validation (LOOC)

To investigate the accuracy of the regression kriging, the Leave-One-Out Cross-Validation (LOOC) method is applied. A code is developed in R to perform the spatiotemporal cross validation. During this process, each space-time data is removed once, while the remaining data predicts the value of the removed point. This process is repeated for all values in the data pool. Finally, the predicted values and observed values are compared (using Root Mean Square Error (RMSE)) to examine the accuracy of the prediction (Learning E.O.M, 2010).

7.2.3 Principal Component Analysis (PCA)

In this study, the built-in R functions prcomp() is used to perform the PCA. This function determines rotation and shift of the original data to a new coordinate system, in which the covariates are independent. For the current work, the two groups of covariates for PCA analysis are Harvey digital elevation model (DEM) and the extended boundary of the

catchment (i.e., Longitude and Latitude of the catchment), as suggested by (Ruybal et al., 2019).

7.2.4 Time-series Analysis

Time-series analysis is carried out, for forty randomly selected grid points, to better understand interrelationship between estimated GWL and ΔGWL, and rainfall time-series. The Cross-Correlation function (CCF) provides time-lag between the input and output, which suggests the response time of the output time-series. Equations 7.3 and 7.4 represent the mathematical expression of the CCF (Cai and Ofterdinger, 2016; Shi et al., 2019).

$$C_{xy}(k) = \frac{1}{n}\sum_{t=1}^{n-k}(x_t - \bar{x}).(y_{t+k} - \bar{y}) \quad (7.3)$$

$$\gamma_{xy}(k) = \frac{C_{xy}(k)}{\sigma_x \sigma_y} \quad (7.4)$$

where *Cxy(k)* is the cross-covariance between x_t (input time-series) and y_t (output time-series), *k* and *n* are the time-lag and the length of the time-series, respectively, and σ is the standard deviation of *x* and *y*.

The Auto-Correlation Function (ACF), on the other hand, is cross-correlation of the time-series with itself, at different time-lags. This parameter provides the "memory effect" of the dataset, which shows interdependency of the time-series to its historical values. For an uncorrelated time-series, the ACF shows sharp decrease within a short period, while a gradual decline shows strong interdependency and a long memory effect (Cai and Ofterdinger, 2016; Larocque et al., 1998).

7.3 Groundwater change detection

The study area is divided into 450×450 meter grids. For each grid a monthly temporal data-frame is provided to produce a uniform spatiotemporal structure and cover the temporal and spatial gaps in the observed data.

7.3.1 PCA calculation

Figure 7.3 is a pair-plot showing the dependency of each pair of the three covariates/ variables (i.e, longitude (Long), latitude (Lat) and elevation or DEM (Elev) of the Harvey Catchment). The lower diagonal shows each pair of variables as scatterplots, on the diagonal is the histogram which shows the Probability Distribution of the variables (PDF), and in the upper

diagonal, their correlations are stated which shows Elevation and Longitude are highly correlated (correlation factor 0.89).

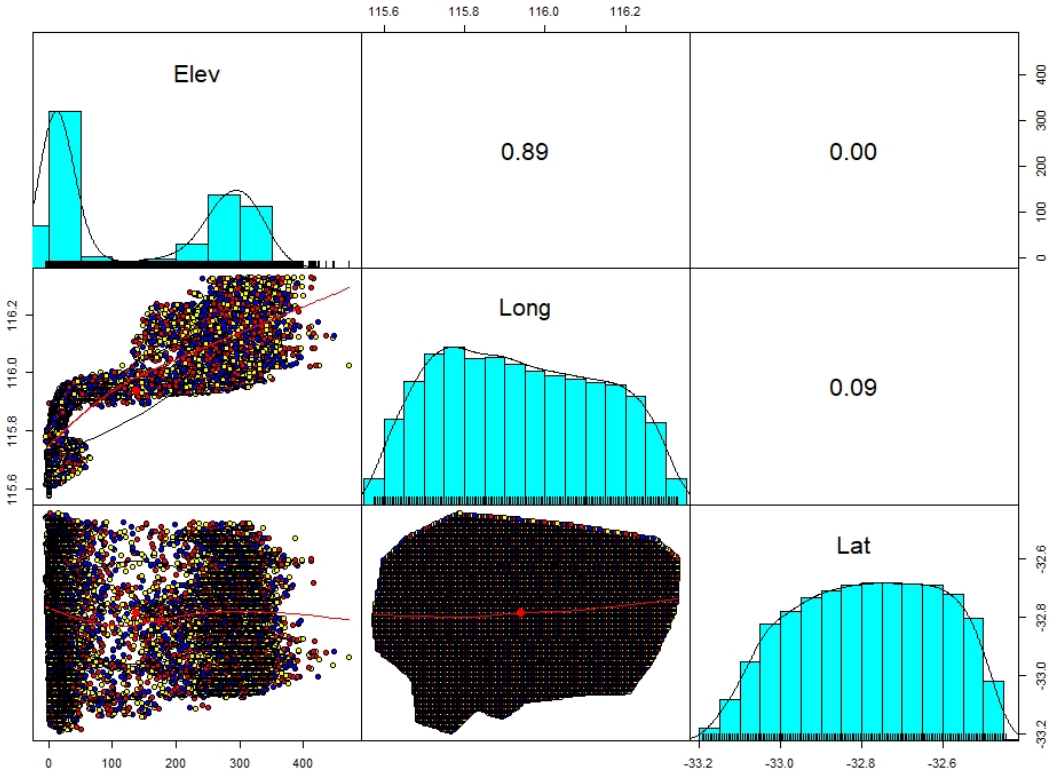

Fig. 7.3 Correlation between the covariates of the Harvey Catchment, WA

Table 7.1 shows the PCA conversion of the original covariates (i.e., longitude, latitude and elevation) explained more than 96% of the variance with two components (i.e. PCA1 and PCA2).

Table 7.1 PCA conversion of the original covariates longitude, latitude and elevation explaining 96% of the variance, Harvey Catchment, WA

Parameters	PCA1	PCA2	PCA3
Standard deviation	1.375	0.9998	0.332
Proportion of Variance	0.63	0.33	0.04
Cumulative Proportion	0.63	0.96	1

As the difference between the variables' ranges and magnitudes might introduce bias to the analysis, all the values were scaled before being projected to the new coordinate system (i.e., PCA provided coordinates). A stepwise regression analysis was performed to provide the subset of optimum regressors, which best describe the trend component. The stepwise regression showed that among the various combinations of the potential predictors (i.e.,

PCA1, PCA2, latitude (Lat), longitude (Long), elevation (Elev), Year the measurement was taken, and Month the measurement was taken), PCA1 and Long give the optimum combination. Hence, the trend component of groundwater level in the Harvey catchment has only the spatial dimension (Eq. (7.5)):

$$m(s) = -4.227 \times Long + 2.398 \times PCA1 + 1740.142 \quad (7.5)$$

Augmented Dickey-Fuller test for stationarity was used to check the stationarity of the input times-series. The test showed that before the trending decomposition the data was non-stationary with P-value = 0.3 and after decomposing and trend deduction, the residual became stationary with the P-value of 0.01.

Figure 7.4 shows the trend component of groundwater level. The trend is constant in time, for each month of the study, as *m* in Eq (7.5) does not have any temporal components. The values are in meter above mean sea level. The green dots are the monitoring wells.

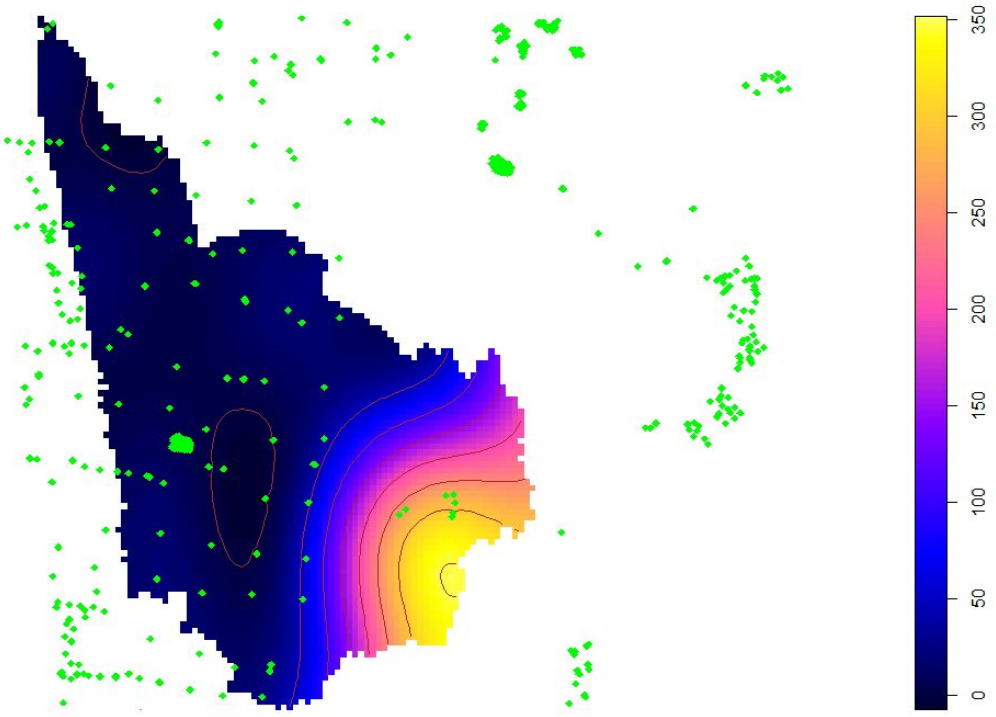

Figure 7.4 Trend component of groundwater level (meter) in the Harvey Catchment, WA

7.3.2 Spatiotemporal variogram (STvariogram) model for residuals

Each component of the STvariogram can be described by a model such as spherical, exponential, Gaussian or power models. Different configuration of these models were tested for three widely used STvariograms (i.e., Separable, Product-sum and Sum-metric), to

determine the best model. The combination of the spherical and exponential model were chosen for spatial and temporal components of the STvariograms, respectively. For the joint component of the sumMetric STvariogram, the Exponential model was the best option (Table 7.2). The initial values of sill, range and nugget were chosen based on the sample spatial and temporal variograms and then adjusted to minimize the mean square error between the sample and modeled STvariogram. In this case study, the directional sample variogram did not show strong anisotropic behavior, therefore the value of anisotropy (k) is set to minimum.

Table 7.2 Parameters of the fitted models and comparison of the goodness of fit to choose the best STvariogram for the Harvey Catchment GWL

Variogram components	Model	Sill (km)	Range (km/day)	Nugget (km^2)	MSE (mean square error)		
					Separable	Product-sum	sumMetric
Spatial	Exponential	60	10	0			
Temporal	Gaussian	50	1000	0			
Joint (only for sumMetric)	Exponential	80	20	40	231	212	209

Fit.StVariogram function in the gstat package was used to fit the model against the empirical variogram from sample. The embedded L-BFGS-B algorithm was used to minimize the error between the model and the sample.

The optimum number of spatiotemporal observations was determined by trial and error method. Comparing the STvariograms with the empirical variogram surface showed that both spatial closeness and number of available data in individual wells, play important roles in accuracy of the variograms. Congested number of wells in one location causes overfitting and scattered temporal data leads to unrealistic variogram. Finally, 641 wells, with at least 10 available temporal data, were selected, for this study.

As suggested in Table 7.2, the two non-separable models perform better than the separable model implying importance of the link between the spatial and temporal domains of the variogram. Among the three employed models, the sumMetric model outperforms the other STvariograms with lower Mean Square Error Value (MSE). The sumMetric model is a combination of sum and metric models (Eq.6) (Derakhshan and Leuangthong, 2006; Dimitrakopoulos and Luo, 1994; Rouhani and Hall, 1989).

$$\gamma_{ST}(s,t) = \gamma_S(h) + \gamma_T(u) + \gamma_J\left(\sqrt{h^2 + (ku)^2}\right) \quad (6)$$

where κ is the spatio-temporal ratio of anisotropy, which combines spatial distances with temporal distances, and $\gamma_S, \gamma_T, \gamma_J$ are the spatial, temporal, and joint components of the STvariograms, with separate nugget effects.

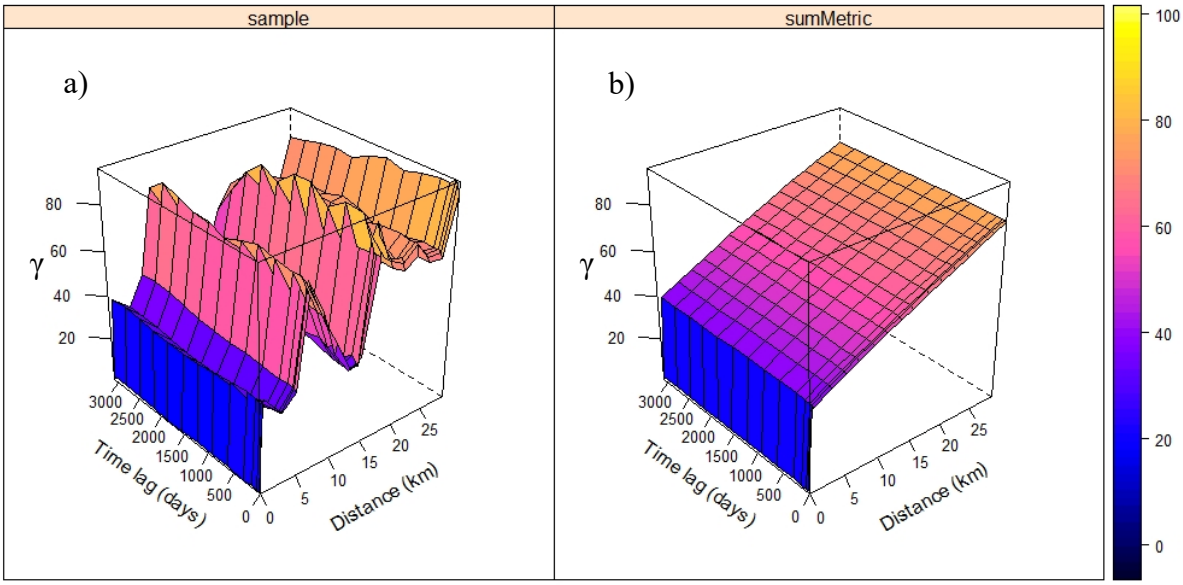

Fig.7.5 a) The empirical surface of the GWL residuals for the Harvey Catchment, WA and b) the fitted spatiotemporal variogram of the residuals (using sumMetric model)

Figure 7.5 compares the empirical surface variogram and the best fitted STvariograms (i.e., sumMetric estimated STvariogram). The general increasing tendency of gamma (γ) with distance suggest that the correlation between the residuals decreases as the distance between the wells increases. The value of γ, however, shows less sensitivity to time-lag. Figure 7.6 presents residual (stochastic) component of the kriging model, in meter, for the selected years of (1982, 1997, 2007 and 2017).

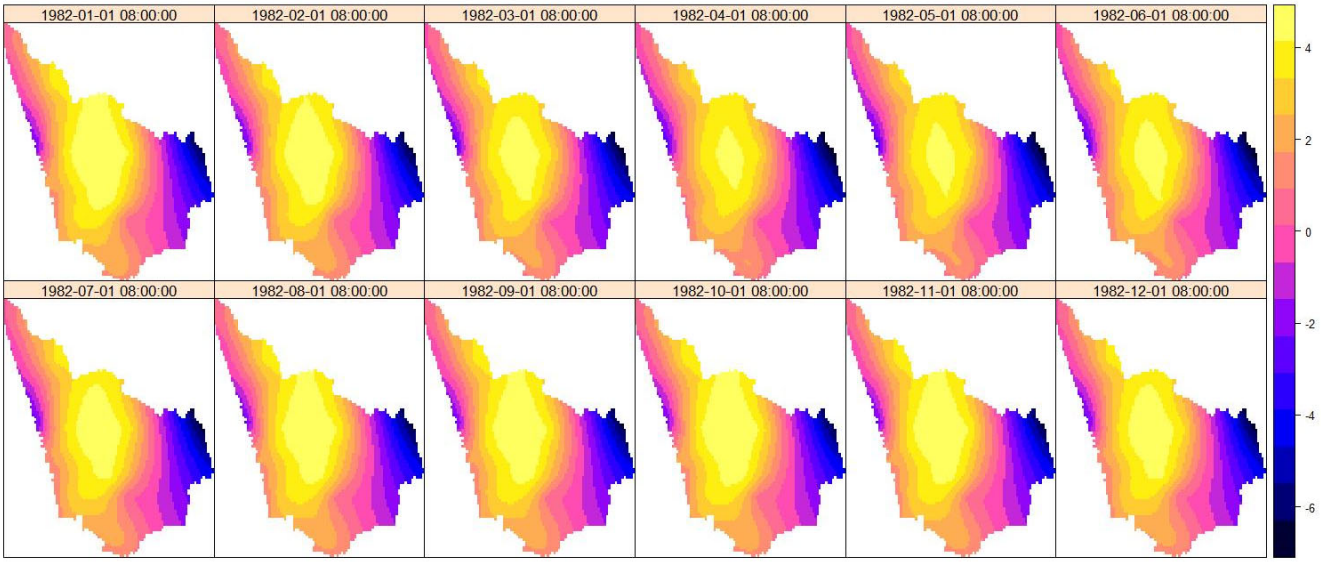
1982-01-01 08:00:00
1982-02-01 08:00:00
1982-03-01 08:00:00
1982-04-01 08:00:00
1982-05-01 08:00:00
1982-06-01 08:00:00
1982-07-01 08:00:00
1982-08-01 08:00:00
1982-09-01 08:00:00
1982-10-01 08:00:00
1982-11-01 08:00:00
1982-12-01 08:00:00
4
2
0
-2
-4
-6

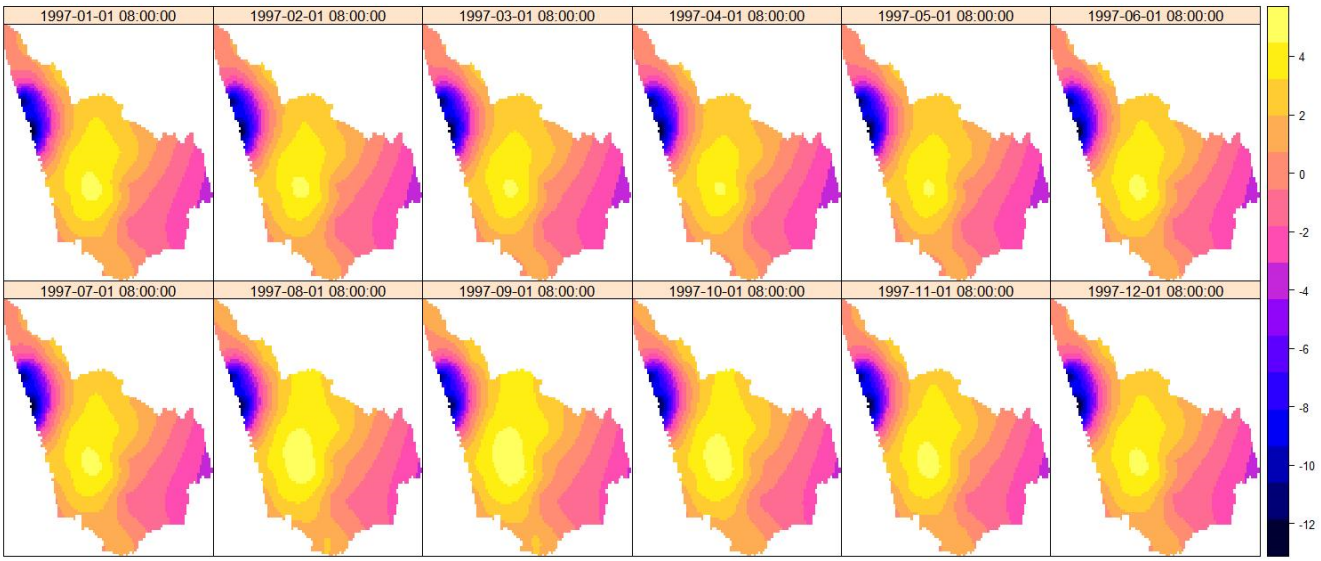
1997-01-01 08:00:00
1997-02-01 08:00:00
1997-03-01 08:00:00
1997-04-01 08:00:00
1997-05-01 08:00:00
1997-06-01 08:00:00
1997-07-01 08:00:00
1997-08-01 08:00:00
1997-09-01 08:00:00
1997-10-01 08:00:00
1997-11-01 08:00:00
1997-12-01 08:00:00
4
2
0
-2
-4
-6
-8
-10
-12

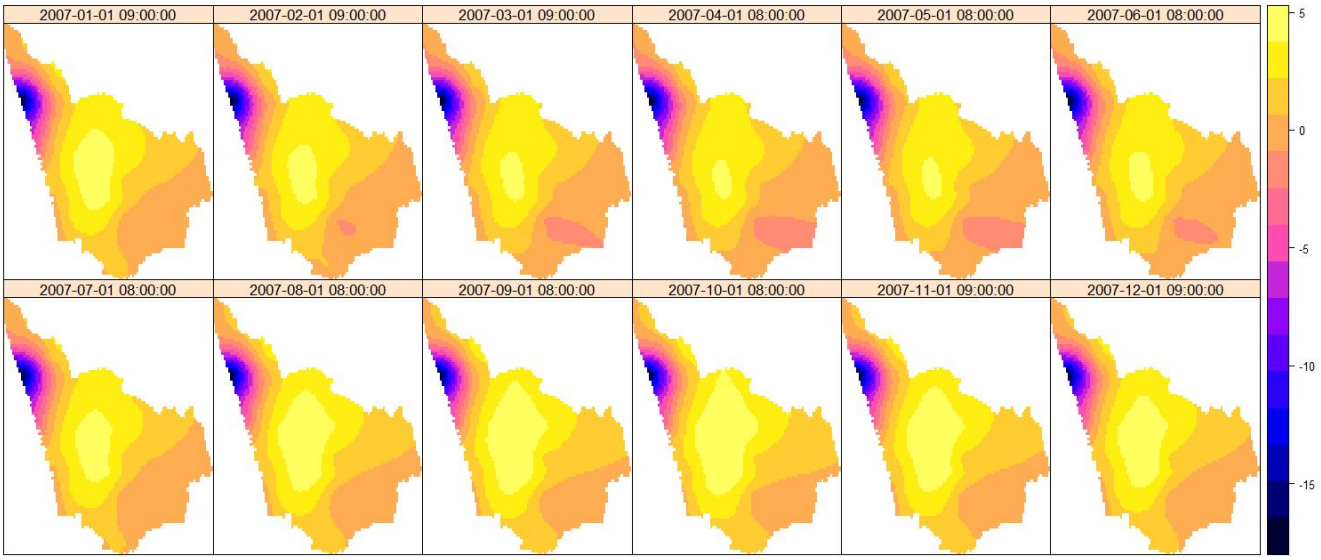
2007-01-01 09:00:00
2007-02-01 09:00:00
2007-03-01 09:00:00
2007-04-01 08:00:00
2007-05-01 08:00:00
2007-06-01 08:00:00
2007-07-01 08:00:00
2007-08-01 08:00:00
2007-09-01 08:00:00
2007-10-01 08:00:00
2007-11-01 09:00:00
2007-12-01 09:00:00
5
0
-5
-10
-15

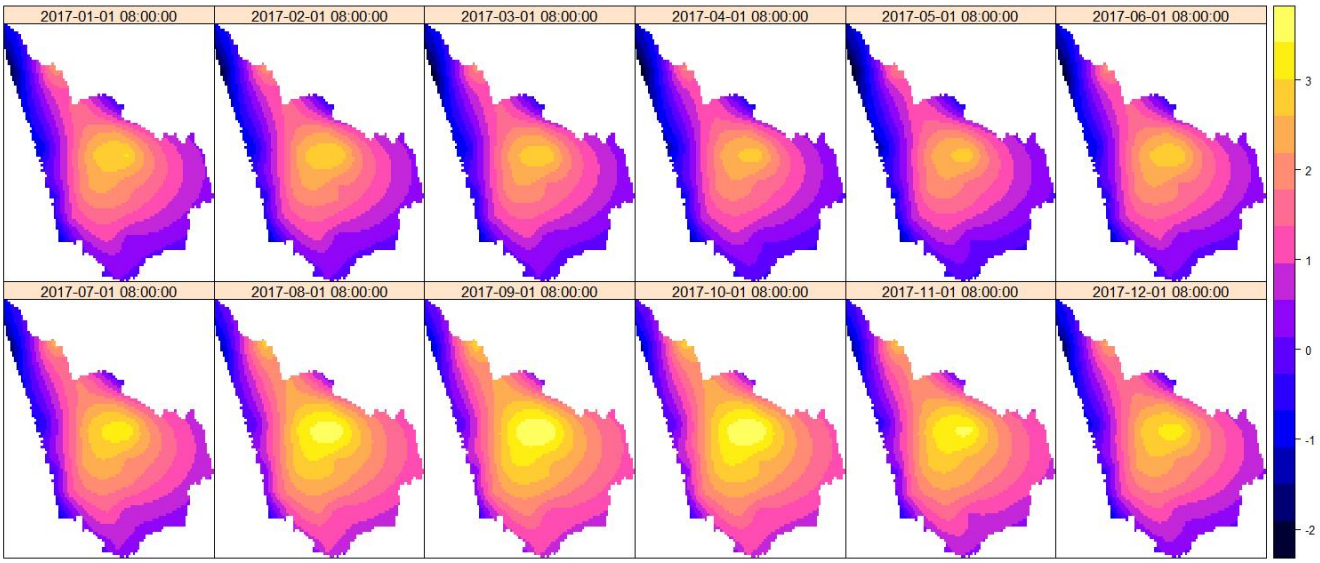

Fig. 7.6 Estimated Residual component of GWL (meter) in the Harvey Catchment, WA, for the selected years using Rkriging method

7.3.3 Spatiotemporal Kriging Predicted Groundwater Levels

The trend (determinist component) and residual (stochastic component) together provide the final estimation of the groundwater level at any grid points in each month, based on which monthly GWL maps can be produced for the study years (i.e., 1982-2017). Due to the length of requirement for the manuscript, Figure 7.7 presents GWL maps for the selected years of 1982, 1997, 2007 and 2017. As expected, the deeper water table is located in south-eastern part of the catchment and shallower water table (the dark blue color) is in the coastal area (i.e., the north-western part, where the catchment meets the sea). It is also shown that GWL follows the same trend over the years although the actual GWL at each grid vary from year to year.

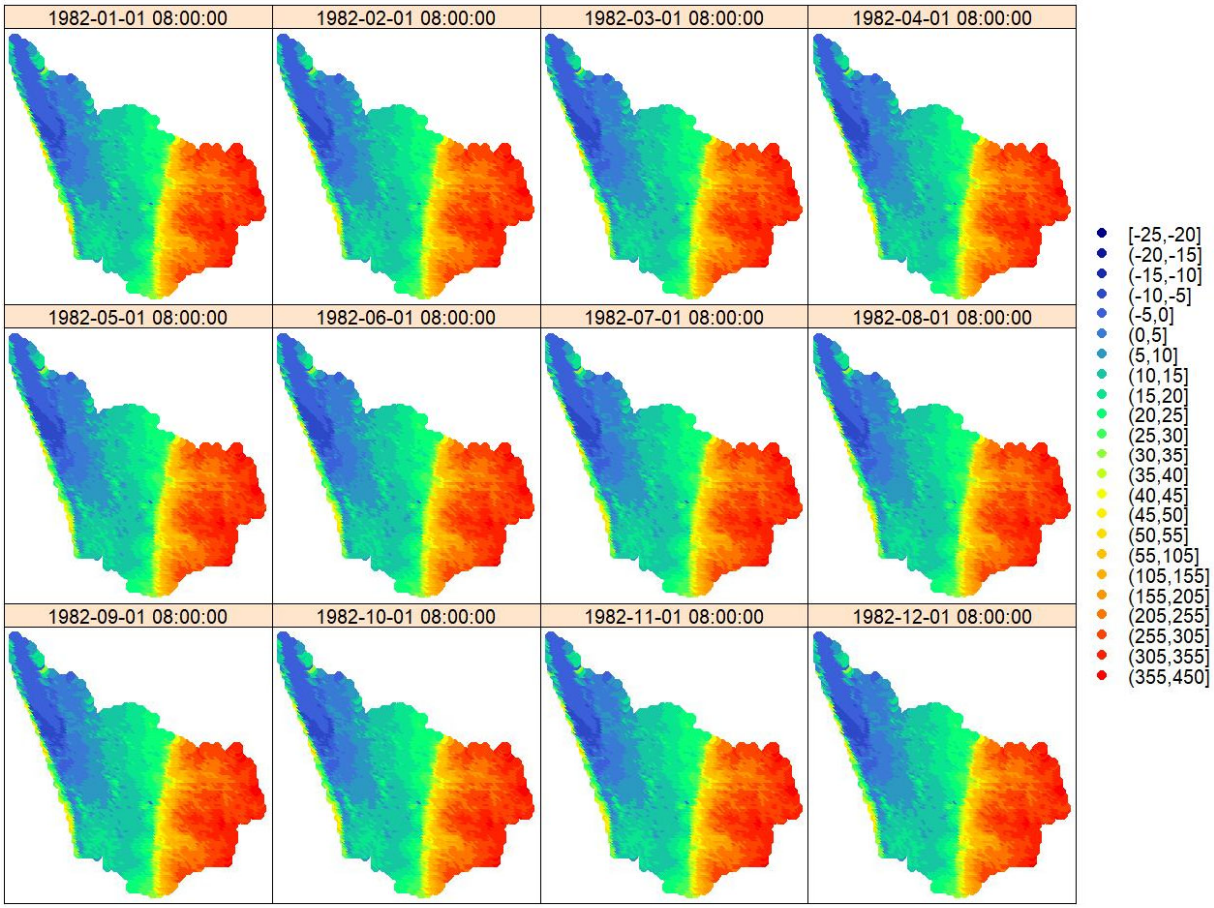
1982-01-01 08:00:00
1982-02-01 08:00:00
1982-03-01 08:00:00
1982-04-01 08:00:00
1982-05-01 08:00:00
1982-06-01 08:00:00
1982-07-01 08:00:00
1982-08-01 08:00:00
1982-09-01 08:00:00
1982-10-01 08:00:00
1982-11-01 08:00:00
1982-12-01 08:00:00
[-25,-20]
(-20,-15]
(-15,-10]
(-10,-5]
(-5,0]
(0,5]
(5,10]
(10,15]
(15,20]
(20,25]
(25,30]
(30,35]
(35,40]
(40,45]
(45,50]
(50,55]
(55,105]
(105,155]
(155,205]
(205,255]
(255,305]
(305,355]
(355,450]

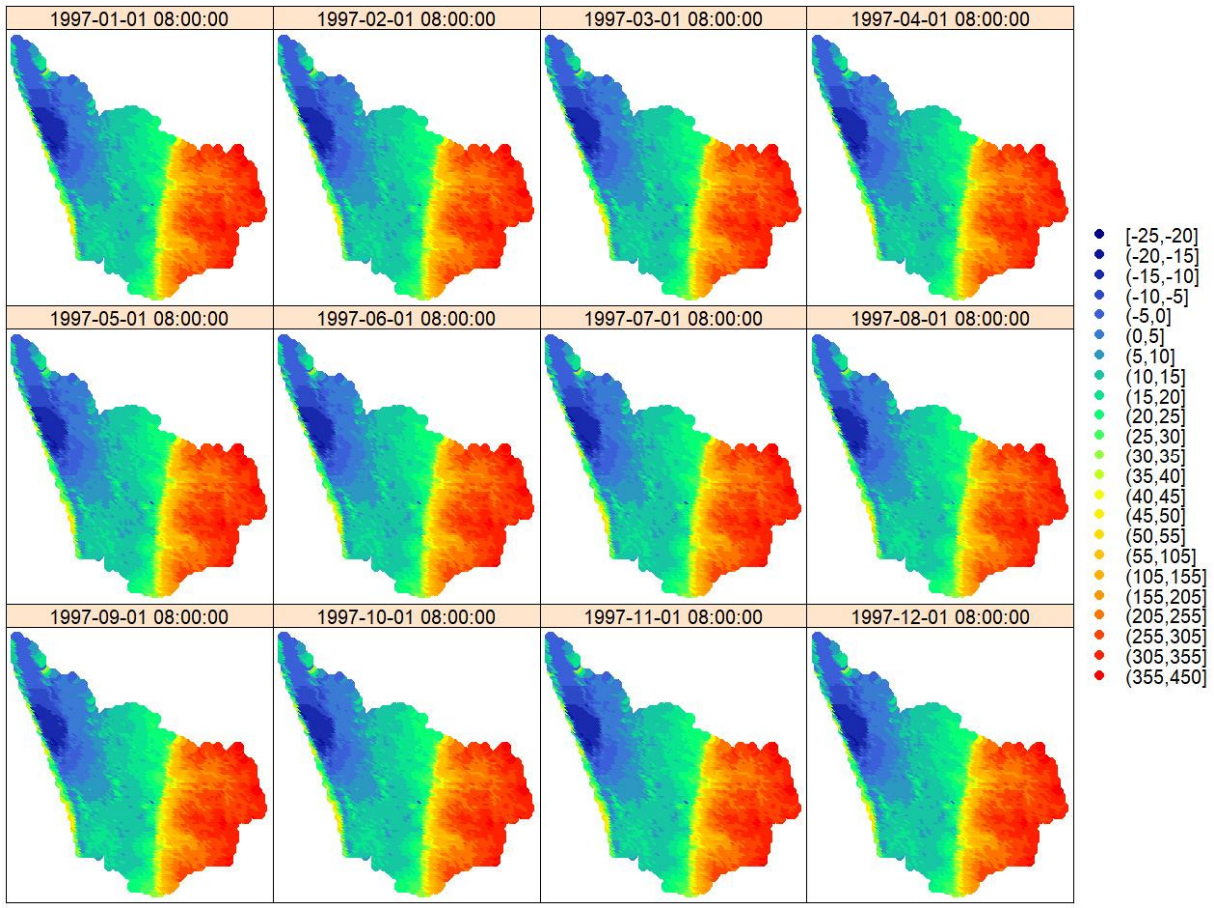
1997-01-01 08:00:00
1997-02-01 08:00:00
1997-03-01 08:00:00
1997-04-01 08:00:00
1997-05-01 08:00:00
1997-06-01 08:00:00
1997-07-01 08:00:00
1997-08-01 08:00:00
1997-09-01 08:00:00
1997-10-01 08:00:00
1997-11-01 08:00:00
1997-12-01 08:00:00
[-25,-20]
(-20,-15]
(-15,-10]
(-10,-5]
(-5,0]
(0,5]
(5,10]
(10,15]
(15,20]
(20,25]
(25,30]
(30,35]
(35,40]
(40,45]
(45,50]
(50,55]
(55,105]
(105,155]
(155,205]
(205,255]
(255,305]
(305,355]
(355,450]

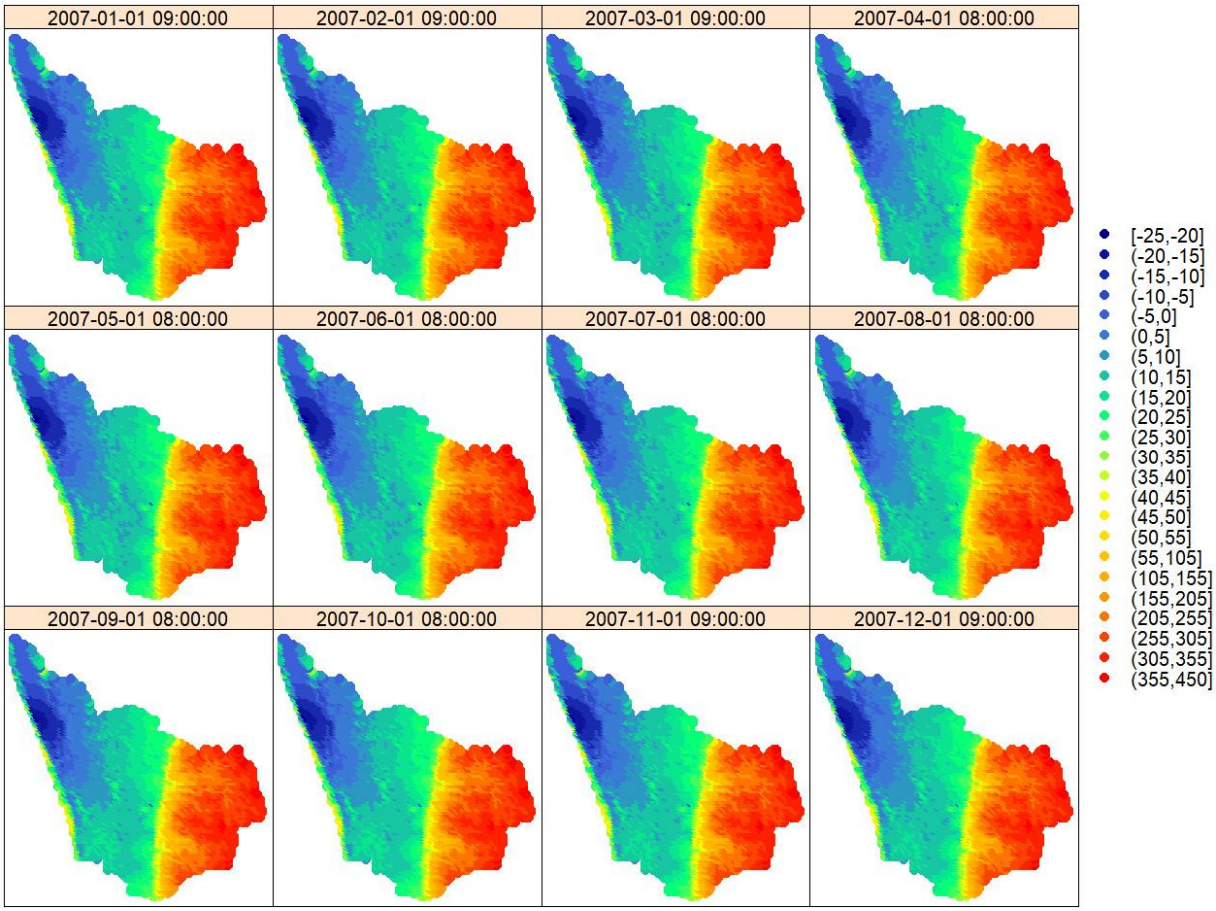
2007-01-01 09:00:00
2007-02-01 09:00:00
2007-03-01 09:00:00
2007-04-01 08:00:00
2007-05-01 08:00:00
2007-06-01 08:00:00
2007-07-01 08:00:00
2007-08-01 08:00:00
2007-09-01 08:00:00
2007-10-01 08:00:00
2007-11-01 09:00:00
2007-12-01 09:00:00
[-25,-20]
(-20,-15]
(-15,-10]
(-10,-5]
(-5,0]
(0,5]
(5,10]
(10,15]
(15,20]
(20,25]
(25,30]
(30,35]
(35,40]
(40,45]
(45,50]
(50,55]
(55,105]
(105,155]
(155,205]
(205,255]
(255,305]
(305,355]
(355,450]

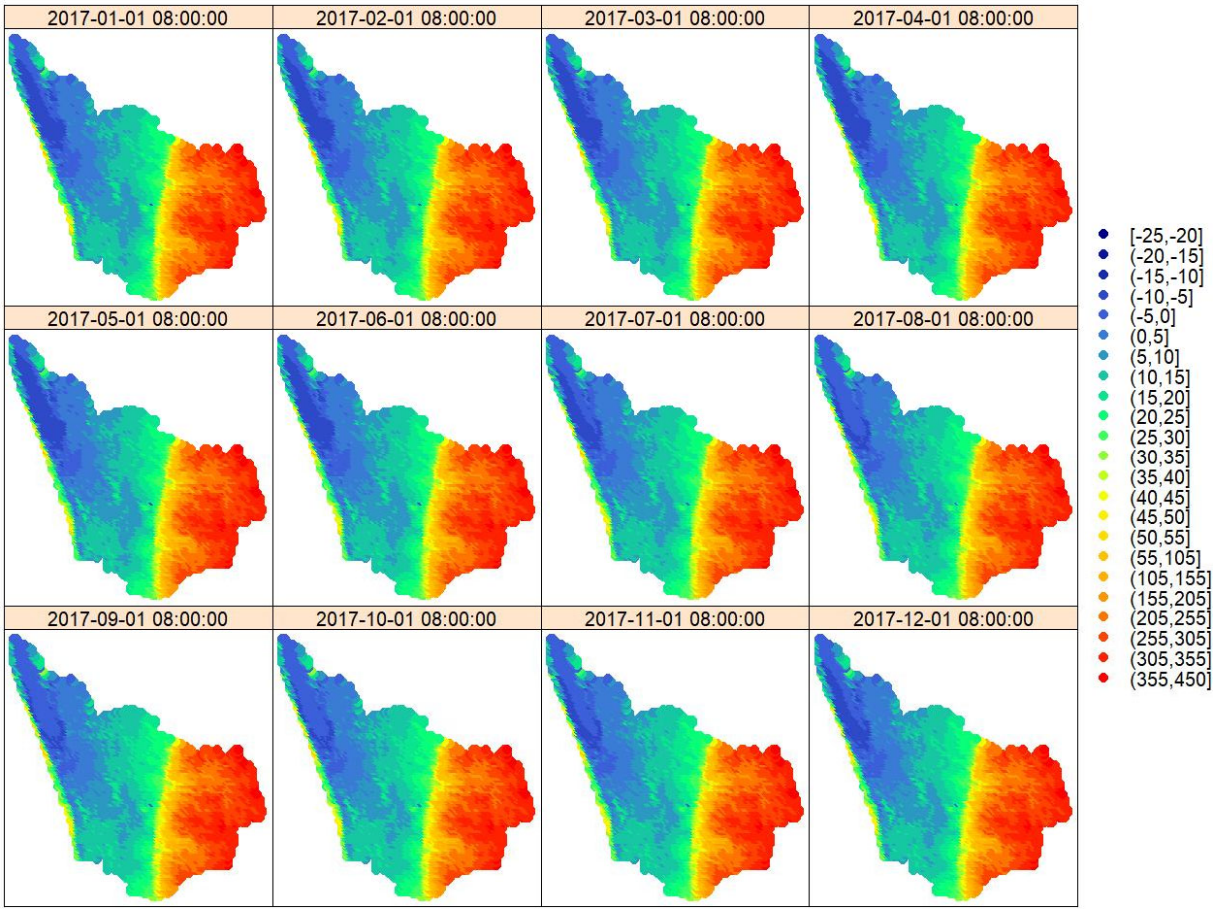
2017-01-01 08:00:00
2017-02-01 08:00:00
2017-03-01 08:00:00
2017-04-01 08:00:00
2017-05-01 08:00:00
2017-06-01 08:00:00
2017-07-01 08:00:00
2017-08-01 08:00:00
2017-09-01 08:00:00
2017-10-01 08:00:00
2017-11-01 08:00:00
2017-12-01 08:00:00
[-25,-20]
(-20,-15]
(-15,-10]
(-10,-5]
(-5,0]
(0,5]
(5,10]
(10,15]
(15,20]
(20,25]
(25,30]
(30,35]
(35,40]
(40,45]
(45,50]
(50,55]
(55,105]
(105,155]
(155,205]
(205,255]
(255,305]
(305,355]
(355,450]

Fig.7.7 Created maps of estimated Harvey catchment GWL (m) for the selected years using Rkriging method

7.3.4 Cross-validation

The "Leave-one-out" cross-validation was carried out for almost 44000 spatiotemporal points to compare the estimated values with the observed values (Figure 7.8). These spatiotemporal points are the observed GWL data from the wells, during the 36 years of study period. Non-uniformity of the observed data can also be observed from the figure where there is a lack of information within some ranges of elevation. It suggests the Rkriging method is well capable of estimating groundwater level in the catchment, with the R-square value closing to 1.

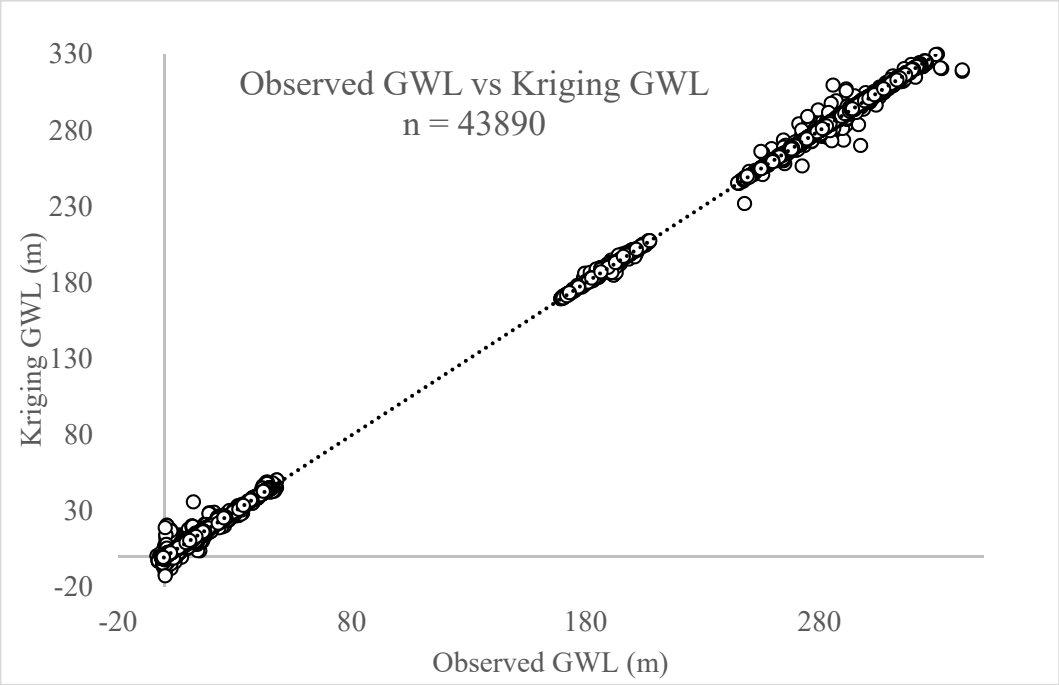

Fig.7.8 Leave–One-Out Cross Validation result showing the goodness of fit between Rkriging predicted GWL and observed GWL information from the 641 wells in the Harvey Catchment.

7.3.5 Time-series Analysis

Forty randomly selected samples (as hypothetical wells) were chosen to perform the auto-correlation and cross-correlation analysis. The samples are almost uniformly distributed in the catchment and cover all of the elevation classes. Figure 7.9 shows the values of auto-correlation function for GWL themselves and ΔGWL. The gradual decline in the ground water level indicates the autocorrelation can last for at least four years (ACF above 0.2). Those samples which show sinusoidal, yet gradually decreasing patterns, are mainly located on the Collins Pool or very close to the pool. The ACF for ΔGWL shows completely different behavior. For most of the cases, the ACF graphs for ΔGWL follow a sinusoidal pattern with

12 month circle but the seasonality and correlation are negligible as they are mostly about or less than 0.3 (the significance level). The aforementioned samples, located on or close to the Collins pool, perform higher seasonal auto-correlation values. As the pool is connected to the ocean (Fig.7.1), the unusual trend of these samples can be because of the influence of ocean water.

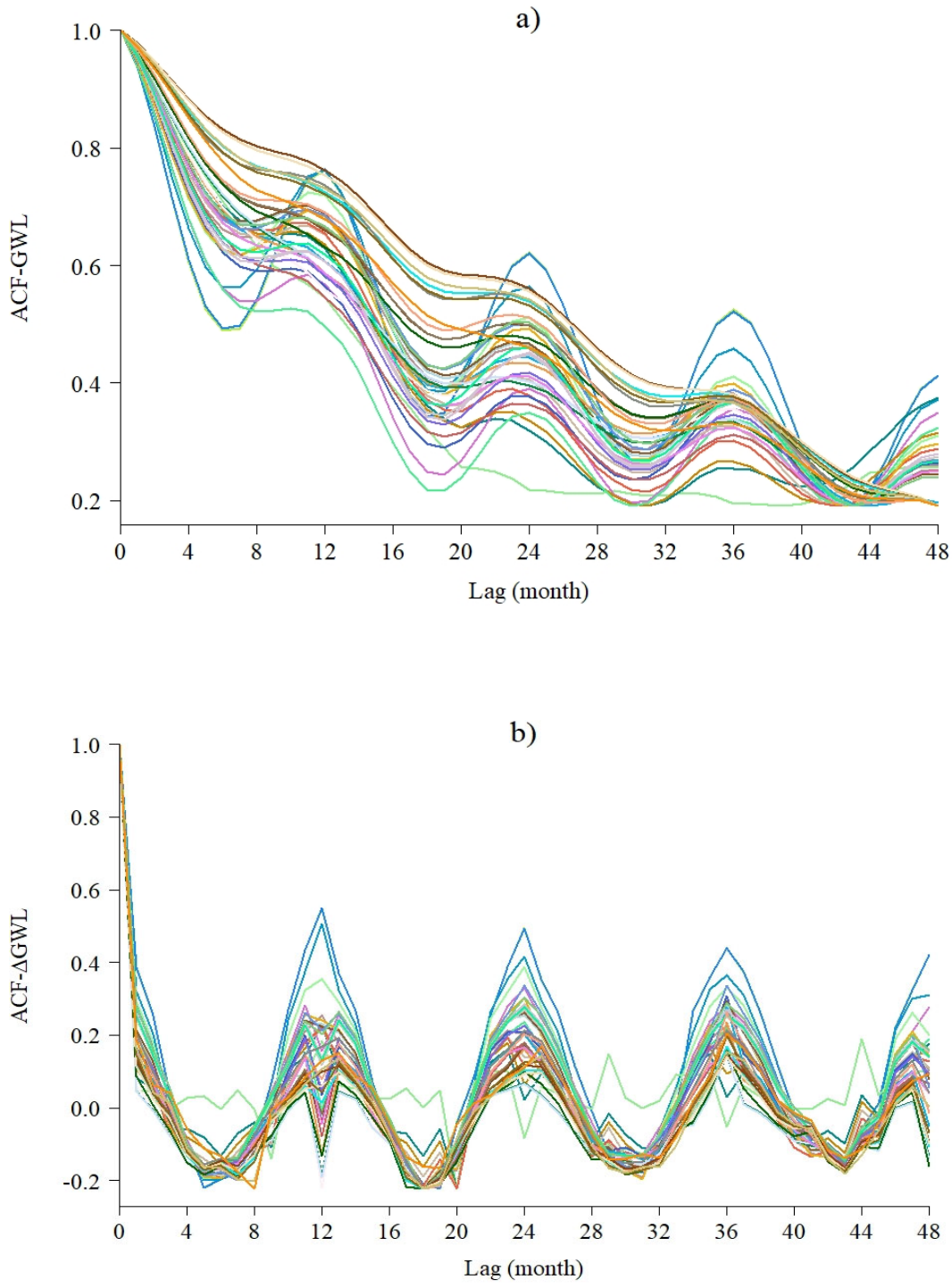

Figure 7.9 a) Auto Correlation Function (ACF) for GWL and b) ΔGWL in 48 months showing the autocorrelation values between the time-series in the Harvey Catchment

Figure 7.10 represents the cross-correlation analysis between ΔGWL and rainfall. It suggests that the time-lag between ΔGWL and rainfall is zero months meaning that rainfall needs less than a month to affect groundwater level change in the catchment.

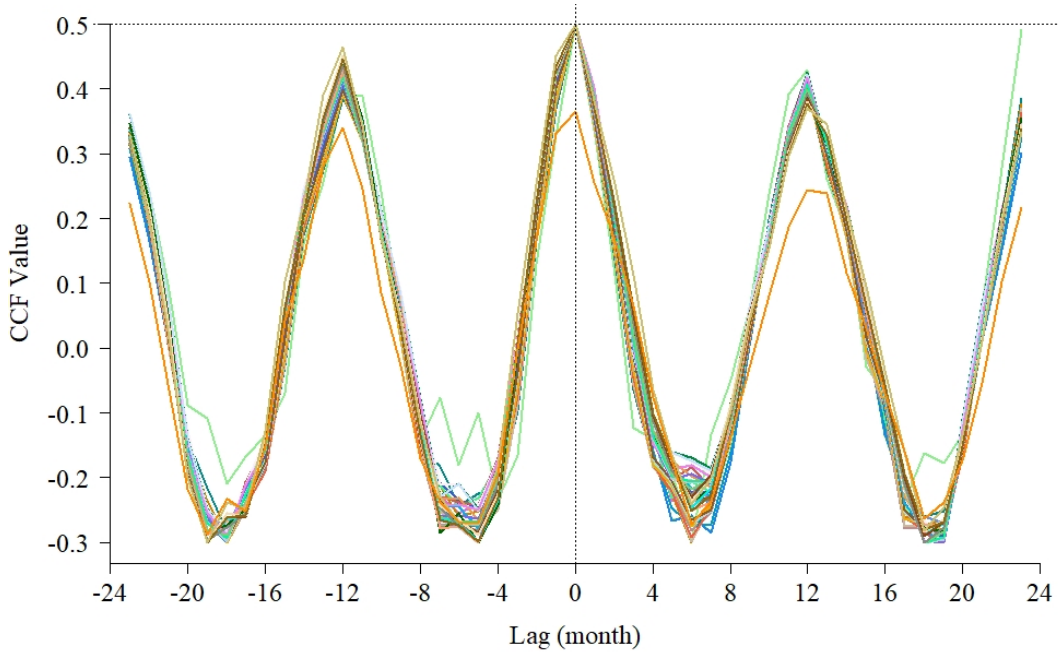

Fig.7.10 Cross-correlation between ΔGWL values and Precipitation (P) values showing time-lag between ΔGWL and precipitation is less than a month (the dashed lines show lag month during which the highest CCF value occurs between the two time-series in the Harvey Catchment)

According to Figure 7.11 the mean monthly GWL has increased during 1988-1993 and decreased afterward. The previous studies for the Harvey region reported decrease in groundwater level since 1980s (Ali et al., 2012; CSIRO, 2009; Kelsey et al., 2010) mainly due to extensive agricultural activities, urban development, and rainfall reduction. The current research confirmed these findings, showing that groundwater level in the catchment has decreased after a short period of increasing.

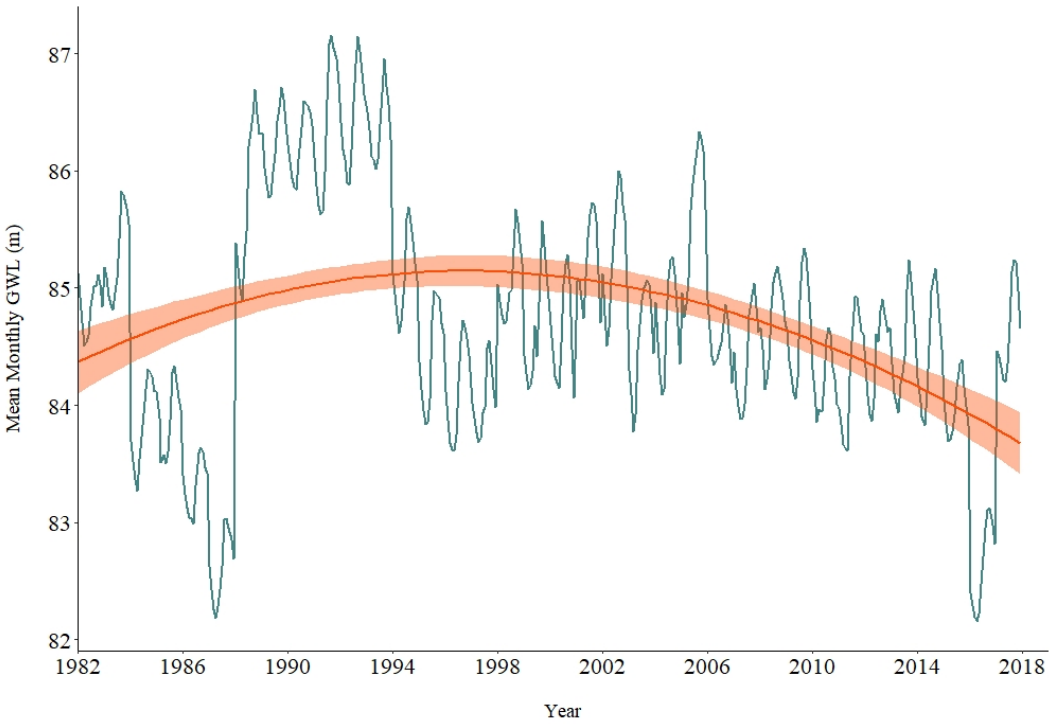

Fig.7.11 Mean Monthly GWL temporal trend in the Harvey Catchment, WA

Figure 7.12 (a and b) provides more detailed information. Although precipitation follows a decreasing trend, the annual rainfall during 1988 – 1993 is significantly above the average which coincides with those years in which groundwater level experienced a brief increase.

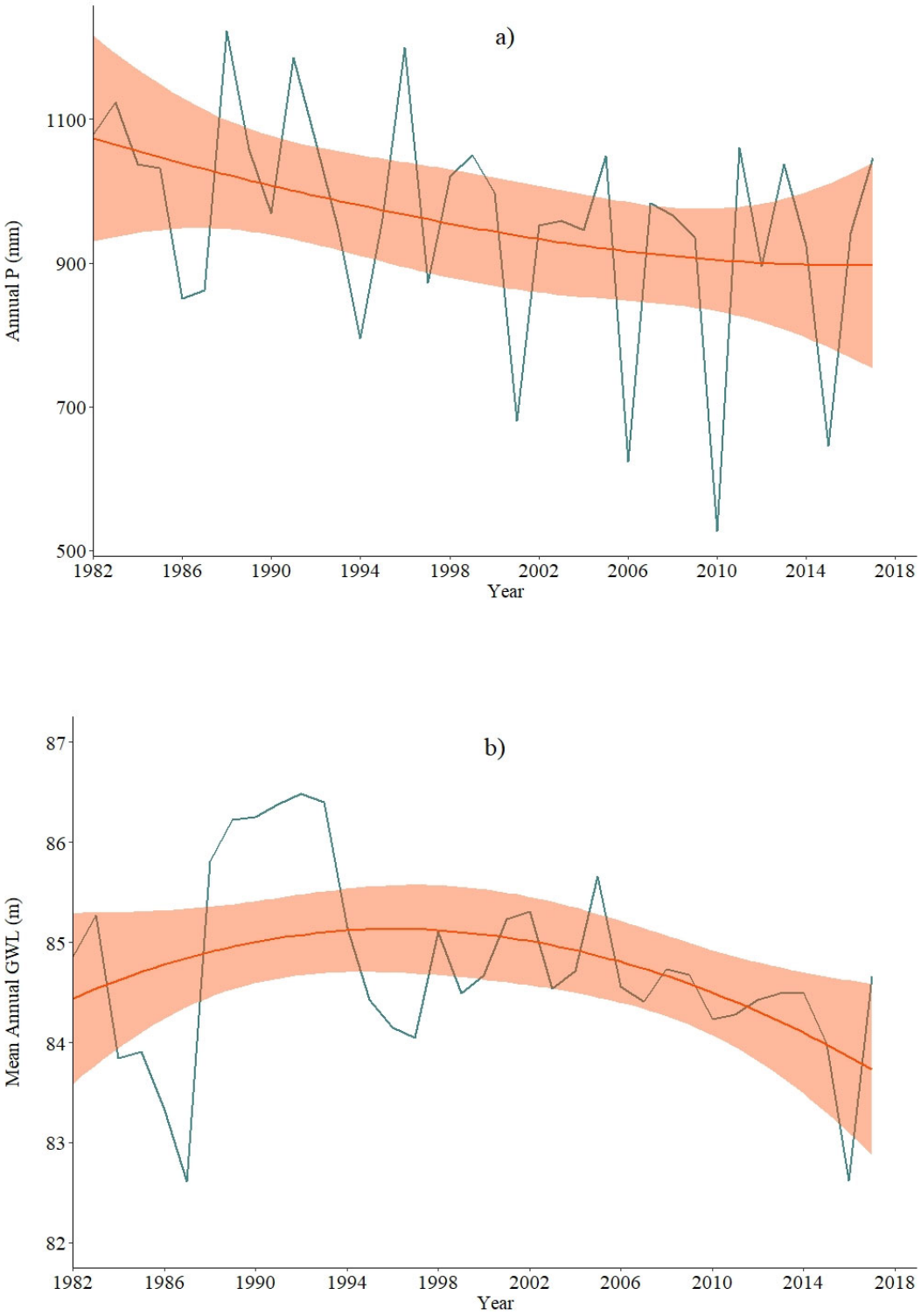

Fig.7.12 a) Annual Precipitation and b) Mean annual GWL trends in the Harvey Catchment, during the study period

The Harvey Catchment, specifically in the coastal area, is reported to have a shallow water table. By deducting earth elevation from estimated GWL at each grid point, it was confirmed that the catchment is shallow, and water level almost stands within 10 meters below the earth

surface. The deepest water table is located in the southeastern part of the catchment (Fig.7.1), where water level stands between 10 to 16 meters from the surface. Shallow catchments, especially in cases like Harvey, where the rainfall is highly seasonal, rejects recharging, after being full during winter time. Therefore the catchment is more vulnerable to water loss. On the other hand, rapid and extensive development in the study area causes higher rate of discharge than recharge, and hence results in more water loss. Decreasing water level increases the risk of ocean water intrusion, and deteriorates water quality (Ali et al., 2012). Because of the shallow groundwater, high permeability (i.e., high hydraulic gradient) and sandy soil of the catchment, a short time-lag between rainfall and ΔGWL was expected. The cross-correlation analysis showed the time-lag between the two time-series is less than a month (Fig. 7.10). However, because of the chosen monthly time step in this study, it was not possible to detect the exact response time of less than a month. In future studies, with a finer temporal grid (e.g., daily scale), it might be possible to track the possible weekly or daily time-lag. Although, due to the extensive computational process, probably, a shorter time period should be adopted.

The Rkriging method is a beneficial, yet, computationally extensive task. The model should perform the inversion covariance matrix, which makes the calculation process massive. Unlike spatial or temporal kriging, the method considers the time and space dependency of the variables by building a correlation between the parameters so that even when some of the spatial or/and temporal points are missing (Varouchakis and Hristopulos, 2019).

7.4 Conclusion

The proposed method showed that groundwater level has decreased in the catchment, during the study period. In order to further investigate this reduction and its correlation with temporal precipitation change, time-series analysis was performed. The results showed there is a short time-lag between the precipitation and ΔGWL time-series (less than a month), which is expected considering Harvey Catchment has relatively shallow groundwater table. The estimated groundwater level provides valuable information about hydrogeological condition of the catchment, and hence can be useful for predicting future change and distinguishing potential environmental threats to the catchment (Ferdowsian and Pannell, 2009). Furthermore, the GWL information is important to accurately quantify water extraction capacity and amount of discharge and recharge to the groundwater system, which in return, is essential for proposing sustainable water supply plan (John and John, 2019; Kotchoni et al.,

2019). Therefore, the outcome of this study is, also, useful for policymakers and water resources manager in developing sustainable plans. The proposed method can be used for other catchments where limited groundwater data is available. In the absence of hydrological modelling and complex dataset, this method can provide valuable information. Moreover, the Rkriging method is a competent approach for cases with sparse non-uniform data, in fields such as hydrology, pollution tracking or other environmental studies. It increases the spatiotemporal understanding of the studied parameters where irregular temporal and spatial data is the only available information. Next, outcome of the current chapter will be applied to investigate water resources variations in the Harvey Catchment, during 1982-2017.

Chapter 8
Improving the assessment of monthly streamflow change using the statistical model

8.1 Background and method

In this chapter, application of the extended Budyko model (Budyko-Du) in estimation of monthly and annual streamflows will be compared with other conceptual models (i.e., the ABCD and ABCD-GE). To be able to use the Budyko model for inter-annual studies, both effective groundwater level change (ΔG) and soil water storage change (ΔS) is considered. Hence, the effective precipitation parameter in the Budyko-Du equation (2.7) is updated to include effective ΔGWL (i.e., $P_e = P - \Delta S - \Delta G$). The ΔGWL data, resulted from Chapter 7, is used to estimate the effective groundwater level data which is involved in evapotranspiration. Accordingly, the chosen study area is the same as Chapter 7 (i.e., the Harvey-Forrest Catchment).

Last but not least, to overcome the simplification assumptions necessary for the conceptual models, the hybrid conceptual-statistical models are developed to use the capability of the time series and increase the accuracy of the models. This new hybrid model combines the conceptual module (i.e., Budyko type or ABCD type models) with the statistical SARIMAX module. The results are discussed and compared with the original conceptual models.

Prior to model the time-series with SARIMAX, stationarity of Y_t should be investigated. Stationary time-series means that the mean and variance of the data are constant over time. Many hydrological parameters experience nonstationary, including trend, seasonality or cycles, which makes them unpredictable and unfitted for modelling (Abbas and Ilyas, 2018). If the time-series is not stationary, it needs to be transformed to stationary using differencing operator (Andrews et al., 2013; Fathi et al., 2019). After stationarity of the time-series (or the differenced time-series) is confirmed, the SARIMAX model is built. Next, the resulted residuals are investigated to make sure they are uncorrelated and follow the white noise.

In order to check the robustness of the model, the data is divided into two groups; calibration data (almost 70% of the data) and validation data (almost 30% of the data). The model should be able to pass the aforementioned criteria (i.e., uncorrelated and white noise residuals) for both data sets. If the model satisfies the criteria with both data sets, it is assumed to be robust and ready for estimation (Fathi et al., 2019).

Here, the SARIMAX model is coupled with Budyko, Budyko-Du and ABCD-GE models to investigate if the hybrid statistical-conceptual models significantly outperform the conceptual models. The SARIMAX module models the error between estimated values from the conceptual models and observed values, using interconnection between exogenous variables and estimated streamflow. The two exogenous variables (here, precipitation and actual evapotranspiration) were suggested by Stepwise Regression Function. Three actual evapotranspiration dataset are provided from Budyko, ABCD-GE and Budyko-Du models.

8.2 Analysis monthly streamflow change

The proposed models were employed to estimate the streamflow variation during 1983-2018. First, the conceptual models were employed and in the next step, their performances were compared with the developed conceptual-statistical model. The period of 1983 to 2007 is selected as the calibration period and the chosen validation period is from 2007 to 2018.

8.2.1 Conceptual models

The estimated monthly streamflow from the ABCD, ABCD-GE and Budyko-Du models are presented in Fig.8.1 Since, the original Budyko equation is not applicable for monthly analysis, under unsteady condition, only Budyko-Du model is presented. The parameters of ω and λ for Budyko-Du model were defined by calibration to be 1.5 and -0.8, respectively. These parameters were calibrated using monthly estimated streamflow and observed values.

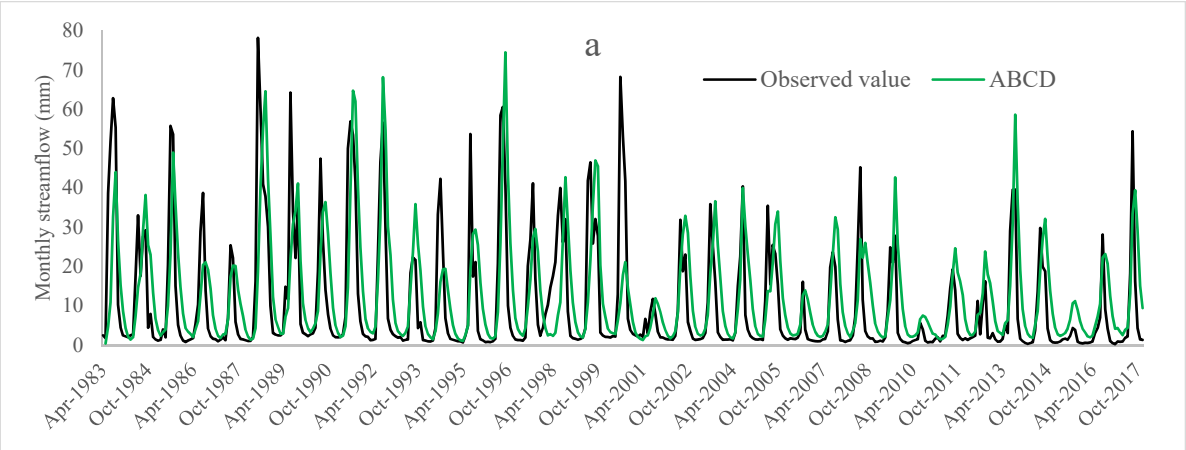

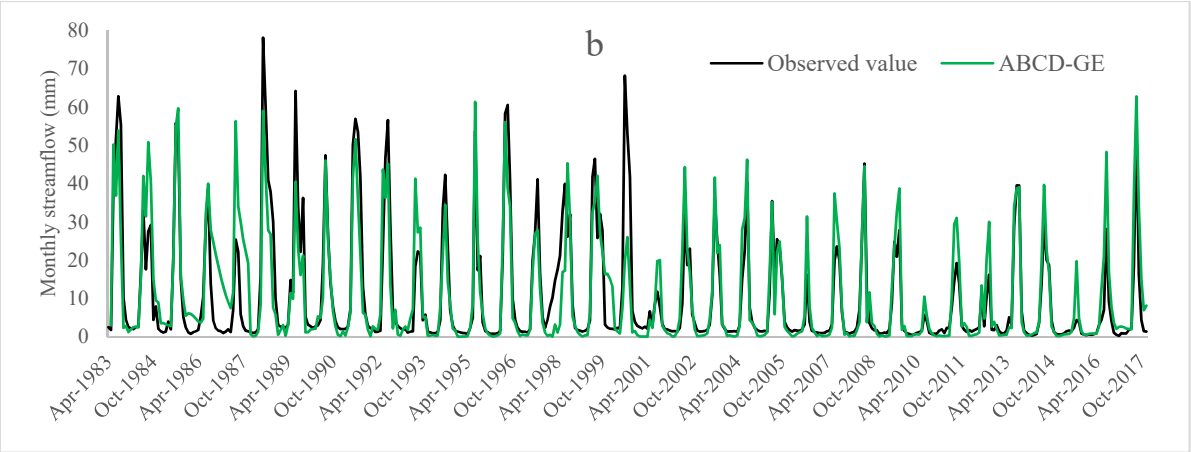

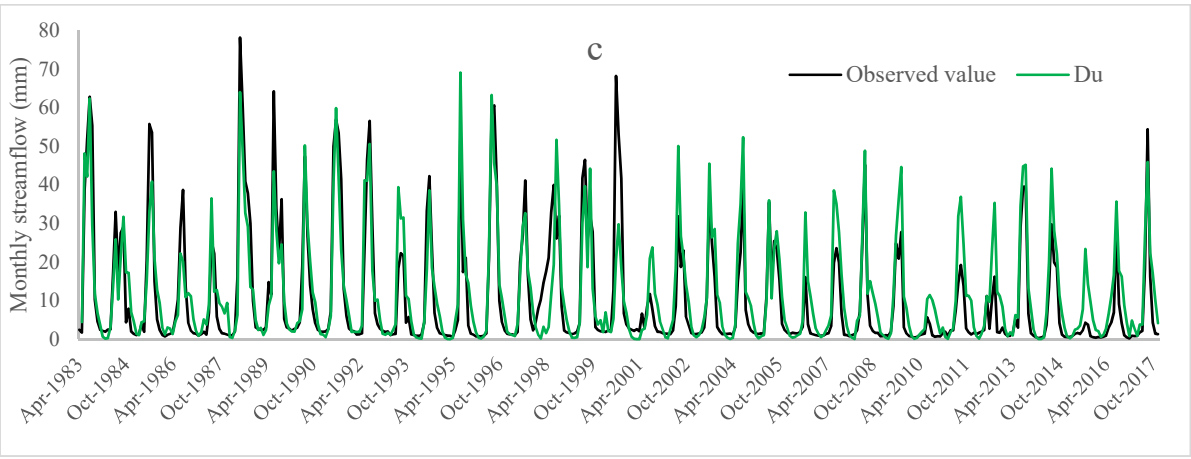

Fig.8.1 Monthly estimated and observed streamflow of the Harvey River using (a) ABCD, (b) ABCD-GE and (c) Budyko-Du models

8.2.2 Hybrid conceptual-statistical models

Augmented Dickey-Fuller test for stationarity was used to check the stationarity of the streamflow times-series. The test showed that streamflow is stationary (with statistical significance (i.e., P-value) less than 0.05), for both monthly and annual timescale (Table 8.1); suggesting the time-series analysis can be proceeded without further manipulation of the data.

Table 8.1 Augmented Dickey-Fuller test parameters for stationarity of the Harvey River streamflow time-series

Timescale	Monthly	Annual
Dickey-Fuller Value	-11.45	-5.52
P-value	0.01	0.01

For the monthly scale, various SARIMAX models, with different orders, were tested to select the best configuration that minimizes the AIC parameter. As the annual observed streamflow does not show any seasonality, seasonal component of SARIMAX is ignored and the

statistical module is downgraded to ARIMAX model. The selected configurations and the goodness of fit parameters are presented in Table 8.2.

Table 8.2 Configurations and goodness of fit parameters for the hybrid SARIMAX-Conceptual models estimating Harvey River monthly streamflow

Model	Scale	Configuration	AIC	P-value
Budyko	Monthly	(2,0,0)(0,1,1)12	393	0.08
ABCD-GE		(2,0,3)(0,1,1)12	309	0.36
Budyko-Du		(2,0,3)(0,1,1)12	303	0.22
Budyko	Annual	(0,1,1)	18	0.21
ABCD		(0,1,1)	15	0.16

It is believed that by coupling the original Budyko and SARIMAX models, the statistical module is able to rectify the errors, which make the Budyko model applicable for monthly time-scale (Fathi et al., 2019).

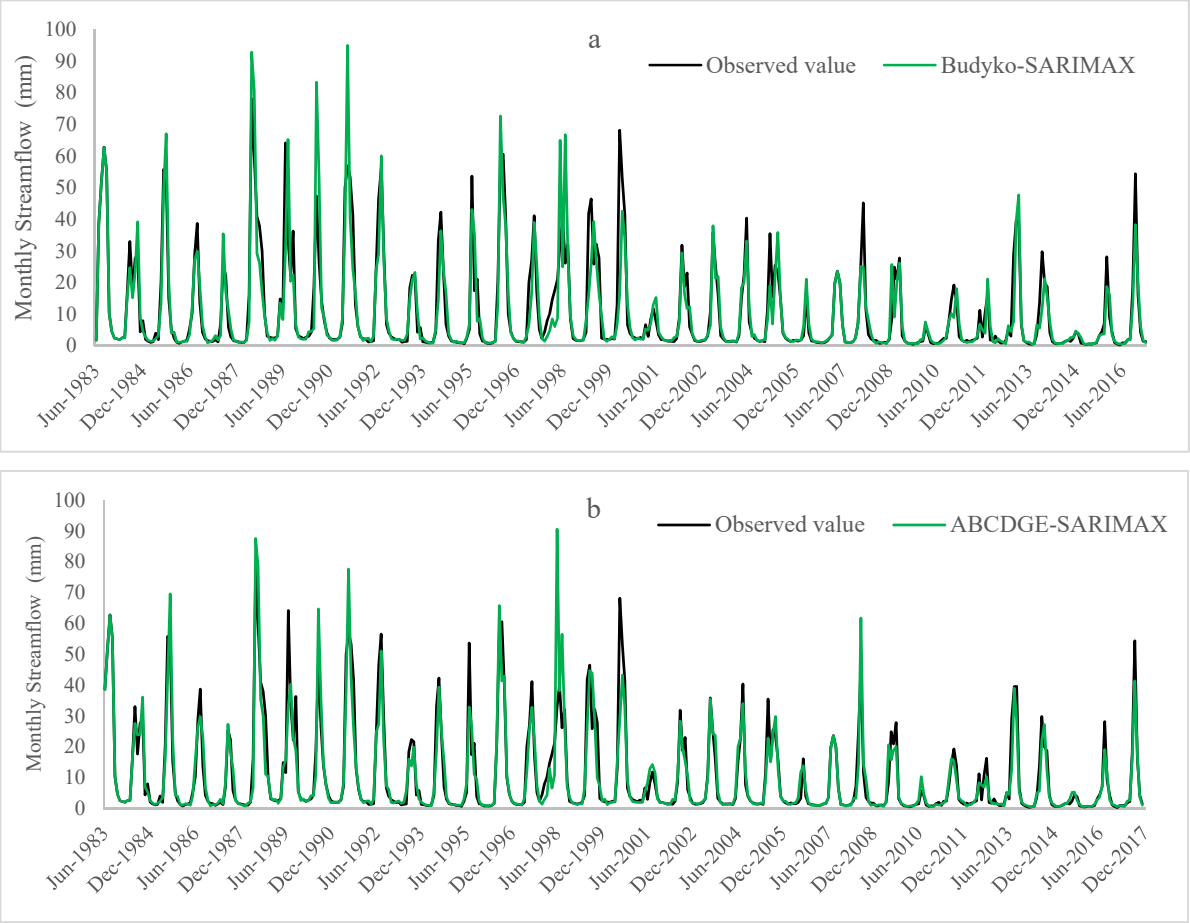

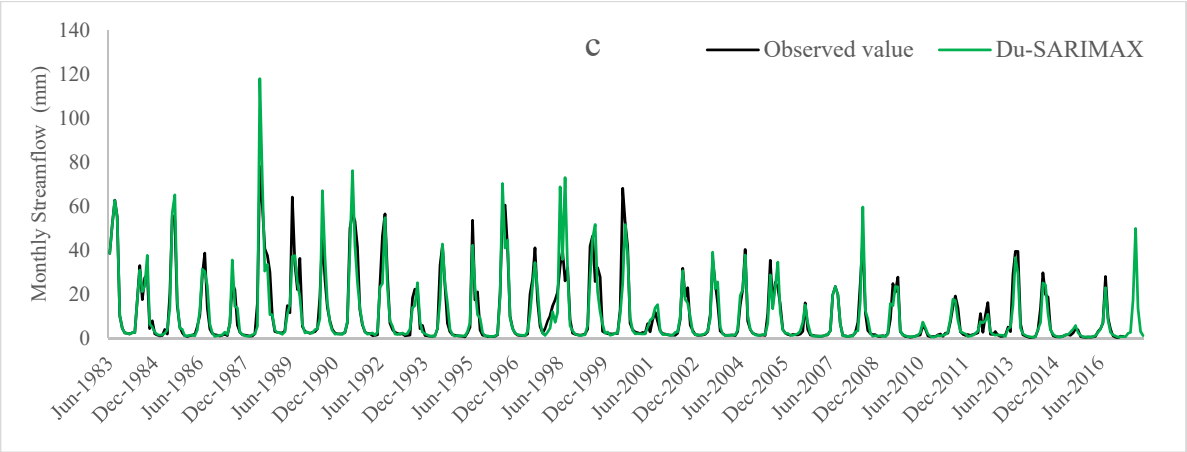

Fig.8.2 Monthly estimated and observed streamflow of the Harvey Catchment using Hybrid models a) ABCD-SARIMAX, b) ABCD-GE-SARIMAX and c) Du-SARIMAX

On the other hand, from, it was shown that ABCD-GE model outperforms ABCD model, hence, the ABCD-SARIMAX results are not presented. Accordingly, fig.8.2 shows monthly streamflow estimation from the three hybrid conceptual-statistical models (i.e., Budyko-SARIMAX, ABCD-GE-SARIMAX and Budyko-Du-SARIMAX models).

Tables 8.3 and 8.4 compare the hybrid models with the original models and show the improvement of estimations after applying the statistic module.

Table 8.3 Fitness values between estimated and observed monthly streamflow of the Harvey River, before and after implementing SARIMAX

Period		Calibration (1983-2007)				Validation (2007-2018)			
Model		Budyko-Du	Budyko	ABCD	ABCD-GE	Budyko-Du	Budyko	ABCD	ABCD-GE
Before	R^2	0.77	-	0.39	0.71	0.84	-	0.46	0.88
SARIMAX	KGE	0.82	-	0.57	0.81	0.54	-	0.47	0.67
After	R^2	0.82	0.66	-	0.81	0.85	0.61	-	0.82
SARIMAX	KGE	0.89	0.78	-	0.9	0.81	0.7	-	0.8

For the annual scale, since the mean annual water storage change estimated from ABCD-GE model showed the catchment has steady state condition (fig.8.3), only the original Budyko and ABCD model were employed to estimate the annual streamflow. The average of water storage change, including effective groundwater change (ΔG) and soil water storage change (ΔS), was -0.63mm, during the study period, which means the water storage change is insignificant.

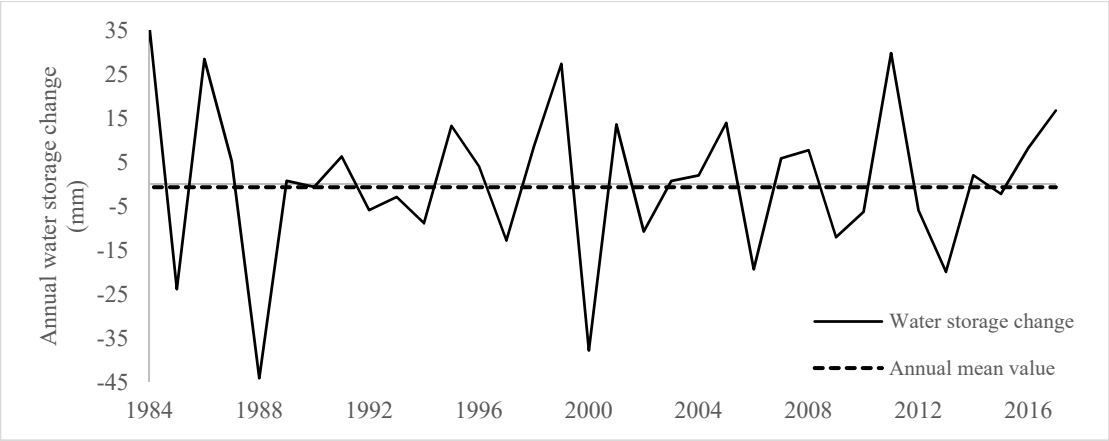

Fig.8.3 Estimated annual water storage change (mm) in the Harvey Catchment, using ABCD model

Input annual data (i.e. P and E_0) were calculated by summation of monthly values. The result from the annual hybrid models (i.e., ABCD-ARIMAX, Budyko-ARIMAX) are presented in table 8.4.

Table 8.4 Fitness values between estimated and observed annual streamflow of the Harvey River, before and after implementing ARIMAX

Period		Calibration (1983-2007)		Validation (2007-2018)	
Model		Budyko	ABCD	Budyko	ABCD
Before ARIMAX	R2	0.53	0.58	0.71	0.89
	KGE	0.73	0.76	0.6	0.7
After ARIMAX	R2	0.67	0.69	0.82	0.85
	KGE	0.77	0.81	0.71	0.7

For the monthly scale modelling, the original Budyko model is not applicable under unsteady conditions. Therefore, the ABCD, ABCD-GE and Budyko-Du models were used. As presented in Table 8.4 and Figure 8.2, both extended versions (ABCD-GE and Budyko-Du) outperformed the ABCD model which suggests the importance of effective groundwater change and groundwater-dependent evapotranspiration. Comparing the Budyko-Du model with the ABCD-GE model, it is shown that the former performs slightly better. The ABCD-GE model in many occasions, underestimate the low flow and high flows, while Budyko-Du model performs better in low flow estimation.

For the annual scale, the mean annual water storage change derived from ABCD-GE model suggested the catchment has steady state condition and water storage change is negligible. The same concept was mentioned by Du et al (2016) which suggested extension of the Budyko

model is not necessary for annual scale (Du et al., 2016). Accordingly, for the annual scale only the original models (i.e., ABCD and Budyko) were used.

The conceptual models use simplification assumptions which can introduce inaccuracy to the modelling. For instance, the two parameters of a and b in the ABCD model are controlling parameters for storage evapotranspiration equation whose physical explanation is not straightforward (Wang and Zhou, 2016). Another example is dividing the catchment into the two shallow and deep zones for the ABCD-GE model, without considering complicated groundwater distribution system of the catchment. The model also assumes that there is a direct correlation between groundwater and the dependent evapotranspiration (Wang and Zhou, 2016). For the case of Budyko-type models, it assumes that the parameters (i.e., ω for the Budyko and ω and λ for Budyko-Du model) are constant, during the study period, while these parameters can vary in respect to environment and land use cover change.

Considering above, the hybrid conceptual-statistical models were developed. The stochastic component of the models (i.e., SARIMAX for the monthly scale and ARIMAX for the annual scale) rectify the limitation of the conceptual components, which arises from oversimplification of the hydrological systems. Figure 8.2, Table 8.3 and 8.4 show that the hybrid versions of the models outperformed the original models in both monthly and annual scales. The hybrid model uses the time-series capabilities and historical information and improves the streamflow estimations. Hence, it can be suggested that using only conceptual models may not be able to capture all the aspects of a water balance model. Although the hybrid conceptual-statistical models are more complex than their original versions, they require few data-sets for operation and are competent alternatives for data-scares region.

Conceptual models are popular methods to investigate hydrogeological system of catchments (Mianabadi et al., 2020; Wang et al., 2020). Coupling these models with statistical models as presented in the current study, makes the model more robust and accurate to study water resources variation. The proposed model require less input data comparing to detailed hydrological models, which makes it competent alternative for data scarce regions. The models proved to be successful in both monthly and annual scales and is suggested to be applied to other catchments around the globe. The framework successfully presented an approach to provide uniform data which can be applied for regional estimates of water balance dynamics, water and land resource development and decision-making for watershed management.

8.3 Conclusion

In this study, two common conceptual models and their extended versions (i.e., ABCD, ABCD-GE, Budyko and Budyko-Du models) were used to estimate the monthly and annual streamflow in Harvey-Forrest catchment. The results show the ABCD model was unable to accurately estimate the base-flows and peak-flows in monthly scale, which can be due to ignoring groundwater dependent evapotranspiration parameter and show the importance of groundwater level change in monthly studies. To overcome the inaccuracy arises from over-simplification of the conceptual models, the models were combined with SARIMAX module. The final conceptual-statistical model outperformed the original conceptual models.

Chapter 9
Conclusions and recommendations

9.1 Conclusions

Studying a catchment water balance is vitally important for understanding water circulation and water availability of the catchment. Accordingly, analysing water balance components, such as streamflow, can help tracking the hydrologic responses of any given catchment to climate and land use change in long-term scales or, to climate parameters fluctuations in short-term scales. Studying impacts of climate change and regional human activities on water resources provides critical information for authorities and decision-makers to develop sustainable water resources management plans. Any hydrological variation due to these two factors (i.e., climate change and human activities) can alter status of streamflow, evapotranspiration, surface storage, and soil moisture, directly impacting a watershed's hydro-environmental and hydro-ecological values. It can affect vegetation, flora and fauna, and due to strong interconnection between vegetation and hydrology, the impact can intensify the hydrological changes. Therefore, variation in climate status and regional activities can change the hydrological cycle, both directly through the water supply demands, and indirectly through climate-induced vegetation change.

Short-term studies, on the other hand, investigate short-term fluctuations of climate parameters such as temperature and precipitation. The parameters' inter-annual or monthly variability controls short-term water balance of the system by affecting evapotranspiration, soil moisture of the catchment, and therefore, streamflow.

There are several methods to assess long-term and short-term water balance of a catchment, among which conceptual models are widely used due to simple parametrization and easy implementation. Hence, this study successfully applied one of the most common conceptual models (i.e., the Budyko model) to investigate catchment scale water balance in both long-term and short-term scales. Finally, the study developed a hybrid conceptual-statistical framework to accurately evaluate the water balance components (such as streamflow and water storage change).

For the first approach in this study, the Budyko model was used to explore long-term impacts of climate change and human activities on annual streamflow. The long-term assessment showed that, in all of the study areas (Harvey catchment in Western Australia; Beardy catchment and Goulburn catchment in New South Wales; Karkheh basin in Western Iran)

streamflow has significantly changed during the last decades. Those case studies, clearly, showed that not only the climate change had impacts on streamflow, but also human activities significantly contributed to the streamflow reduction. Although, these case studies are selected from different parts of the globe and have different physical and catchment characteristics, they were significantly affected by change in precipitation and actual evapotranspiration, caused by climate and land use and land cover change. Outcome of the Budyko model was cross-validated, quantitatively, with the HBV model and, qualitatively, with remote sensing technique. The results verified performance of the Budyko model in assessing streamflow. The Budyko model also was employed for predicting streamflow variation under the two climate scenarios (i.e. RCP4.5 and RCP8.5) and its result was compared with the HBV model. The Budyko model proved to be a very reliable, simple and user-friendly tool for predicting future streamflow.

In the second approach (i.e., short-term approach), importance of monthly water storage change in the catchment's water balance was confirmed. Since the original Budyko model is not applicable for short-term studies, the extended version of the model (the Budyko-Du model) was employed. Moreover, another common conceptual model (i.e., ABCD-GE model) was used to compare the performance of the Budyko-Du model with.

For this phase of the study, the Harvey Catchment in Western Australia was chosen because of the importance of the catchment for the region and the physical characteristics of the catchment. Due to sandy soil profile of the area, rainfall infiltration is the only reliable means to replenish water table in the Harvey Catchment. Rainfall reduction and increased groundwater consumption have dramatically decreased groundwater level in the area. Excessive water withdrawal for domestic, agricultural and industrial purposes, has affected GWL, and therefore, has disturbed the dependent ecosystem. Furthermore, the Harvey Catchment, has both shallow and deep groundwater areas which enabled the research probe the importance of shallow groundwater in providing an extra source of water for evapotranspiration.

Unavailability of uniformly distributed groundwater data was the main challenge in assessing short-term water balance of the catchment. Therefore, this study successfully applied Rkriging method to investigate the catchment's groundwater level change. The method displayed spatiotemporal interpolation between the non-uniform observed groundwater data. To overcome temporal and spatial gap in the data, a uniform spatiotemporal grid was produced

and accordingly monthly uniform GWL data was estimated and monthly GWL maps were created.

The proposed Rkriging method confirmed groundwater level reduction in the area, following the literature. The estimated decreasing GWL trend also matched rainfall pattern of the catchment. Using the estimated groundwater level and soil water storage change resulted from extended ABCD model (i.e., ABCD-GE), improved performance of the Budyko-Du model. It was shown that for short-term scales, both soil water storage and groundwater storage change have significant roles in streamflow variation, hence, in order to produce a realistic results, studies need to consider both parameters.

And last but not least, to further increase performance of the conceptual models (i.e., ABCD and Budyko type models) in streamflow estimation, the Hybrid Conceptual-Statistical model (Conceptual-SARIMAX model) was developed. The statistical module of the developed model (i.e., SARIMAX) uses time-series capabilities and learns from the errors between the estimated values from the conceptual module and observed data to improve the model. The results were carefully validated with several performance criteria and showed significant improvement comparing to the original models.

9.2 Recomendatoions for further research

Effective long-term water management strategies at local-scale require an appropriate awareness of the eco-hydrological processes of a catchment and more attention and effort should be allocated to future water resources management and ecosystem planning in the study regions. The research can be expanded to investigate hydro-ecological responses of a system due to water resources change resulted from climate variation and human activites. Warmer and drier climate condition of the studied areas predicted by most of the future climate scenarios can affect the water resources (including groundwater and streamflow) of the catchmnets differently based on the future human activities. In this study human activites was defined as the regional impacts of human considering the fact that dam construction and land use change, including urbanization and agricultural activities, etc., are intimately embedded in the human impact. Hence, proposing differnet anthropogenic scenarios and separating different components of human activities such as land use change, forestation and deforestation, excess water withdrawals, can increase our knowledge of the systems' responses.

The proposed Rkriging method should be applied to other catchments where limited groundwater data is available and can be a useful approach for catchments with irregular temporal and spatial data. The method increases the spatiotemporal understanding of the studied parameter/s in the region. With a finer temporal grid (e.g., daily scale) the method can track the possible weekly or daily time-lag between rainfall and groundwater change which increases our knowledge of the catchment and its sensitivity to rainfall change. Should finer time scale be chosen, a shorter time period need to be adopted due to the extensive computational process. For future studies, by adding other covariate (such as rainfall) it might be possible to assess the impacts of climate parameters change on groundwater level.

The developed conceptual-statistical model can be easily used for other environmental cases and water resources problems where time-series information is employed for investigations. The statistical modules using time-series capabilities and learning from previous errors, can be coupled with other well-known conceptual hydrological models to overcome disadvantages of oversimplification embedded in conceptual models. Future research can use this method to other regions to further verify the findings of this work.

References

Abbaspour, K. C., M. Faramarzi, S. S. Ghasemi and H. Yang (2009) "Assessing the impact of climate change on water resources in Iran", Water resources research 45(10).

Afshar A, Kazemi H (2012) "Multi objective calibration of large scaled water quality model using a hybrid particle swarm optimization and neural network algorithm". KSCE Journal of Civil Engineering 16:913-918

Afshar A, Kazemi H, Saadatpour M (2011) "Particle swarm optimization for automatic calibration of large scale water quality model (CE-QUAL-W2): application to Karkheh Reservoir, Iran". Water resources management 25:2613-2632

Ahmad, M. U. D., and Giordano, M (2010) "The Karkheh River basin: the food basket of Iran under pressure". Water Int., 35, 522–544, https://doi.org/10.1080/02508060.2010.510326.

Ahmad, M. U. D., Islam, M. A., Masih, I., Muthuwatta, L., Karimi, P., and Turral, H (2009) "Mapping basin-level water productivity using remote sensing and secondary data in the Karkheh River Basin, Iran". Water Int., 34, 119–133, https://doi.org/10.1080/02508060802663903.

Al-Safi HIJ, Kazemi H, Sarukkalige PR (2020) "Comparative study of conceptual versus distributed hydrologic modelling to evaluate the impact of climate change on future runoff in unregulated catchments". Journal of Water and Climate Change

Al-Safi HIJ, Sarukkalige PR (2017a) "Assessment of future climate change impacts on hydrological behavior of Richmond River Catchment". Water Science and Engineering 10:197-208

Al-Safi HIJ, Sarukkalige PR (2017b) "Potential climate change impacts on the hydrological system of the Harvey River Catchment". World Academy of Science, Engineering and Technology, International Journal of Environmental, Chemical, Ecological, Geological and Geophysical Engineering 11:296-306

Al-Safi HIJ, Sarukkalige PR (2018) "The application of conceptual modelling to assess the impacts of future climate change on the hydrological response of the Harvey River catchment". Journal of Hydro-environment Research

Ali, R., McFarlane, D., Varma, S., Dawes, W., Emelyanova, I., Hodgson, G., & Charles, S. (2012). "Potential climate change impacts on groundwater resources of south-western Australia". Journal of Hydrology, 475, 456-472.

Alimohammadi N (2012) "Modeling Annual Water Balance In The Seasonal Budyko Framework". University of Central Florida Orlando, Florida

Andrews, B. H., M. D. Dean, R. Swain and C. Cole (2013). "Building ARIMA and ARIMAX models for predicting long-term disability benefit application rates in the public/private sectors." Society of Actuaries: 1-54.

Ashofteh P-S, Bozorg-Haddad O, Loáiciga HA, Marino MA (2016) "Evaluation of the impacts of climate variability and human activity on streamflow at the basin scale". Journal of Irrigation and Drainage Engineering 142:04016028

Australian Bureau of Meteorology. Climate Data Online. Retrieved January 20, 2020, from http://www.bom.gov.au/climate/data/index.shtml

Badrzadeh H, Sarukkalige R, Jayawardena A (2013) “Impact of multi-resolution analysis of artificial intelligence models inputs on multi-step ahead river flow forecasting”. Journal of Hydrology 507:75-85

Barron O et al. (2011) “Climate change impact on groundwater resources in Australia: Summary Report”. CSIRO Water for a Healthy Country Flagship, Australia,

Belinda PKJHPK, Shakya QD (2011) “Hydrological and nutrient modelling of the Peel-Harvey catchment”. vol WST 33. Department of Water, Western Australia, Water Science Technical Series

Beven, K (2001) “Rainfall-runoff modelling”. The Primer, John Wiley and Sons Press, Department of Geography Royal Holloway, University of London Egham, Surrey.

Birhanu, A., Masih, I., van der Zaag, P., Nyssen, J., and Cai, X (2019) “Impacts of land use and land cover changes on hydrology of the Gumara catchment, Ethiopia”. Physics and Chemistry of the Earth.

BOM (2018) Harvey at Dingo road, average annual streamflow. Australian Bureau of Metrology.

Brilliant.org (2018) “Feedforward Neural Network”. https://brilliant.org/wiki/feedforward-neural-networks/. 2018

Budyko M (1974) “Climate and Life”, 508 pp. Academic Press, New York,

Cai, Z., & Ofterdinger, U. (2016). “Analysis of groundwater-level response to rainfall and estimation of annual recharge in fractured hard rock aquifers, NW Ireland”. Journal of Hydrology, 535, 71-84.

Chang J, Zhang H, Wang Y, Zhu Y (2016) “Assessing the impact of climate variability and human activities on streamflow variation”. Hydrology and Earth System Sciences 20:1547-1560

Chauvin, G., G. Flerchinger, T. Link, D. Marks, A. Winstral and M. Seyfried (2011). "Long-term water balance and conceptual model of a semi-arid mountainous catchment." Journal of Hydrology 400(1-2): 133-143.

Chiew F, Teng J, Vaze J, Post D, Perraud J, Kirono D, Viney N (2009) “Estimating climate change impact on runoff across southeast Australia: Method, results, and implications of the modeling method”, Water Resources Research 45

CSIRO (2009) “Groundwater yields in south-west Western Australia”. A report to the Australian Government from the CSIRO South-WestWestern Australia Sustainable Yields Project. CSIRO Water for a Healthy Country Flagship, Australia.

CSIRO. (2009). “Water yields and demands in south-west Western Australia”. A report to the Australian Government from the CSIRO South-West Western Australia Sustainable Yields Project.

Cong, Z., Zhang, X., Li, D., Yang, H., and Yang, D (2015) “Understanding hydrological trends by combining the Budyko hypothesis and a stochastic soil moisture model”. Hydrological Sciences Journal, 60(1), 145-155.

Dash, J., Sarangi, A., & Singh, D. (2010). “Spatial variability of groundwater depth and quality parameters in the national capital territory of Delhi”. Environmental Management, 45(3), 640-650.

De Vries, J. J., & Simmers, I. (2002). “Groundwater recharge: an overview of processes and challenges”. Hydrogeology Journal, 10(1), 5-17.

Derakhshan, H., & Leuangthong, O. (2006). “A Review of Separable Spatiotemporal Models of Regionalization”.

Dimitrakopoulos, R., & Luo, X. (1994). “Spatiotemporal modelling: covariances and ordinary kriging systems”. Geostatistics for the next century (pp. 88-93): Springer.

Dey P, Mishra A (2017) “Separating the impacts of climate change and human activities on streamflow: a review of methodologies and critical assumptions”. Journal of Hydrology

Donohue RJ, McVicar TR, Roderick ML (2010) “Assessing the ability of potential evaporation formulations to capture the dynamics in evaporative demand within a changing climate”, Journal of Hydrology 386:186-197

Dooge JC (1992) “Sensitivity of runoff to climate change: A Hortonian approach Bulletin of the American Meteorological Society” 73:2013-2024

Du, C., F. Sun, J. Yu, X. Liu and Y. Chen (2016) “New interpretation of the role of water balance in an extended Budyko hypothesis in arid regions”. Hydrology and Earth System Sciences 20(1): 393.

Du, J., L. Qian, H. Rui, T. Zuo, D. Zheng, Y. Xu and C.-Y. Xu (2012). "Assessing the effects of urbanization on annual runoff and flood events using an integrated hydrological modeling system for Qinhuai River basin, China." Journal of Hydrology 464: 127-139.

Durrant J, Byleveld S (2009) “Streamflow trends in south-west Western Australia”. Department of Water, Western Australia

Duvert, C., Jourde, H., Raiber, M., & Cox, M. E. (2015). “Correlation and spectral analyses to assess the response of a shallow aquifer to low and high frequency rainfall fluctuations”. Journal of Hydrology, 527, 894-907.

Emam, A. R., M. Kappas and S. Z. Hosseini (2015) “Assessing the impact of climate change on water resources, crop production and land degradation in a semi-arid river basin”. Hydrology Research 46(6): 854-870.

Engineers, JAMAB Consulting (1999) “Karkheh Comprehensive Report”.

Engineers, JAMAB Consulting (2006) “Water balance report of Karkheh River Basin area: Preliminary analysis”. Ministry of Energy, Tehran, Iran (in Farsi).

Environmental Protection Authority (2008). “Water Quality Improvement Plan for the Rivers and Estuary of the Peel-Harvey System - Phophorus Management”, Environmental Protection Authority, Perth, Western Australia.

Fan H, Xu L, Tao H, Feng W, Cheng J, You H (2017) “Accessing the Difference in the Climate Elasticity of Runoff across the Poyang Lake Basin, China”. Water 9:135

Fathi, M. M., A. G. Awadallah, A. M. Abdelbaki and M. Haggag (2019). "A new Budyko framework extension using time series SARIMAX model." Journal of Hydrology 570: 827-838.

Ferdowsian, R., & Pannell, D. (2009). “Explaining long-term trends in groundwater hydrographs”. Paper presented at the Proceedings of the 18th World IMACS/MODSIM Congress, Cairns, Australia.

Fu G, Charles SP, Chiew FH (2007) “A two-parameter climate elasticity of streamflow index to assess climate change effects on annual streamflow”. Water Resources Research 43

Geris, J., Tetzlaff, D., Seibert, J., Vis, M., and Soulsby, C (2015) “Conceptual modelling to assess hydrological impacts and evaluate environmental flow scenarios in montane river systems regulated for hydropower”. River Research and Applications, 31(9), 1066-1081.

Geniaux, G. (2017). Analyzing spatio-temporal data with R: everything you always wanted to know-but were afraid to ask. Journal de la Société Française de Statistique, 158(3), 124-158.

Ghobadi, Y., Pradhan, B., Kabiri, K., Pirasteh, S., Shafri, H. Z. M., and Sayyad, G. A (2012) “Use of multi-temporal remote sensing data and GIS for wetland change monitoring and degradation”. In 2012 IEEE Colloquium on Humanities, Science and Engineering (CHUSER), 103–108, IEEE, DOI: 10.1109/CHUSER.2012.6504290.

Ghobadi, Y., Pradhan, B., Shafri, H. Z. M., and Kabiri, K (2012) “Assessment of spatial relationship between land surface temperature and landuse/cover retrieval from multi-temporal remote sensing data in South Karkheh Sub-basin, Iran”. Arabian J. Geosci., 8, 525–537, https://doi.org/10.1007/s12517-013-1244-3.

Green, T. R., Taniguchi, M., Kooi, H., Gurdak, J. J., Allen, D. M., Hiscock, K. M., Aureli, A. (2011). “Beneath the surface of global change: Impacts of climate change on groundwater”. Journal of Hydrology, 405(3-4), 532-560.

Guo, L., Lei, L., Zeng, Z.-C., Zou, P., Liu, D., & Zhang, B. (2014). “Evaluation of spatio-temporal variogram models for mapping Xco 2 using satellite observations: A case study in China”. IEEE Journal of Selected Topics in Applied Earth Observations and Remote Sensing, 8(1), 376-385.

Guo Y, Li Z, Amo-Boateng M, Deng P, Huang P (2014) “Quantitative assessment of the impact of climate variability and human activities on runoff changes for the upper reaches of Weihe River”. Stochastic environmental research and risk assessment 28:333-346

Gupta, H. V., Kling, H., Yilmaz, K. K., & Martinez, G. F. (2009). “Decomposition of the mean squared error and NSE performance criteria: Implications for improving hydrological modelling”. Journal of hydrology, 377(1-2), 80-91.

Guyennon N, Salerno F, Portoghese I, Romano E (2017) “Climate change adaptation in a Mediterranean semi-arid catchment: Testing managed aquifer recharge and increased surface reservoir capacity”. Water 9:689

Götzinger, J., and Bárdossy, A (2007) “Comparison of four regionalisation methods for a distributed hydrological model”. J. Hydrol., 333, 374–384, https://doi.org/10.1016/j.jhydrol.2006.09.008.

Goovaerts, P. (2000). “Geostatistical approaches for incorporating elevation into the spatial interpolation of rainfall”. Journal of Hydrology, 228(1-2), 113-129.

Greve, P., L. Gudmundsson, B. Orlowsky and S. I. Seneviratne (2016). "A two-parameter Budyko function to represent conditions under which evapotranspiration exceeds precipitation." Hydrology and Earth System Sciences 20(6): 2195-2205.

Haddeland I et al. (2014) “Global water resources affected by human interventions and climate change”. Proceedings of the National Academy of Sciences 111:3251-3256

Hardwinarto S, Aipassa M (2015) “Rainfall Monthly Prediction Based on Artificial Neural Network: A Case Study in Tenggarong Station, East Kalimantan-Indonesia”. Procedia Computer Science 59:142-151

Hashemi, H (2015) “Climate change and the future of water management in Iran”. Middle East Critique, 24(3), 307-323, https://doi.org/10.1080/19436149.2015.1046706.

Hashemi, H., Berndtsson, R., Kompani-Zare, M. and Persson, M (2013) “Natural vs. artificial groundwater recharge, quantification through inverse modeling”. Hydrol. Earth Syst. Sci, 17(2), 637-650. https://doi.org/10.5194/hess-17-637-2013.

Hashemi, H., Uvo, C. B., and Berndtsson, R (2015) “Coupled modeling approach to assess climate change impacts on groundwater recharge and adaptation in arid areas”. Hydrol. Earth Syst. Sci., 19, 4165–4181, https://doi.org/10.5194/hess-19-4165-2015, 2015.

Hashim Alsafi RS, Jun Magome, (2017) Hydrological impacts of Climate Change on the Future Streamflow of Unregulated Catchments of the Australian Hydrologic Reference Stations climate change

Haylock, M., Hofstra, N., Klein Tank, A., Klok, E., Jones, P., & New, M. (2008). “A European daily high-resolution gridded data set of surface temperature and precipitation for 1950–2006”. Journal of Geophysical Research: Atmospheres, 113(D20).

Han, S., H. Hu, D. Yang and Q. Liu (2011). "Irrigation impact on annual water balance of the oases in Tarim Basin, Northwest China." Hydrological Processes 25(2): 167-174.

HBV-manual (2013) IHMS, Integrated Hydrological Modelling System Manual, Version 6.3.

Hsu, Y. J., Fu, Y., Bürgmann, R., Hsu, S. Y., Lin, C. C., Tang, C. H., & Wu, Y. M. (2020). “Assessing seasonal and interannual water storage variations in Taiwan using geodetic and hydrological data”. Earth and Planetary Science Letters, 550, 116532.

Hu S, Liu C, Zheng H, Wang Z, Yu J (2012) “Assessing the impacts of climate variability and human activities on streamflow in the water source area of Baiyangdian Lake”. Journal of Geographical Sciences 22:895-905

Hu, D., Shu, H., Hu, H., & Xu, J. (2017). “Spatiotemporal regression Kriging to predict precipitation using time-series MODIS data”. Cluster Computing, 20(1), 347-357.

Huang S, Chang J, Huang Q, Chen Y, Leng G (2016) “Quantifying the Relative Contribution of Climate and Human Impacts on Runoff Change Based on the Budyko Hypothesis and SVM Model”. Water Resources Management 30:2377-2390

Islam S, Bari M, Anwar F (2014) “Hydrologic impact of climate change on Murray–Hotham catchment of Western Australia: a projection of rainfall–runoff for future water resources planning”. Hydrology and Earth System Sciences 18:3591-3614

Jafari, R., and Hasheminasab, S (2017) “Assessing the effects of dam building on land degradation in central Iran with Landsat LST and LULC time series”. Environ. Monit. Assess., 189, 74, https://doi.org/10.1007/s10661-017-5792-y, 2017.

Jalota, S. and V. Arora (2002). "Model-based assessment of water balance components under different cropping systems in north-west India." Agricultural Water Management 57(1): 75-87.

Jamali, S., A. Abrishamchi, M. A. Marino and A. Abbasnia (2013) "Climate change impact assessment on hydrology of Karkheh Basin, Iran", Proceedings of the Institution of Civil Engineers-Water Management, Thomas Telford Ltd.

Jamali, S., Jönsson, P., Eklundh, L., Ardö, J., and Seaquist, J (2015) "Detecting changes in vegetation trends using time series segmentation". Remote Sens. Environ., 156, 182–195, https://doi.org/10.1016/j.rse.2014.09.010.

Jeffrey SJ, Carter JO, Moodie KB, Beswick AR (2001) "Using spatial interpolation to construct a comprehensive archive of Australian climate data". Environmental Modelling & Software 16:309-330

Jones, D. A., Wang, W., and Fawcett, R (2009) "High-quality spatial climate data-sets for Australia". Aust. Meteorol. Oceanogr. J., 58, 233.

John, R., & John, M. (2019). "Adaptation of the visibility graph algorithm for detecting time lag between rainfall and water level fluctuations in Lake Okeechobee". Advances in Water Resources, 134, 103429.

Kahya, E. and S. Kalaycı (2004). "Trend analysis of streamflow in Turkey." Journal of Hydrology 289(1-4): 128-144.

Kapangaziwiri, E., Hughes, D., and Wagener, T (2009) "Towards the development of a consistent uncertainty framework for hydrological predictions in South Africa". IAHS publication, 333, 84.

Karimi, H., J. Jafarnezhad, J. Khaledi and P. Ahmadi (2018) "Monitoring and prediction of land use/land cover changes using CA-Markov model: a case study of Ravansar County in Iran", Arabian Journal of Geosciences 11(19): 592.

Kazemi, H., Sarukkalige, R., and Badrzadeh, H (2019) "Evaluation of streamflow changes due to climate variation and human activities using the Budyko approach". Environmental Earth Sciences., 78(24), 713.

Kelsey, P., Hall, J., Kretschmer, P., Quinton, B., & Shakya, D. (2010). "Hydrological and nutrient modelling of the Peel-Harvey catchment". Water Science Technical Series, Report.

Kim, J.-M., & Lee, J. (2017). "Time series analysis for evaluating hydrological responses of pore-water pressure to rainfall in a slope". Hydrological Sciences Journal, 62(9), 1412-1421.

Kim, J., J. Choi, C. Choi and S. Park (2013) "Impacts of changes in climate and land use/land cover under IPCC RCP scenarios on streamflow in the Hoeya River Basin, Korea", Science of the Total Environment 452: 181-195.

Knoben, W. J., Freer, J. E., & Woods, R. A. (2019). "Inherent benchmark or not? Comparing Nash–Sutcliffe and Kling–Gupta efficiency scores". Hydrology and Earth System Sciences, 23(10), 4323-4331.

Kotchoni, D. V., Vouillamoz, J.-M., Lawson, F. M., Adjomayi, P., Boukari, M., & Taylor, R. G. (2019). "Relationships between rainfall and groundwater recharge in seasonally humid Benin: a comparative analysis of long-term hydrographs in sedimentary and crystalline aquifers". Hydrogeology Journal, 27(2), 447-457.

Lambert, L., and Chitrakar, B. D (1989) “Variation of potential evapotranspiration with elevation in Nepal”. Mt. Res. Dev., 145–152, doi:10.2307/3673477.

Larocque, M., Mangin, A., Razack, M., & Banton, O. (1998). “Contribution of correlation and spectral analyses to the regional study of a large karst aquifer (Charente, France)”. Journal of Hydrology, 205(3-4), 217-231.

Learning, E. o. M. (2010). “Leave-One-Out Cross-Validation”. In C. Sammut & G. I. Webb (Eds.), Encyclopedia of Machine Learning (pp. 600-601). Boston, MA: Springer US.

Lee, L., Lawrence, D., & Price, M. (2006). “Analysis of water-level response to rainfall and implications for recharge pathways in the Chalk aquifer, SE England”. Journal of Hydrology, 330(3-4), 604-620.

Lehmann, A., & Rode, M. (2001). “Long-term behaviour and cross-correlation water quality analysis of the river Elbe, Germany”. Water Research, 35(9), 2153-2160.

Legesse, D., C. Vallet-Coulomb and F. Gasse (2013) “Hydrological response of a catchment to climate and land use changes in Tropical Africa: case study South Central Ethiopia”, Journal of hydrology 275(1-2): 67-85.

Li, D., Y. Tian and C. Liu (2004) “Distributed hydrological simulation of the source regions of the Yellow River under environmental changes”, Acta Geographica Sinica/Dili Xuebao 59(4): 565-573.

Li D, Pan M, Cong Z, Zhang L, Wood E (2013) “Vegetation control on water and energy balance within the Budyko framework”. Water Resources Research 49:969-976

Li H, Zhang Y, Vaze J, Wang B (2012) “Separating effects of vegetation change and climate variability using hydrological modelling and sensitivity-based approaches”. Journal of Hydrology 420:403-418

Li, J., and Zhou, S (2015) “Quantifying the contribution of climate-and human-induced runoff decrease in the Luanhe river basin, China”. J. Water Clim. Change., 7, 430–442, https://doi.org/10.2166/wcc.2015.041.

Li, L. J., Zhang, L., Wang, H., Wang, J., Yang, J. W., Jiang, D. J., and Qin, D. Y (2007) “Assessing the impact of climate variability and human activities on streamflow from the Wuding River basin in China”. Hydrol. Processes., 21, 3485–3491, https://doi.org/10.1002/hyp.6485.

Li, Y., He, D., Li, X., Zhang, Y., and Yang, L (2016) “Contributions of climate variability and human activities to runoff changes in the upper catchment of the Red River Basin, China”. Water, 8, 414, https://doi.org/10.3390/w8090414.

Liang W et al. (2015) “Quantifying the impacts of climate change and ecological restoration on streamflow changes based on a Budyko hydrological model in China's Loess Plateau”. Water Resources Research 51:6500-6519

Lidén, R., and Harlin, J (2000) “Analysis of conceptual rainfall–runoff modelling performance in different climates”. J. Hydrol., 238(3-4), 231–247, https://doi.org/10.1016/S0022-1694(00)00330-9.

Lindström G, Johansson B, Persson M, Gardelin M, Bergström S (1997) Development and test of the distributed HBV-96 hydrological model Journal of hydrology 201:272-288

Liu, J., Zhang, Q., Singh, V. P., and Shi, P.: Contribution of multiple climatic variables and human activities to streamflow changes across China. J. Hydrol., 545, 145–162, https://doi.org/10.1016/j.jhydrol.2016.12.016, 2017.

Love, D., Uhlenbrook, S., Corzo-Perez, G., Twomlow, S., and van der Zaag, P (2010) "Rainfall–interception–evaporation–runoff relationships in a semi-arid catchment, northern Limpopo basin, Zimbabwe". Hydrol. Sci. J., 55, 687–703, https://doi.org/10.1080/02626667.2010.494010.

Marjanizadeh, S., de Fraiture, C., and Loiskandl, W (2010) "Food and water scenarios for the Karkheh River Basin, Iran". Water Int., 35, 409–424, https://doi.org/10.1080/02508060.2010.506263.

Masih, I.: Understanding Hydrological Variability for Improved Water Management in the Semi-Arid Karkheh Basin, Iran: UNESCO-IHE PhD Thesis. CRC Press, 2011.

Masih, I., S. Uhlenbrook, H. Turral and P. Karimi (2009) "Analysing streamflow variability and water allocation for sustainable management of water resources in the semi-arid Karkheh river basin, Iran", Physics and Chemistry of the Earth, Parts A/B/C 34(4-5): 329-340.

Masih, I., S. Uhlenbrook, S. Maskey and M. Ahmad (2010) "Regionalization of a conceptual rainfall–runoff model based on similarity of the flow duration curve: A case study from the semi-arid Karkheh basin, Iran". Journal of hydrology 391(1-2): 188-201.

Masih, I., Uhlenbrook, S., Maskey, S., and Smakhtin, V(2011) "Streamflow trends and climate linkages in the Zagros Mountains, Iran". J. Clim. Change., 104, 317–338, https://doi.org/10.1007/s10584-009-9793-x.

McFarlane D, Stone R, Martens S, Thomas J, Silberstein R, Ali R, Hodgson G (2012) "Climate change impacts on water yields and demands in south-western Australia". Journal of Hydrology 475:488-498

McMahon T, Peel M, Lowe L, Srikanthan R, McVicar T (2013) "Estimating actual, potential, reference crop and pan evaporation using standard meteorological data: a pragmatic synthesis". Hydrology and Earth System Sciences 17:1331

Mekonnen, D. F., Duan, Z., Rientjes, T., and Disse, M (2018) "Analysis of combined and isolated effects of land-use and land-cover changes and climate change on the upper Blue Nile River basin's streamflow". Hydrol. Earth Syst. Sci., 22, 6187–6207, https://doi.org/10.5194/hess-22-6187-2018.

Merz, R., and Blöschl, G (2004) "Regionalisation of catchment model parameters". J. Hydrol., 287, 95–123, https://doi.org/10.1016/j.jhydrol.2003.09.028.

Mesgaran, M., Madani, K., Hashemi, H., and Azadi, P (2017) "Iran's land suitability for agriculture". Sci. Rep., 7, 7670, https://doi.org/10.1038/s41598-017-08066-y,.

Mianabadi, A., K. Davary, M. Pourreza-Bilondi and A. Coenders-Gerrits (2020). "Budyko framework; towards non-steady state conditions." Journal of Hydrology: 125089.

Michelle Antao, B. D., Adrian Goodreid. (2015). Peel Coastal groundwater allocation plan: Groundwater-dependent ecosystems. Environmental Water Report series, Department of Water, Government of Western Australia: 87.

Mitchell, V. G., T. A. McMahon and R. G. Mein (2003). "Components of the total water balance of an urban catchment." Environmental Management 32(6): 735.

Modarres, R. and T. B. Ouarda (2013). "Modelling heteroscedasticty of streamflow times series." Hydrological Sciences Journal 58(1): 54-64.

Mohammadi, B., F. Ahmadi, S. Mehdizadeh, Y. Guan, Q. B. Pham, N. T. T. Linh and D. Q. Tri (2020). "Developing novel robust models to improve the accuracy of daily streamflow modeling." Water Resources Management 34(10): 3387-3409.

Montenegro, A. and R. Ragab (2010) "Hydrological response of a Brazilian semi-arid catchment to different land use and climate change scenarios: a modelling study", Hydrological Processes 24(19): 2705-2723, 2010.

Mouelhi, S., C. Michel, C. Perrin and V. Andréassian (2006). "Stepwise development of a two-parameter monthly water balance model." Journal of Hydrology 318(1-4): 200-214.

Muthuwatta, L. P., Bos, M. G., and Rientjes, T. H. M (2010) "Assessment of water availability and consumption in the Karkheh River Basin, Iran—using remote sensing and geo-statistics". Water Resour. Manage., 24, 459–484, https://doi.org/10.1007/s11269-009-9455-9, 2010.

Muttitanon, W., and Tripathi, N. K (2005) "Land use/land cover changes in the coastal zone of Ban Don Bay, Thailand using Landsat 5 TM data", Int. J. Remote Sens., 26, 2311–2323, https://doi.org/10.1080/01431160512331326666.

Nasta, P., C. Allocca, R. Deidda and N. Romano (2020). "Assessing the impact of seasonal-rainfall anomalies on catchment-scale water balance components." Hydrology and Earth System Sciences 24(6): 3211-3227.

Noori, N. and L. Kalin (2016). "Coupling SWAT and ANN models for enhanced daily streamflow prediction." Journal of Hydrology 533: 141-151.

Oliveira, P. T. S., M. A. Nearing, M. S. Moran, D. C. Goodrich, E. Wendland and H. V. Gupta (2014). "Trends in water balance components across the Brazilian Cerrado." Water Resources Research 50(9): 7100-7114.

Patterson LA, Lutz B, Doyle MW (2013) "Climate and direct human contributions to changes in mean annual streamflow in the South Atlantic, USA". Water Resources Research 49:7278-7291

Pebesma, E. J. (2004). Multivariable geostatistics in S: The gstat package. Computers & Geosciences, 30(7), 683–691. https://doi.org/10.1016/j.cageo.2004.03.012

Pebesma, E., & Heuvelink, G. (2016). "Spatio-temporal interpolation using gstat". RFID Journal, 8(1), 204-218.

Petrone KC, Hughes JD, Van Niel TG, Silberstein RP (2010) "Streamflow decline in southwestern Australia", 1950–2008 Geophysical Research Letters 37

Rientjes, T., L. P. Muthuwatta, M. Bos, M. J. Booij and H. Bhatti (2013) "Multi-variable calibration of a semi-distributed hydrological model using streamflow data and satellite-based evapotranspiration". Journal of hydrology 505: 276-290.

Raman, R., S. Mohanty, K. Bhatta, S. Karna, A. Sahoo, B. Mohanty and B. Das (2018). "Time series forecasting model for fisheries in Chilika lagoon (a Ramsar site, 1981), Odisha, India: a case study." Wetlands Ecology and Management 26(4): 677-687.

Rouhani, S., & Hall, T. J. (1989). "Space-time kriging of groundwater data". In Geostatistics (pp. 639-650): Springer.

Ruibal-Conti, A. L. (2014). “Connecting Land to the Ocean: A Restrospective Analysis of Nutrient Flux Pathways Within the Peel-Harvey Catchment-estuary System”. University of Western Australia

Ruybal, C. J., Hogue, T. S., & McCray, J. E. (2019). “Evaluation of groundwater Levels in the Arapahoe Aquifer using Spatiotemporal regression kriging”. Water Resources Research, 55(4), 2820-2837.

Sahoo, G., C. Ray and E. De Carlo (2006). "Calibration and validation of a physically distributed hydrological model, MIKE SHE, to predict streamflow at high frequency in a flashy mountainous Hawaii stream." Journal of Hydrology 327(1-2): 94-109.

Sankarasubramanian A, Vogel RM, Limbrunner JF (2001) “Climate elasticity of streamflow in the United States”. Water Resources Research 37:1771-1781

Santos, L., Thirel, G., & Perrin, C. (2018). “Pitfalls in using log-transformed flows within the KGE criterion”. Hydrology and Earth System Sciences, 22(8), 4583-4591.

Schaake JC (1990) From climate to flow Climate change and US water resources:177-206

Seibert J (2005) “HBV light version 2, User's manual” Stockholm University-available at http://people su se/~ jseib/HBV/HBV_manual_2005 pdf

Shahid, M., Z. Cong and D. Zhang (2018). "Understanding the impacts of climate change and human activities on streamflow: a case study of the Soan River basin, Pakistan." Theoretical and Applied Climatology 134(1-2): 205-219.

Shi, L., Zhang, B., Wang, H.-x., Zhang, H.-j., Peng, Z.-h., & Li, J.-y. (2019). “Investigation on the causes of abnormal increase of water inflow in underground water-sealed storage system”. Tunnelling and Underground Space Technology, 87, 174-186.

Silberstein R et al. (2012) “Climate change and runoff in south-western”. Australia Journal of Hydrology 475:441-455

Sposito G (2017) “Understanding the Budyko Equation”. Water 9:236

Sun, Y., Niu, J., & Sivakumar, B. (2019). “A comparative study of models for short-term streamflow forecasting with emphasis on wavelet-based approach”. Stochastic Environmental Research and Risk Assessment, 33(10), 1875-1891.

Sun Y, Tian F, Yang L, Hu H (2014) “Exploring the spatial variability of contributions from climate variation and change in catchment properties to streamflow decrease in a mesoscale basin by three different methods”. Journal of Hydrology 508:170-180

Tan K, Neal B (2018) “Changes in annual rainfall-runoff responses in Melbourne's major water supply catchments”. Hydrology and Water Resources Symposium (HWRS 2018): Water and Communities,. Engineers Australia, p 827

Taylor, R. G., Scanlon, B., Döll, P., Rodell, M., Van Beek, R., Wada, Y. Edmunds, M. (2013). “Ground water and climate change”. Nature Climate Change, 3(4), 322-329.

Teng J, Chiew F, Vaze J, Marvanek S, Kirono D (2012) “Estimation of climate change impact on mean annual runoff across continental Australia using Budyko and Fu equations and hydrological models”. Journal of Hydrometeorology 13:1094-1106

Timbal B, Jones D (2008) “Future projections of winter rainfall in southeast Australia using a statistical downscaling technique”. Climatic Change 86:165-187

Vaze J, Teng J (2011) “Future climate and runoff projections across New South Wales, Australia: results and practical applications”. Hydrological Processes 25:18-35

Varouchakis, E. A., & Hristopulos, D. T. (2019). “Comparison of spatiotemporal variogram functions based on a sparse dataset of groundwater level variations”. Spatial Statistics, 34, 100245.

Varouchakis, E., & Hristopulos, D. (2013). Comparison of stochastic and deterministic methods for mapping groundwater level spatial variability in sparsely monitored basins. Environmental monitoring and assessment, 185(1), 1-19.

Voss, S., Zimmermann, B., & Zimmermann, A. (2016). Detecting spatial structures in throughfall data: The effect of extent, sample size, sampling design, and variogram estimation method. Journal of Hydrology, 540, 527-537.

Wang, C., Wang, S., Fu, B., and Zhang, L (2016) “Advances in hydrological modelling with the Budyko framework: A review”. Prog. Phys. Geogr., 40, 409–430, https://doi.org/10.1177/0309133315620997.

Wang, D. (2012). "Evaluating interannual water storage changes at watersheds in Illinois based on long-term soil moisture and groundwater level data." Water Resources Research 48(3).

Wang, G., J. Xia and J. Chen (2009) “Quantification of effects of climate variations and human activities on runoff by a monthly water balance model: a case study of the Chaobai River basin in northern China”, Water resources research 45(7).

Wang, H., Bracciano, D., & Asefa, T. (2020). Evaluation of water saving potential for short-term water demand management. Water Resources Management, 34(10), 3317-3330.

Wang, W., Shao, Q., Yang, T., Peng, S., Xing, W., Sun, F., and Luo, Y (2013) “Quantitative assessment of the impact of climate variability and human activities on runoff changes: a case study in four catchments of the Haihe River basin”, China. Hydrol. Processes., 27, 1158–1174, https://doi.org/10.1002/hyp.9299.

Wang, X., B. Gao and X. Wang (2020) “A Modified ABCD Model with Temperature-Dependent Parameters for Cold Regions: Application to Reconstruct the Changing Runoff in the Headwater Catchment of the Golmud River”, China. Water 12(6): 1812.

Wang, X., B. Gao and X. Wang (2020). "A Modified ABCD Model with Temperature-Dependent Parameters for Cold Regions: Application to Reconstruct the Changing Runoff in the Headwater Catchment of the Golmud River, China." Water 12(6): 1812.

Wang, X.-S. and Y. Zhou (2016) “Shift of annual water balance in the Budyko space for catchments with groundwater-dependent evapotranspiration”. Hydrology and Earth System Sciences 20(9): 3673-3690

Wang, Z.-Y., J. Qiu and F.-F. Li (2018). "Hybrid models combining EMD/EEMD and ARIMA for Long-term streamflow forecasting." Water 10(7): 853.

Wu J, Miao C, Zhang X, Yang T, Duan Q (2017) “Detecting the quantitative hydrological response to changes in climate and human activities”. Science of The Total Environment 586:328-337

Xu J, Chen Y, Li W, Nie Q, Song C, Wei C (2014a) “Integrating wavelet analysis and BPANN to simulate the annual runoff with regional climate change: a case study of Yarkand River, Northwest China”. Water resources management 28:2523-2537

Xu X, Liu W, Scanlon BR, Zhang L, Pan M (2013) “Local and global factors controlling water-energy balances within the Budyko framework”. Geophysical Research Letters 40:6123-6129

Xu X, Yang D, Yang H, Lei H (2014b) “Attribution analysis based on the Budyko hypothesis for detecting the dominant cause of runoff decline in Haihe basin”. Journal of Hydrology 510:530-540

Yang H, Yang D (2011) “Derivation of climate elasticity of runoff to assess the effects of climate change on annual runoff”. Water Resources Research 47

Yang H, Yang D, Lei Z, Sun F (2008) “New analytical derivation of the mean annual water-energy balance equation” Water Resources Research 44

Yao, L., Huo, Z., Feng, S., Mao, X., Kang, S., Chen, J. Steenhuis, T. S. (2014). “Evaluation of spatial interpolation methods for groundwater level in an arid inland oasis, northwest China”. Environmental Earth Sciences, 71(4), 1911-1924.

Yaseen, Z. M., O. Kisi and V. Demir (2016). "Enhancing long-term streamflow forecasting and predicting using periodicity data component: application of artificial intelligence." Water resources management 30(12): 4125-4151.

Ye, X., Q. Zhang, J. Liu, X. Li and C.-y. Xu (2013) “Distinguishing the relative impacts of climate change and human activities on variation of streamflow in the Poyang Lake catchment”, China. Journal of Hydrology 494: 83-95.

Yin, L., Y. Zhou, J. Huang, J. Wenninger, E. Zhang, G. Hou and J. Dong (2015). "Interaction between groundwater and trees in an arid site: Potential impacts of climate variation and groundwater abstraction on trees." Journal of Hydrology 528: 435-448.

Yokoo, Y., M. Sivapalan and T. Oki (2008). "Investigating the roles of climate seasonality and landscape characteristics on mean annual and monthly water balances." Journal of Hydrology 357(3-4): 255-269.

Zaidi, S. M., Akbari, A., Abu Samah, A., Kong, N. S., Gisen, A., and Isabella, J (2017) “Landsat-5 Time Series Analysis for Land Use/Land Cover Change Detection Using NDVI and Semi-Supervised Classification Techniques”, Polish Journal of Environmental Studies, 26, https://doi: 10.15244/pjoes/68878.

Zeng, S., J. Xia and H. Du (2014) “Separating the effects of climate change and human activities on runoff over different time scales in the Zhang River basin. Stochastic environmental research and risk assessment” 28(2): 401-413.

Zeng, S., Zhan, C., Sun, F., Du, H., and Wang, F (2015) “Effects of climate change and human activities on surface runoff in the Luan River Basin”. Adv. Meteorol., http://dx.doi.org/10.1155/2015/740239.

Zhang, L., C. Podlasly, Y. Ren, K. H. Feger, Y. Wang and K. Schwärzel (2014). "Separating the effects of changes in land management and climatic conditions on long-term streamflow trends analyzed for a small catchment in the Loess Plateau region, NW China." Hydrological Processes 28(3): 1284-1293.

Zhang, L., N. Potter, K. Hickel, Y. Zhang and Q. Shao (2008). "Water balance modeling over variable time scales based on the Budyko framework–Model development and testing." Journal of Hydrology 360(1): 117-131.

Zheng, H., L. Zhang, R. Zhu, C. Liu, Y. Sato and Y. Fukushima (2009). "Responses of streamflow to climate and land surface change in the headwaters of the Yellow River Basin." Water Resources Research 45(7).

Zhou, X., Y. Zhang, Y. Wang, H. Zhang, J. Vaze, L. Zhang, Y. Yang and Y. Zhou (2012). "Benchmarking global land surface models against the observed mean annual runoff from 150 large basins." Journal of hydrology 470: 269-279.

Zheng H, Zhang L, Zhu R, Liu C, Sato Y, Fukushima Y (2009) “Responses of streamflow to climate and land surface change in the headwaters of the Yellow River Basin Water” Resources Research 45

Appendices

Authorship Approval

Journal Paper: **Comparative study of conceptual versus distributed hydrologic modelling to evaluate the impact of climate change on future runoff in unregulated catchments** (2020). Journal of Water and Climate Change, 11(2), 341-366.						
Authors	Contribution					
	Conception and design	Acquisition of data & method	Data conditioning & manipulation	Analysis & statistical method	Interpretation & discussion	Final approval
Dr Hashim Al-Safi	✔	✔	✔	✔	✔	✔
Hamideh Kazemi	✔	✔	✔	✔	✔	✔
Dr Ranjan Sarukkalige	✔	✔			✔	✔

Journal Paper: **Evaluation of streamflow changes due to climate variation and human activities using the Budyko approach** (2019). Environmental Earth Sciences, 78(24), 1-17.						
Authors	Contribution					
	Conception and design	Acquisition of data & method	Data conditioning & manipulation	Analysis & statistical method	Interpretation & discussion	Final approval
Hamideh Kazemi	✔	✔	✔	✔	✔	✔
Dr Ranjan Sarukkalige	✔			✔	✔	✔
Dr Honey Badrzadeh		✔				✔

Rights & Permissions from Journals

Springer www.springer.com

Permissions

Get permission to reuse Springer Nature content

Springer Nature is partnered with the Copyright Clearance Center to meet our customers' licensing and permissions needs.

Copyright Clearance Center's RightsLink® service makes it faster and easier to secure permission for the reuse of Springer Nature content to be published, for example, in a journal/magazine, book/textbook, coursepack, thesis/dissertation, annual report, newspaper, training materials, presentation/slide kit, promotional material, etc.

Simply visit SpringerLink and locate the desired content;

Go to the article or chapter page you wish to reuse content from. (Note: permissions are granted on the article or chapter level, not on the book or journal level). Scroll to the botton of the page, or locate via the side bar, the "Reprints and Permissions" link at the end of the chapter or article.

Select the way you would like to reuse the content;

Complete the form with details on your intended reuse. Please be as complete and specific as possible ao as not to delay your permission request;

Create an account if you haven't already. A RightsLink account is different than a SpringerLink account, and is necessary to receive a licence regardless of the permission fee. You will receive your licence via the email attached to your RightsLink receipt;

Accept the terms and conditions and you're done!

For questions about using the RightsLink service, please contact Customer Support at Copyright Clearance Center via phone +1-855-239-3415 or +1-978-646-2777 or email springernaturesupport@copyright.com.

How to obtain permission to reuse Springer Nature content not available online on SpringerLink

Requests for permission to reuse content (e.g. figure or table, abstract, text excerpts) from Springer Nature publications currently not available online must be submitted in writing. Please be as detailed and specific as possible about what, where, how much, and why you wish to reuse the content.

Your contacts to obtain permission for the reuse of material from:

- books: bookpermissions@springernature.com
- journals: journalpermissions@springernature.com

Author reuse

Please check the Copyright Transfer Statement (CTS) or Licence to Publish (LTP) that you have signed with Springer Nature to find further information about the reuse of your content.

Authors have the right to reuse their article's Version of Record, in whole or in part, in their own thesis. Additionally, they may reproduce and make available their thesis, including Springer Nature content, as required by their awarding academic institution. Authors must properly cite the published article in their thesis according to current citation standards.
Material from: 'AUTHOR, TITLE, JOURNAL TITLE, published [YEAR], [publisher - as it appears on our copyright page]'

If you are any doubt about whether your intended re-use is covered, please contact journalpermissions@springernature.com for confirmation.

Self-Archiving

- Journal authors retain the right to self-archive the final accepted version of their manuscript. Please see our self-archiving policy for full details:
https://www.springer.com/gp/open-access/authors-rights/self-archiving-policy/2124

- Book authors please refer to the information on this link:
https://www.springer.com/gp/open-access/publication-policies/self-archiving-policy

IWA PUBLISHING

Select Language ▼

Rights & Permissions

Author Rights

An author's right to reuse and post their work published by IWA Publishing is defined by IWA Publishing's copyright policy. For papers which are not published "open access", authors transfer copyright to IWA Publishing, but have the right to:

- Share their article for personal (scholarly) purposes (including scholarly rights to create certain derivative works), so long as they give proper attribution and credit to the published work*.
- Retain patent, trademark and other intellectual property rights (including raw research data).
- Proper attribution and credit for the published work.

*Authors can share their article in the following ways:

- At a conference, meeting, or for teaching purposes
- Internal training
- Scholarly sharing with colleagues
- In a subsequent compilation of the author's works
- In a thesis or dissertation
- Reuse of portions in other works
- Preparation of derivative works for non-commercial purposes

For **IWA Publishing Open papers** (published as open access), authors sign an exclusive licence agreement. Authors retain copyright but licence exclusive rights in their article to the publisher. Authors have the right to:

Skip to Main Content